

TECHNIQUES UTILIZED IN THE CHARACTERIZATION OF EXISTING  
MATERIALS FOR IMPROVED MATERIAL DEVELOPMENT

Gary Withaeger, B.S.

Problems in Lieu of Thesis Prepared for the Degree of

MASTER OF SCIENCE

UNIVERSITY OF NORTH TEXAS

December 2001

APPROVED:

Witold Brostow, Major Professor

Kevin Menard, Minor Professor

Bruce Gnade, Committee Member and Chair of the  
Department of Materials Science

C.Neal Tate, Dean of the Robert B. Toulouse  
School of Graduate Studies

Withaeger, Gary, Techniques Utilized in the Characterization of Existing Materials for Improved Material Development. Master of Science (Material Science), December 2001, 157 pp.

It has become increasingly important to remain on the cutting edge of technology for a company to remain competitive and survive in today's high-tech industries. To do this, a company needs various resources dedicated to this cause. One of these resources is the use of existing materials, as starting points, for which improved materials can be based. For this, a company must rely on the characterization of existing materials to bring that base technology into their company. Through this evaluation, the base materials properties can be obtained and a material with improved properties can be developed.

There are many techniques that can be used in characterizing an existing material, but not every technique is required to obtain the desired goal. The techniques utilized depend upon the depth of identification required. This report summarizes several techniques utilized in the characterization of existing materials and provides some examples of evaluated products.

Copyright 2001

by

Gary Withaeger

## ACKNOWLEDGEMENTS

This paper was prepared to accomplish two main goals. The first was to fulfill my requirements to obtain my Masters Degree from the Robert B. Toulouse School of Graduate Studies. The second goal was to write a reference paper that could be utilized for students and professionals who are not familiar with or are new to the characterization techniques that are included in this Thesis. I want to thank both the University of North Texas Material Science Department and Corning Cable Systems for allowing me to accomplish these goals.

## Table of Contents

Chapter		
<b>1.</b>	<b>Introduction</b>	<b>6</b>
<b>2.</b>	<b>Theory of Instrumentation</b>	<b>9</b>
2.1	Rheological Characterization Techniques	9
2.2	Dynamic Mechanical Analysis	27
2.3	Differential Scanning Calorimetry	42
2.4	Thermal Mechanical Analysis	51
2.5	Thermogravimetric Analysis	62
2.6	Dielectric Analysis	74
2.7	Fourier Transform Infrared Spectrometry	81
<b>3.</b>	<b>Experimental</b>	<b>93</b>
3.1	Sample 1	93
3.1a	Equipment	93
3.1b	Procedures	93
3.2	Sample 2	99
3.2a	Equipment	99
3.2b	Procedures	100
3.3	Sample 3	105
3.3a	Equipment	105
3.3b	Procedures	106

<b>4. Results</b>	111
4.1 Sample 1	111
4.2 Sample 2	125
4.3 Sample 3	134
<b>5. Discussion and Recommendations</b>	144
5.1 Sample 1	144
5.2 Sample 2	148
5.3 Sample 3	150
<b>6. Conclusion</b>	153
References	156

## CHAPTER 1

### INTRODUCTION

It has become increasingly important to remain on the cutting edge of technology for a company to remain competitive and survive in today's high-tech industries. To do this, a company needs various resources dedicated to this cause. One of these resources is the use of existing materials, as starting points, for which improved materials can be based. For this, a company must rely on the characterization of existing materials to bring that base technology into their company. Through this evaluation, the base materials properties can be obtained and a material with improved properties can be developed.

This type of material development has many positive attributes. It can save a company time and money. By characterizing a material that already performs a specific function you do not have to reinvent the wheel. You are relying on previous scientists work and knowledge to create a starting point from which improvements can be made. This can save a company years and thousands of dollars. By characterizing a material that already performs a specific function, a base technology can be gained on specific applications of materials. This technology can be applied to future and current material development programs.

The first sample that is going to be characterized for base technological knowledge and possible material improvement is going to be called Sample 1 throughout this entire program. This name will keep the material manufacturer secret so that there is no corporate interest in this evaluation. This sample is used as an outdoor enclosure for telecommunication products. In its operation, it is exposed to UV radiation, extreme thermal cycling, rain, ice, and generally any other element possible in the continental United States. Sample 1 was evaluated to find an improved replacement for similar enclosures. The identification is unknown, so initially it is not known if the new material will represent a cost savings over the current material. Once the material has been characterized, it will be decided whether the properties should be improved or if they can be utilized without alteration.

The second sample characterized in this program is going to be called Sample 2 for the same reasons as stated before. This sample is used in telecommunication connectors. The sample is a part of a main component used in indoor applications. Sample 2 is exposed to moderate temperatures. Sample 2 was characterized to determine if it was a suitable base material for improved component development or other similar application.

The third sample (Sample 3) characterized in this program is a fiber optic boot. It is the soft cone shaped polymer that surrounds the fiber just behind a fiber optic plug. The boot is used to avoid the fiber from becoming pulled too far to either side and being broken. This material is totally an indoor application. The elements it will face include small temperature variations (less than 20°C) and very low or no UV radiation. Sample 3

was characterized to develop a base technology of these soft polymers and as a base for new material development.

There are many techniques that can be used in characterizing an existing material, but not every technique is required to obtain the desired goal. The techniques utilized depend upon the depth of identification that is required. For example, if the base polymer of a component is the only information needed, this can usually be determined with only a few techniques. If the exact make up of a material needs to be known, including its base polymer, filler content, filler particle size and distribution, molecular weight and distribution, rheological characteristics, thermal properties, electrical properties, etc, it could take approximately ten or twelve different techniques. Generally, for a quick overview of the sample's properties, most labs utilize the Fourier Transform Infrared Spectrophotometer (FTIR), Differential Scanning Calorimeter (DSC), Thermogravimetric Analyzer (TGA), Capillary Extrusion Rheometer, and Parallel Plate Rheometer in the characterization of various products. These techniques combined usually provide us with the base polymer composition, percent inorganic filler, operational temperature range of the material, molding temperature range, the material processing rheology, and other various properties. This report summarizes several techniques utilized in the characterization of existing materials and provides some examples of evaluated products.

## CHAPTER 2

### THEORY

#### 2.1 Rheological Characterization Method

Rheology is the deformation and flow of materials. Rheological property testing may be utilized for several purposes, including incoming inspection, identifying processability, predicting properties, and determining the quality of the material.

Rheological data can be used to determine lot to lot differences of thermoplastic upon incoming inspection. This can be performed by comparing relevant data of new lots of material against previously cataloged data. This can identify several problems with the new material before any is used in production. This type of inspection is capable of identifying changes in base polymer molecular weight (MW), filler quantity, end polymer performance, and problems the polymer will create in the injection molding process.

The viscosity function is necessary in order to determine the processability of a material over a given operational range of shear rates. This information is critical for molding equipment design and processing condition optimization. This data can be used to model the injection molding processing of critical components through computerized mold filling, packing, and cooling simulations. These simulations are very important for the proper sizing of mold part, runner, gate, and sprue dimensions.

Another useful tool of rheology is to predict the end product properties. This can be done in several ways by comparing zero shear viscosities of materials or by determining the shear rate dependence of the material, but the most important and most widely used prediction tool is Time Temperature Superposition (TTS). This method is used to predict the modulus – time behavior of a polymer at constant temperature. This will be discussed further later in this section.

Rheological characterizations can be performed on the reground molded parts and then compared to the virgin resin behavior. A significant shift in the measured viscosity function of the reground material serves as an effective indicator of degradation taking place in the plastic during the molding cycle. This is because the melt viscosity of a polymer is strongly dependent upon its weight average molecular weight (MW).

Rheological characterization techniques supply vital information regarding polymer material processability and possible MW changes(degradation) resulting from processing or conditioning. The storage modulus of a material is the portion of the samples modulus that is in phase with the strain. (1) This in phase stress and strain result in elastically stored energy which is completely recoverable. Storage modulus ( $G'$ ) is represented by  $G' = \sigma'/\gamma$  where  $\sigma$  = stress and  $\gamma$  = strain. The viscous (loss) modulus is the portion that is 90° out of phase with the strain. (1) The loss modulus is the portion of energy that is lost due to friction and internal motion. It is not recoverable. Loss modulus ( $G''$ ) is represented by  $G'' = \sigma''/\gamma$ . The Tan  $\delta$  of a material is the ratio of the viscous to elastic component of the material it is represented by the formula:  $\text{Tan } \delta = G''/G'$ . The relationship of these can be seen in Fig 1. The measured visco-elastic moduli of the sample consists of storage and viscous contributions. Of these two moduli

the useful one correlating to end-product performance (i.e., heat distortion) is the storage modulus as discussed earlier. By analyzing the storage modulus and  $\text{Tan } \delta$ , we can determine how the material reacts under the testing conditions.

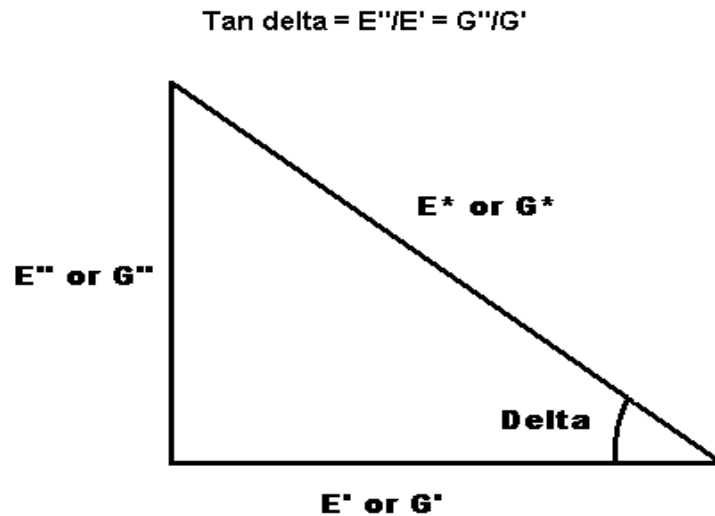


Fig 1: Triangle of Viscoelastic Relations

Viscoelastic materials can be characterized by a simple model put together by Maxwell called the Maxwell model. (2) It incorporates the spring and dashpot elements in series. If we first look at the spring element in a tensile elongation experiment, the uniaxial elongation is a pure Hookean spring. See Fig 2.



Fig2: Hookean Spring Element

This model is purely elastic. If the spring has an instantaneous stress ( $\sigma_0$ ) applied to it, the spring would respond with an instantaneous strain ( $\epsilon_0$ ). The instantaneous stress and strain are related by the following equation  $\sigma_0 = E\epsilon_0$  ; where E is the Youngs modulus. The purely viscous element is characterized by a dashpot. Newtons law:  $\sigma = \eta d\epsilon/dt$  is the model for a linear viscous behavior. This equation can be drawn as the dashpot, which is basically a piston with it's cylinder that has a liquid of viscosity  $\eta$  as seen in Fig 3.

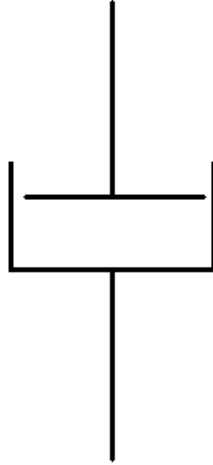


Fig 3: Dashpot Element

Viscoelastic materials are not represented by either of these elements very accurately. A more accurate representation of a viscoelastic material is the Maxwell element. The Maxwell element is the combination of the spring and dashpot in series as seen in Fig 4. The elastic response of the viscoelastic material is represented by the instantaneous tensile modulus,  $E$ , while the viscous response of the material is represented by the viscosity,  $\eta$ , of the dashpot. In this model,  $\eta = \tau E$ , where  $\tau$  is the relaxation time of the Maxwell element. A linear combination of the perfectly elastic and viscous motions in the Maxwell model is given by  $d\epsilon/dt = 1/E d\sigma/dt + \sigma/\eta$ . (2)

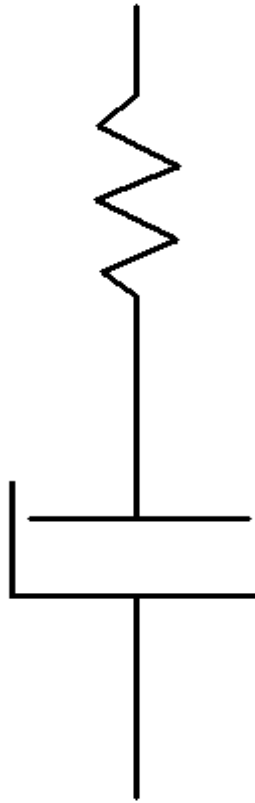


Fig 4: Maxwell Element

Materials have different responses to different environments. If we take a plot of shear rate vs relaxation time as in Fig 5 for different materials, we can see four distinct differences in behavior. These four types of behavior are named Newtonian, Bingham, dilatant, and pseudo-plastic. Newtonian behavior is characterized by a viscosity that is independent of shear. The shear rate of a Newtonian fluid is directly proportional to the shear stress. An example of a Newtonian fluid is water. Bingham plastics are concentrated suspensions of solid particles in Newtonian liquids. These materials often show little or no deformation up to a certain stress, called the yield stress. Above the

yield stress this materials follows a nearly Newtonian flow. An example of a Bingham fluid is toothpaste. Dilant behavior is characterized by an increase in viscosity with increasing shear rate. Dilant behavior is commonly called shear thickening. Pseudo-plastic behavior is characterized by an apparent viscosity decrease with increasing shear rate and stress. Most polymeric materials show pseudo-plastic behavior. A common name for pseudo-plastic is shear thinning.

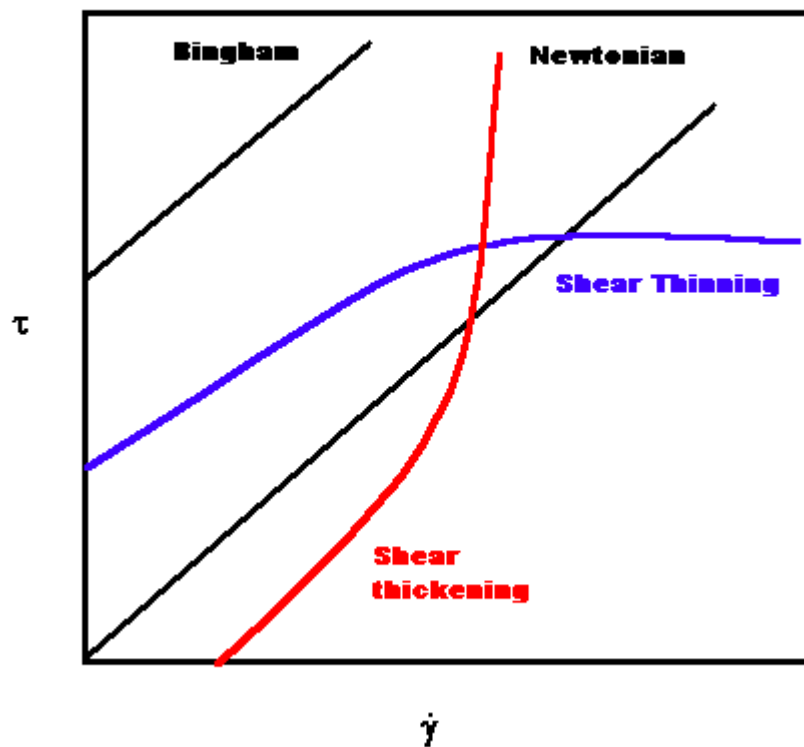


Fig 5: Shear rate vs Relaxation Time

There are several generic conditions that affect rheological data. Viscosity is lower for a material with a lower activation energy. Activation energy is affected by the chain mobility. A material with a high chain mobility will have a low activation energy

and consequently a low viscosity. Pressure also has an effect on viscosity. As pressure is increased for a polymer, the free volume of the polymer is decreased. This decrease in free volume creates an increase in the viscosity of the material due to the fact that chain mobility decreases. Shear rate is not always a way to predict viscosity. As shear rate increases, the viscosity decreases, for shear thinning materials. However, shear thickening materials increase their viscosity with increasing shear rate and Newtonian Fluids are not affected by shear rate. The  $M_w$  also plays a role in rheology. Viscosity( $\eta$ ) is proportional to the  $M_w$  of the polymer to the factor of 3.4 ( $\eta = MW^{3.4}$ ).<sup>(3)</sup> This is because as the molecular weight increases, the chains have a harder time moving around. This creates a higher activation energy and thus a higher viscosity. Base chain branching also plays a role in the viscosity of a material. Generally short branches don't affect the viscosity and long branches of  $M_w < M_e$  decrease the viscosity of the material.  $M_e$  is the molecular weight of entanglements. This is because entanglements increase the viscosity of a material. Fig 6 is a plot of viscosity vs shear rate for HDPE @150°C. This plot represents a shear thinning material.

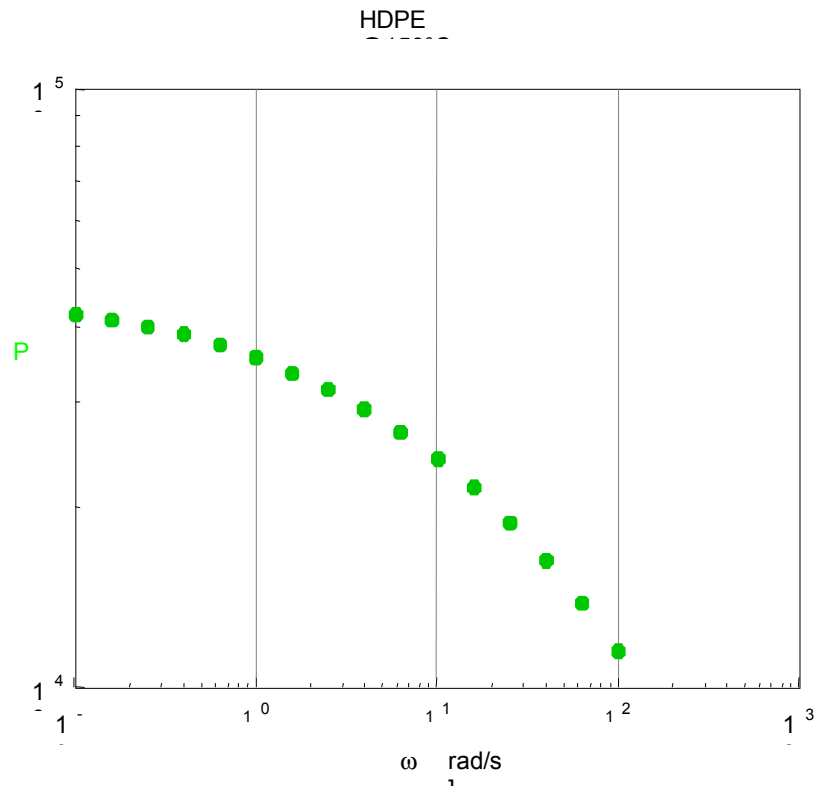


Fig 6: Viscosity / Shear rate for HDPE @ 150°C

Through the combined extrusion and parallel plate rheology, an evaluation can be performed predict important information about a polymer. Data collected on the extrusion rheometer and the parallel plate are fitted to a cross model through the use of the Cox-Mertz Rule. Application of the Cox-Merz rule permits superposition of capillary and parallel plate data on a single shear rate-viscosity plot to yield a broader range of shear rate-viscosity data. The Cox-Merz rule states that for rheologically simple materials the complex viscosity from dynamic measurements at a given frequency is equivalent to the steady shear viscosity at the same numerical value of shear rate.

Rheologically simple materials are those that can be superimposed. A general plot of viscosity vs shear rate for rheologically simple materials is given in Fig 7.

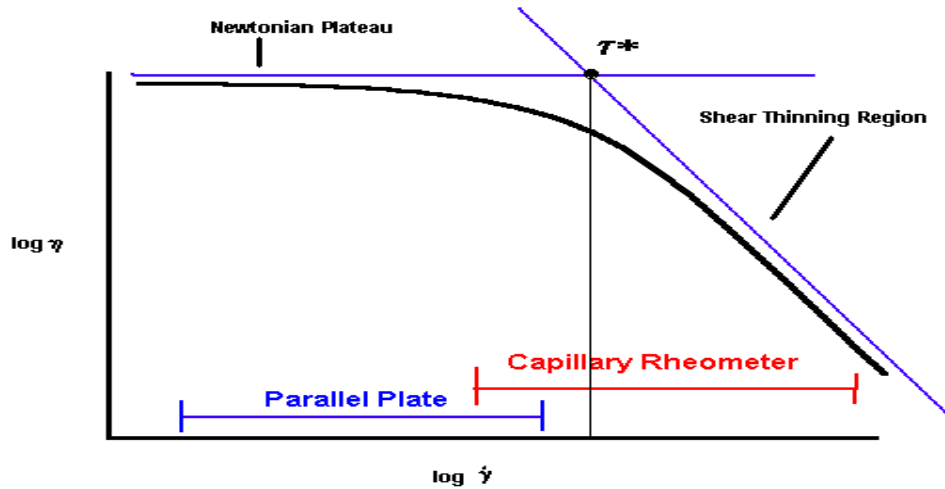


Fig 7: A general plot of viscosity vs shear rate for rheologically simple materials

It can be seen that these materials have an almost perfect Newtonian region followed by a shear thinning region at  $\tau^*$  (discussed next). Thus the combined parallel plate-capillary rheometer plot for a polymer melt can cover a shear rate range of 0.1 to 20,000 s<sup>-1</sup>. This method involves combining higher shear rate viscosity data from capillary rheometer with lower shear rate data from the parallel plate rheometer. By fitting this data to an appropriate steady shear viscosity model such as the “Cross” model critical parameters including the Newtonian plateau viscosity or zero shear viscosity ( $\eta_0$ ), an indication of MWD ( $\tau^*$ ), and a power law or shear thinning index ( $n$ ) are generated.  $\eta_0$  is related to  $M_w$  and thus to the critical part end-use properties. In addition  $\eta_0$ ,  $\tau^*$ , and  $n$  are direct

indicators of extrusion or injection molding melt processability.  $\eta_0$  is the zero shear viscosity which is related to Mw as  $\eta_0 = MW^{3.4}$ . As  $\eta_0$  increases, the MW of the polymer increases.  $\tau^*$  is an indicator of processability of the polymer. As  $\tau^*$  increase the polymer becomes harder to process. A material with a larger  $\tau^*$  takes a larger shear rate to approach the shear thinning region of that material. For example, as glass filler quantity is increased in a polymer, the  $\tau^*$  with also increase and the required shear rate required to shear thin the material will also increase.  $k$  is an indicator of the breadth of the MWD. As  $k$  decreases, the MWD of the material broadens. A material with a broader MWD is easier to process.  $n$  is the shear thinning index. It is inversely proportional to the tendency to shear thin. As  $n$  increases the tendency for the material to shear thin decreases. Once these parameters are established for a given polymeric raw material (resin) they can be used to assess lot-to-lot consistency as well as possible polymer degradation during extrusion or injection molding processing. This latter feature can be clarified by comparing the generated viscosity curves from the initial unprocessed (virgin) plastic resin and the corresponding extruded or injection molded part. Typically a significant downward shift in the viscosity curve for the processed part relative to the virgin resin is indicative of substantial thermal or mechanical degradation during melt processing; however, some materials have an increased viscosity upon degradation due to crosslinking.

Several generic cross model comparisons of various temperatures can be seen for HDPE in Figures 8, 9, and 10. The cross model is based on the combination of Newtonian and non-Newtonian fluids. A Newtonian fluid has the general formula

$$\eta (T) = A_0 e^{\Delta E/T}$$

A non-Newtonian fluid has the general formula  $\eta = A_0 \cdot e^{\Delta E/T} \cdot \dot{\gamma}^{n-1}$ . The power law combines the two regions under one formula through the use of the Cox-Mertz rule,  $\eta \dot{\gamma} = \eta^*(\omega)$ ; with  $\dot{\gamma} = \omega$ . (3) The form of the cross model is:

$$\eta(T, \dot{\gamma}) = \eta_0(T) / [1 + (\eta_0 \dot{\gamma} / \tau^*)^{(1-n)}] = \eta_0(T) / [1 + k^* \dot{\gamma}^{(1-n)}]$$

where

$\eta$  = steady shear viscosity

$\dot{\gamma}$  = shear rate

$\eta_0$  = zero shear

$n$  = power law or shear thinning index

$\tau^*$  = critical shear

$k$  = parameter related to breadth of MWD (s)

In a cross model graph if two tangents are taken from the Newtonian region and the shear thinning region, as in Fig 7,  $\tau^*$  can be estimated.  $\tau^*$  is the critical shear rate for the transformation of the material from Newtonian to shear thinning. Data at lower shear rates than  $\tau^*$  is generally obtained from the parallel plate rheometer. This low shear rate data is an indicator of the packing stage of the injection molding process. At shear rates above  $\tau^*$  the data is mainly obtained from the extrusion rheometer. This data is representative of the injection stroke of injection molding.  $\tau^*$  is not the point at which parallel plate rheology ends and extrusion rheology begins, that can be seen from the shear rates, it is the lowest shear rate that can be used for injection molding or extrusion for a particular material at a particular temperature. The zero shear rate viscosity,  $\eta_0$ , is directly related to  $M_w$ ,  $\eta_0 \propto M_w^n$ , and with the use of the cross model comparison can be calculated. For comparison of different materials, the materials must be at the same temperature and be of the same type (base polymer, filler, etc) to be properly compared.

This can be seen from figures 8, 9, and 10, that increasing the temperature will decrease the zero shear viscosity and since  $\eta_0 \propto M_w^n$  proving that the comparisons must be made within the same temperature. Each of these figures has  $\eta_0$ ,  $k$ , and  $n$  values provided.

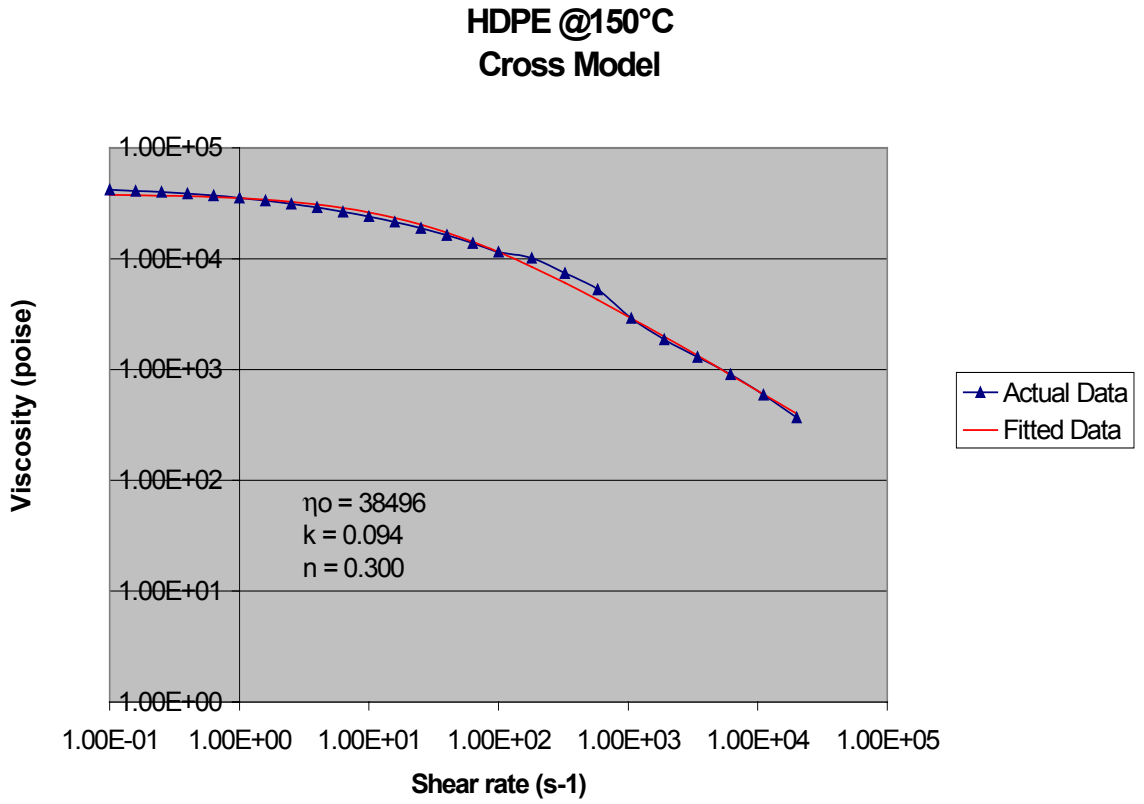


Fig 8: Cross Model of HDPE at 150°C

### HDPE @ 170°C Cross Model

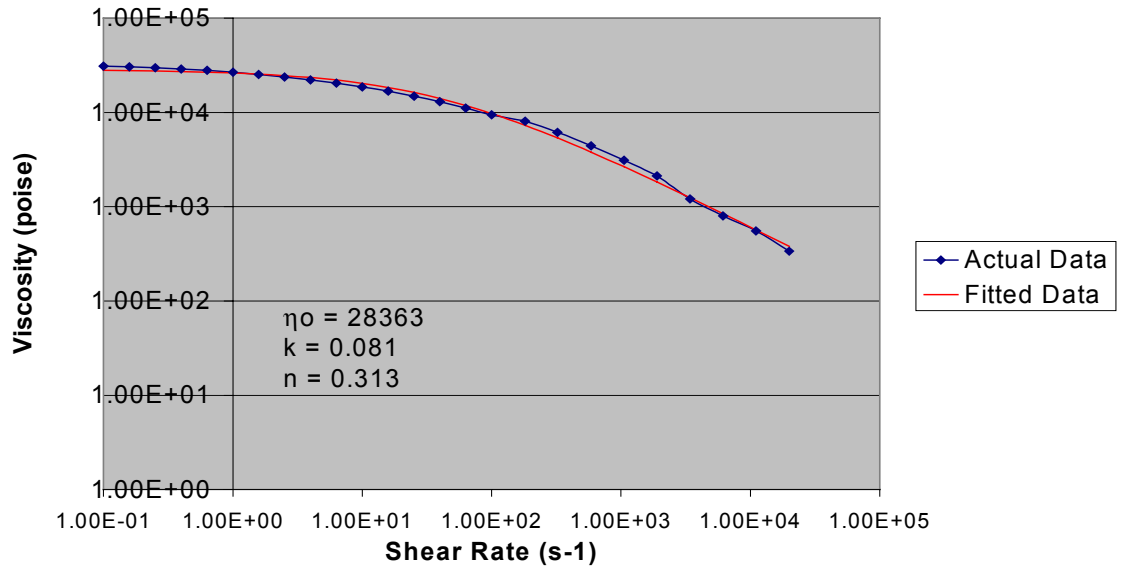


Fig 9: Cross Model of HDPE at 170°C

### HDPE@190°C Cross Model

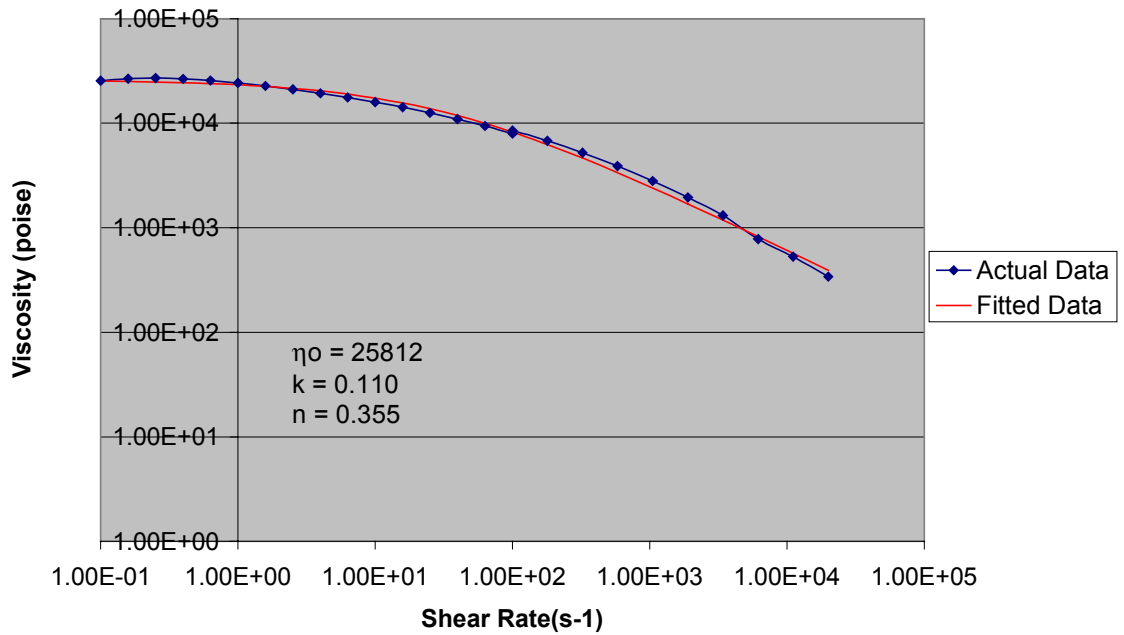


Fig 10: Cross Model of HDPE at 190°C

Modulus is a function of time as well as temperature which leads to the principle of Time Temperature Superposition (TTS).(2) Through the use of TTS a master curve can be generated that predicts moduli-time behavior at constant temperature. The combined parallel plate rheological and DMA data allow for the formation of a master curve of the data to predict storage ( $G'$ ) and loss ( $G''$ ) moduli at long times without having to test for long times. For example, an eight hour test can predict the performance for polymers anywhere from 50 to 80 years. This is done by running a frequency sweep at several temperatures above and below your reference temperature  $T_r$ , usually  $T_g$ , and then shifting the data below the  $T_r$  to the right with increasing shift factors  $a_T$  and the data above  $T_r$  is shifted to the left with decreasing  $a_T$ . The resulting graph is the master curve for that material at the reference temperature. The frequencies

can be converted to time and useful moduli-time data would be produced. Additionally, the slope of the plot of  $1/T(K)$  vs  $\ln aT$  gives the activation energy of flow of the material.

To be able to plot both the parallel plate and the DMA data on the same graph the DMA data needed to be converted to parallel plate data ( $E' \rightarrow G'$  and  $E'' \rightarrow G''$ ). This can be performed from the equation:

$$E = 2G(1 + \nu) \quad \text{where} \quad (2)$$

$\nu =$  Poisson's ratio of the material

The parallel plate rheology consists of two circular parallel plates of the same diameter. The diameter and type of plate used depends upon the sample being evaluated. For example, to run water in a parallel plate system it would be necessary for the plates to be very large and serrated plates are utilized on samples that lack plate adhesion. One plate is connected to the transducer while the other is attached to the instrument motor. The orientation of the motor and transducer varies from instrument to instrument. The plates are surrounded by an environmental chamber that regulates their temperature as seen in Fig 11. The parallel plate was run in oscillatory mode with shear rates ranging from 0.1 - 100 s<sup>-1</sup>. During an experiment the motor rotates at the prescribed frequency and the transducer measures the generated torque and normal forces for the given strain deformation. The valuable rheological properties are then generated with the use of the testing geometry. Parallel plate flow is not homogeneous.

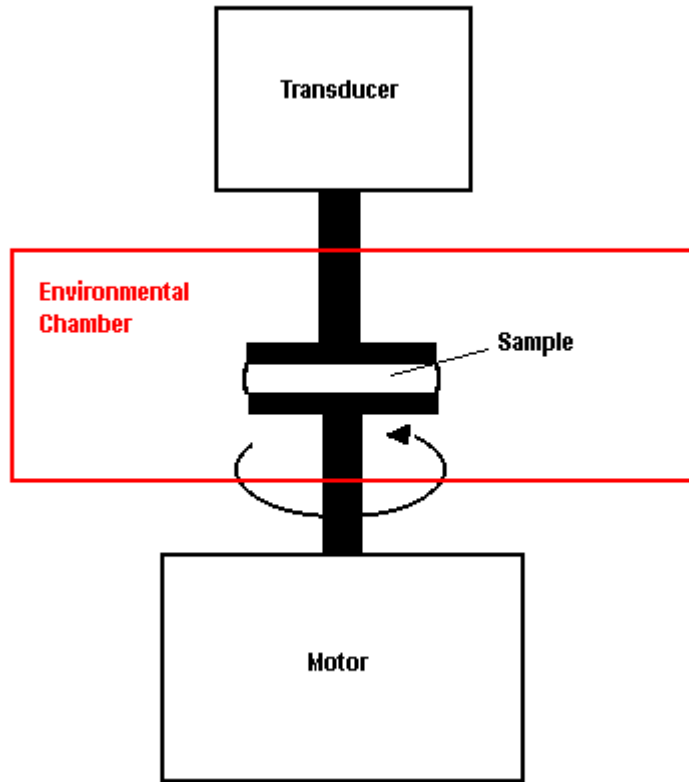


Fig 11: Parallel Plate diagram

Capillary extrusion rheology is performed in steady shear. It's flow is also not homogeneous.(3) In extrusion rheology, high shear rates are obtained. Generally extrusion rheology is run between  $100 - 20000\text{s}^{-1}$ . It is possible to run a lower shear rate but below  $100\text{s}^{-1}$  parallel plate is more accurate. A cross section of the capillary extrusion rheometer can be seen in Fig 12. Basically the rheometer consists of a heater, barrel, and a driving force for the melt. The barrel has thermocouples spaced throughout to maintain a constant temperature. Additionally, some rheometers have a pressure transducer mounted in the barrel to measure the driving pressure. Generally, the flow rate,  $Q$ , and the driving pressure are measured. Instruments that flow the melt with a

moving piston and do not have pressure transducer to measure the driving pressure  
calculate the pressure as follows:

$$P_d = F_d / \pi R_b^2 \quad \text{where}$$

$P_d$  = driving pressure

$F_d$  = piston force that is generated by  
the moving piston

$R_b$  = radius of the barrel

The measured quantities are used with the sample setup parameters (die length, entrance  
angle, and die diameter) to calculate the required rheological properties.

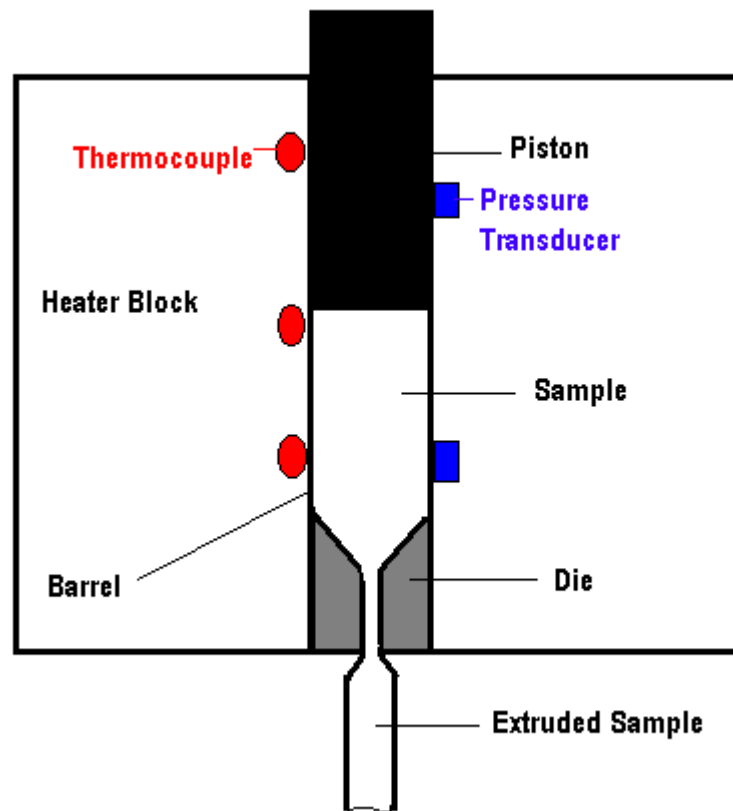


Fig 12: Capillary Rheometer diagram.

## 2.2 Dynamic Mechanical Analysis

In a Dynamic Mechanical Analysis (DMA) experiment the sample is under a constant load. An applied stress is oscillated sinusoidally as seen in Fig 13. Stress( $\sigma$ ) is described as the force multiplied by the area as:  $\sigma = FA$  ; where  $F = ma$ ,  $F =$  Force,  $m =$  mass,  $a =$  acceleration, and  $A =$  area. This experiment is valid as long as the material stays within its elastic limits. For a 100% elastic material, the applied stress and the materials response are in phase.(1) A 100% viscous material has a response that is  $90^\circ$  out of phase with the applied stress.(1) For a viscoelastic material, the materials response will be somewhere between in phase and  $90^\circ$  out of phase with the applied stress. For the viscoelastic materials evaluated, the applied stress and the materials response are out of phase by the phase angle  $\delta$ . This phase angle and the amounts of stress and strain at the peaks of their sine waves are the only parameters required by the DMA to arrive at the required data. The Storage modulus ( $E'$ ) can be calculated by:

$$E' = \sigma^0/\varepsilon^0 \text{ Cos } \delta = (f_0/bk)\text{Cos } \delta \quad (1) \quad \text{where}$$

$\sigma^0 =$  maximum stress

$\varepsilon^0 =$  maximum strain

$\delta =$  phase angle

$f_0 =$  force applied at the peak  
of the sine wave

$b =$  sample geometry term

$k =$  sample displacement at  
peak

The Loss (Viscous) modulus ( $E''$ ) can be calculated by:

$$E'' = \sigma^0 / \epsilon^0 \sin \delta = (f_0 / bk) \sin \delta \quad (1)$$

Tan delta ( $\tan \delta$ ) is calculated by:  $\tan \delta = E'' / E'$ . The compliance ( $J$ ) of a material is its willingness to yield. In a purely elastic material this is the inverse of the modulus.

$$J = 1/E. \quad (1)$$

Additionally, the complex modulus ( $E^*$ ) can be calculated by

$$E^* = E' + iE'' = \text{SQRT}(E'^2 + E''^2). \quad (1)$$

Through the use of the complex modulus, the complex shear modulus ( $G^*$ ) can be determined with  $E^* = 2G^*(1+\nu)$  (2) where  $\nu$  is the Poisson's Ratio of the material tested.

Utilizing the complex shear modulus, the complex viscosity ( $\eta^*$ ) can be determined by  $\eta^* = 3G^* / \omega = \eta'' + i\eta'$ . (1)

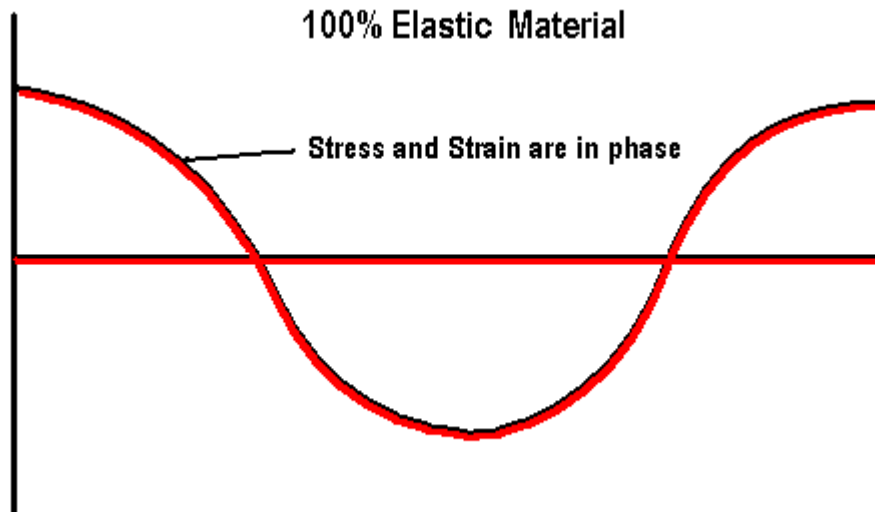


Fig 13: Sinusoidal stress/strain in a 100% Elastic Material

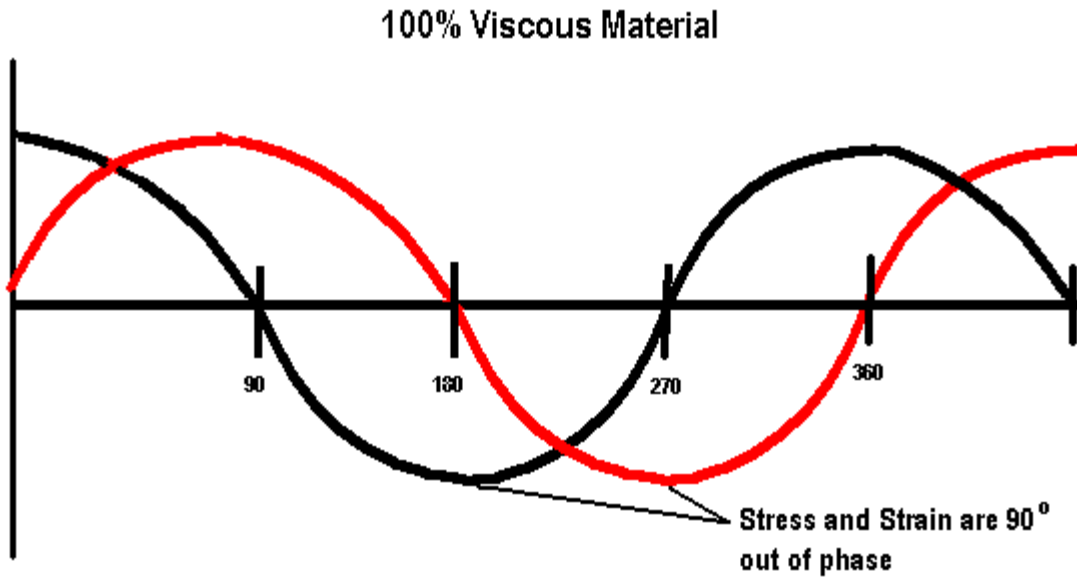


Fig 14: Sinusoidal Stress/Strain for a 100% Viscous Material

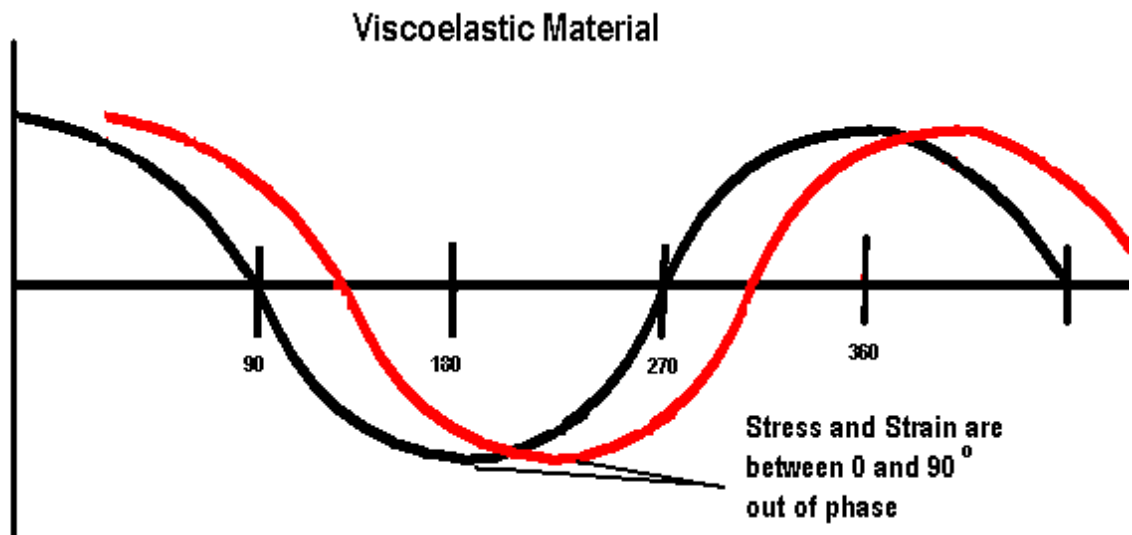


Fig 15: Sinusoidal Stress/Strain for a Viscoelastic Material

The sample size, heating rate, and oven size must be coordinated so as not to introduce extra transitions into an experimental run. For example, a large PPS sample can produce as many as seven glass transitions when heated too fast.

DMA can be tested from the Neutronian to the Hookean regions. Neutronian response is viscous behavior while Hookean response is elastic behavior. Stress –strain curves look at the Hookean response of the material.

DMA is based on a stress strain relationship of the samples. In DMA, a stress is applied to the sample, in the form of a sine wave, and the materials response (strain) is evaluated. The slope of a stress-strain plot represents the modulus of the material. Modulus is dependent upon temperature and applied stress.

A typical stress – strain curve is shown in Fig 16. The following properties are labeled in the figure: Young's tensile modulus ( $E = d\sigma/d\epsilon$ ), yield stress ( $\sigma_Y$ ), yield strain ( $\epsilon_Y$ ), ultimate stress ( $\sigma_U$ ), ultimate strain ( $\epsilon_U$ ), breaking stress ( $\sigma_B$ ), breaking strain ( $\epsilon_B$ ), and the toughness. Young's or tensile modulus is a direct reflection of polymer type and molecular weight (MW). Young's modulus is directly related to the stiffness of the material which is a critical parameter affecting dimensional stability.

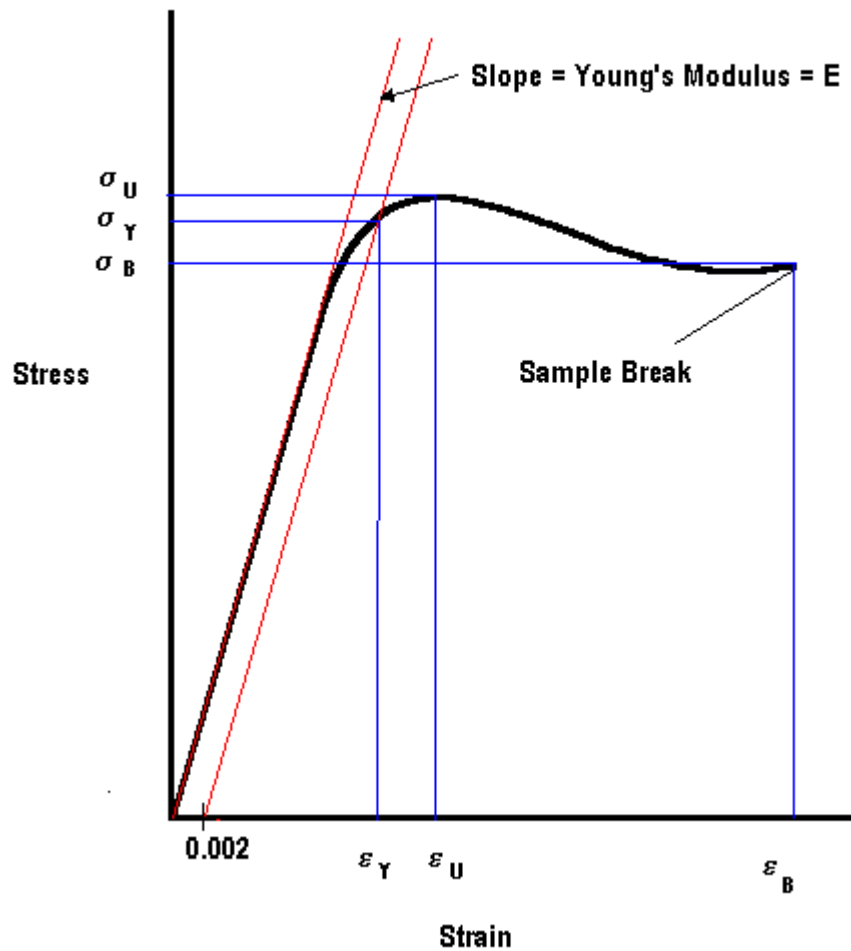


Fig 16: Generic Stress/Strain Curve

In this graph, the yield point is chosen at 2% (0.002) strain. Therefore, you take this point on the x-axis and draw a line from it parallel to the initial tangent of the stress – strain curve which is defining the Young's modulus. This intersection of the 2% strain with the stress-strain curves gives an estimated yield point labeled the yield stress and yield strain. This yield stress and strain represent the practical engineering design limits for a given material. Also the yield point can be labeled the maximum point. Beyond

this second definition of the yield point permanent plastic deformation occurs. The breaking stress and strain represent the ultimate value of stress and strain that the material can withstand before failure. The toughness of the material is represented by the area under the tensile stress-strain curve up to the breaking point. Toughness is a reflection of impact strength and relates to end performance.

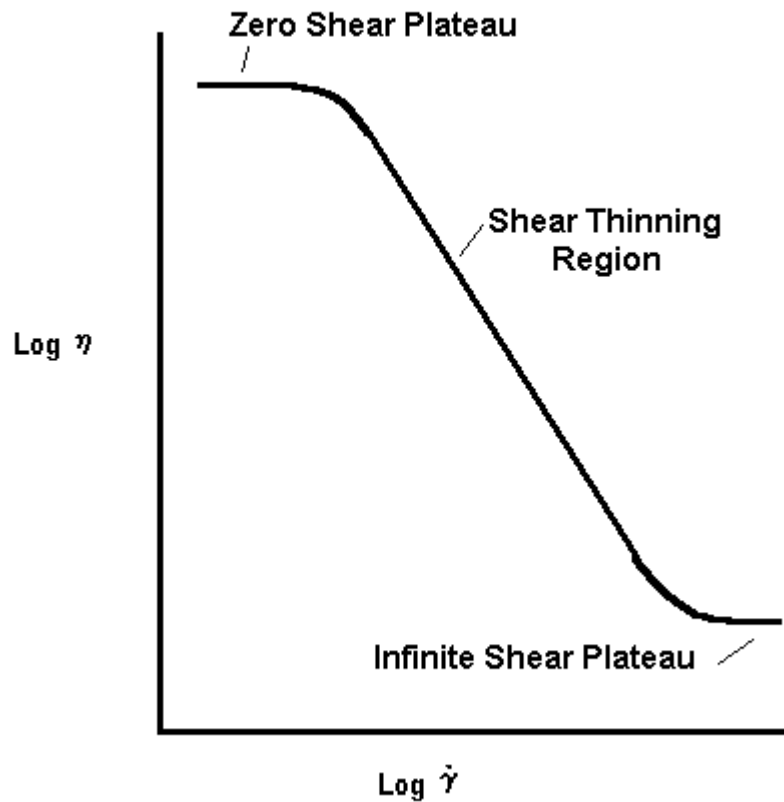


Fig 17: Generic viscosity/ shear rate

Fig 17 gives a generic viscosity vs shear rate plot. In this plot three distinct regions are seen, the zero shear plateau, shear thinning region, and the infinite shear plateau. The zero shear plateau is characterized by the Newtonian behavior at low shear rates. This zero shear viscosity can be related to the molecular weight of the polymer as:

$$\eta_0 = k(MW^{3.4}) \quad (1) \quad \text{where}$$

$\eta_0$  = zero shear viscosity  
 $k$  = a material specific constant  
 $MW$  = molecular weight

At the end of this region, the plot takes a linear dependence with respect to shear rate. This region is called the shear thinning region. The shear thinning region is characterized by a decrease in viscosity with increasing shear rate. The infinite shear plateau region begins at the end of the shear thinning region. It is characterized by a Newtonian behavior at high shear rates.

When comparing materials properties, a material with a higher storage modulus ( $E'$ ) would be stiffer and harder to deform than one with a lower storage modulus. The storage modulus is a materials elastic component. The storage modulus is the materials ability to store or return energy. A material also has a viscous component called the loss modulus. This viscous component relates the materials ability to lose energy. The material's  $\tan \delta$  designates the material's ratio of viscous to elastic components ( $E''/E'$ ) A material with a higher  $\tan \delta$  has a higher viscous percentage than one with a lower  $\tan \delta$ . Therefore the material would be more likely to be able to absorb a vibration or impact and disperse it throughout the material without failure.  $\tan \delta$  is sometimes called the materials damping ability.(1)

A generic DMA plot of the storage modulus vs temperature of a semicrystalline material can be seen in Fig18 . The glass transition( $T_g$ ) is also called the alpha transition ( $T_\alpha$ ). The glass transition is caused by the material gaining enough energy through increased heat to allow gradual chain movements. The glassy region is the region at temperatures below the glass transition. From the  $T_g$  moving toward a lower temperature, the next transition is the beta transition ( $T_\beta$ ) followed by the gamma transition ( $T_\gamma$ ), and then the delta transition ( $T_\delta$ ). The beta transition is caused by side chain and pendent group movements. The beta transition can be related to the toughness of the material through  $\tan \delta$ . The larger  $T_\beta$ , the greater the materials ability to withstand an impact. The main chain has greater mobility due to the increased side chain movements and the material has a less probability of failure.  $T_\gamma$  is caused by the increased free volume allowing localized bond movements and side chain movements to occur. Beta and gamma transitions can not be detected by other thermal analysis techniques. Basically  $T_\gamma$  is caused by localized bond movements (bending and stretching) and side chain movements.  $T_\beta$  is caused by the whole side chains and localized groups of four to eight backbone atoms beginning to have enough space to move causing the material to begin to develop some toughness. The  $T_g$  is caused by the chains in the amorphous region beginning to coordinate large-scale motions. In theory, there are no glass transitions in 100% crystalline materials; however, 100% crystalline materials are impossible to produce. The melting temperature ( $T_m$ ) is caused by large scale chain slippage occurring and the material begins to flow. The region between the glass transition and the melting point is called the rubbery plateau. Thermoset materials do not exhibit a melting point. The crosslinks prevent chains from slipping past each

other in a thermoset preventing the material from melting. Upon excess heating, a thermoset will degrade rather than melt.

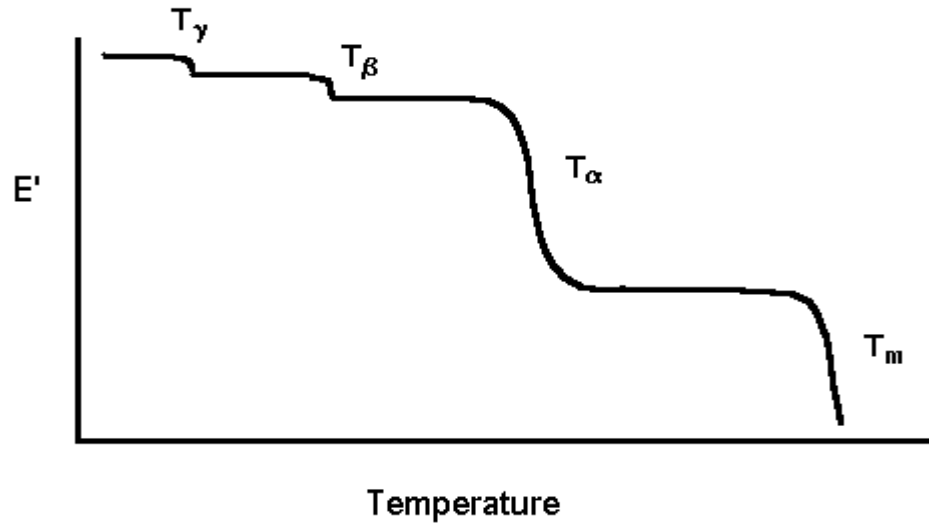


Fig18: Generic  $E'$  vs T for a Semicrystalline Material

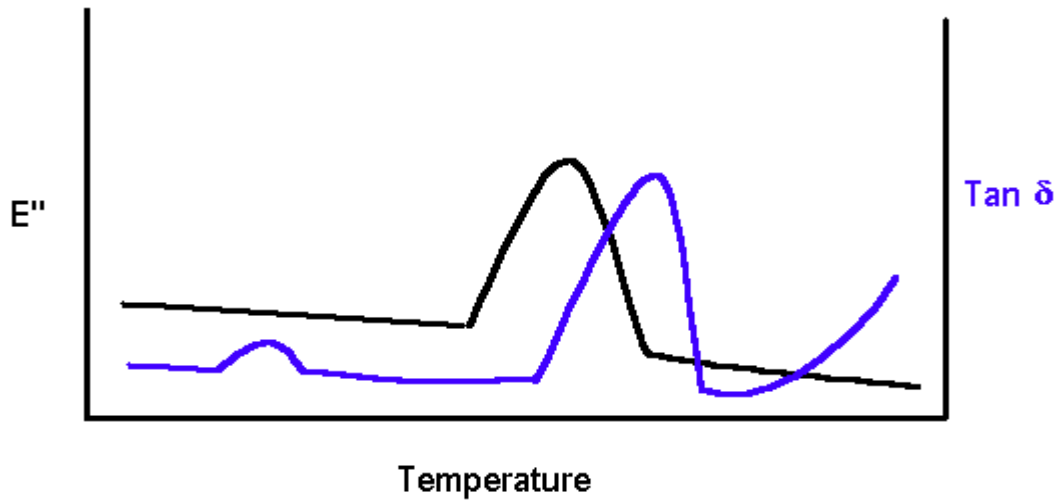


Fig 19: Generic plot of  $E''$  and Tan delta for a Semicrystalline Material

Fig 19 shows a generic plot of a semicrystalline material with the Loss Modulus ( $E''$ ) and the  $\tan \delta$  instead of  $E'$ . When comparing these two plots for actual materials, it can be seen that the peak of the loss modulus plot corresponds with the glass transition range from the storage modulus of the previous figure. In this figure, the  $\tan \delta$  plot has two peaks. The peak at the lower temperature is the beta transition peak. It corresponds with the beta transition of the storage modulus. This peak can be used to compare materials with respect to damping ability as discussed earlier. The second peak on the  $\tan \delta$  plot corresponds with the glass transition region of the storage modulus plot. The glass transition from the  $\tan \delta$  plot is at the upper end of the storage modulus glass transition region. It is also at a higher temperature than the peak of the loss modulus.

There are many circumstances that will alter the properties of a material. The following are only a few material changes that can be seen in a plot of a material's viscoelastic properties. An increase in the cross link density of the material will increase the storage modulus of a given material. It will also decrease the plot of  $\tan \delta$ . These effects are both attributed to the fact that increased cross link density constricts the movements of the polymer chains. The addition of plasticizers decreases a material's storage modulus while broadening its glass transition region. The addition of fillers can either increase or decrease the materials properties. The effect is dependent upon the filler type and filler weight percent. A generic formula to help estimate the properties caused by the addition of a filler is:

$$P_f = P_p w_p + P_a w_a \quad \text{where}$$

$P_f$  = final property  
 $P_p$  = polymer's initial property  
 $w_p$  = weight percent of the polymer  
 $P_a$  = additive's property  
 $w_a$  = weight percent of the additive

The crystallinity of a material is a state of molecular structure attributed to the existence of solid crystals with a definite geometric form. Crystalline structures are characterized by uniformity and compactness. A change in the crystallinity of a material will have significant changes in the materials viscoelastic behavior. For instance, the storage modulus will be increased if the crystallinity of the material is increased. Additionally, the glass transition or melting point of the material would increase in temperature. These two changes in properties are due to the increased compactness of the polymer with increasing crystallinity. This compactness would lead to an increase in elastic modulus and require additional energy (higher temperature) for the molecules to move and cause the glass transition or the melting point. The  $\tan \delta$  of the material is also affected by the change in crystallinity. As the crystallinity of a material is increased, the  $\tan \delta$  and the peaks ( $\beta$  transition peaks) are decreased.  $\tan \delta$  is called the damping ability of the material. As the  $\tan \delta$  increases the material is more likely to absorb a shock and disperse it without fracture. As the crystallinity increases, the material becomes more set in place and has less possible motion, therefore, it would have less motion to move and absorb a shock leading to a smaller  $\tan \delta$  peak. These changes are given in Figures 20 and 21.

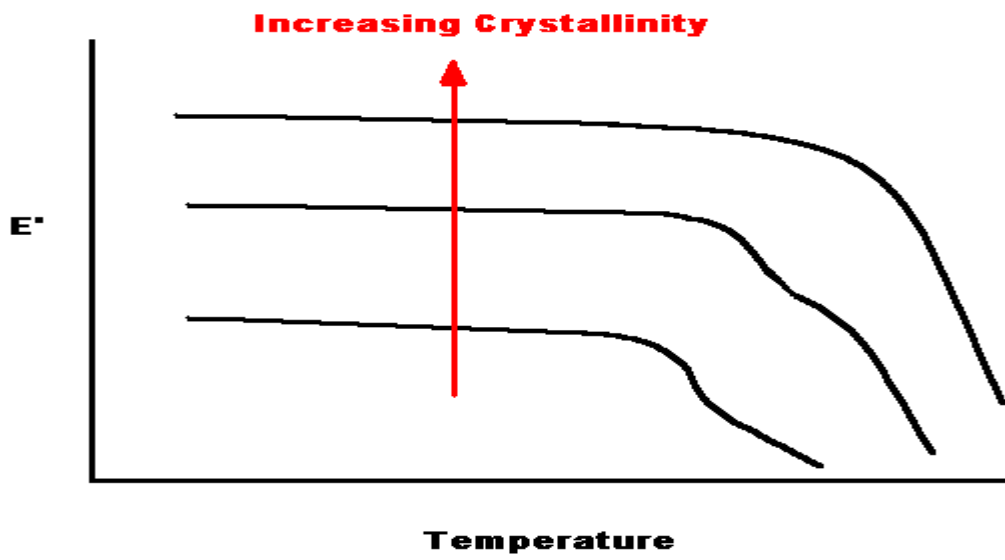


Fig 20: Changes in  $E'$  with respect to crystallinity.

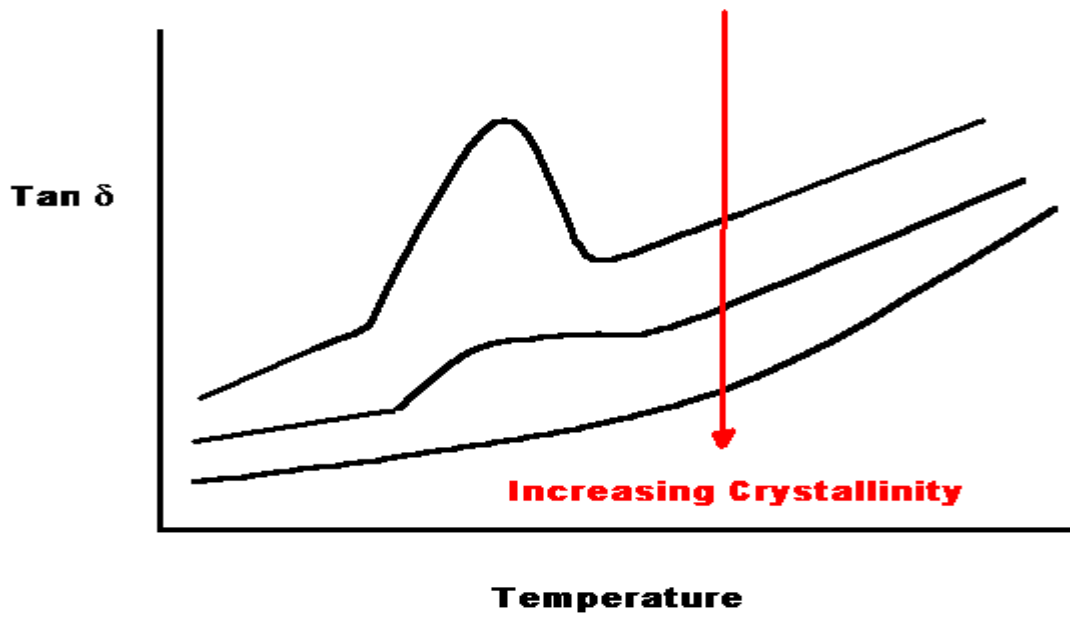


Fig 21: Change in  $\tan \delta$  with respect to crystallinity

Molecular weight variation of a polymer also has a tremendous effect on viscoelastic behavior. A molecular weight increase in a material will increase the storage modulus of that material and increase the glass transition and melting temperatures. The increase in the glass transition or melting point is caused by the increased entanglements associated with the increased molecular weight. The increased entanglements require an increased amount of energy (increased temperature) to allow the movement seen in a glass transition or melting point. Increasing the molecular weight of a material also shifts the peak of  $\tan \delta$  to a higher temperature. The peak of  $\tan \delta$  is in the range of the glass transition of the material. As the molecular weight is increased the glass transition is also increased which leads to this shift in  $\tan \delta$  peaks with respect to increasing molecular weight. These characteristics can be seen in the following plots. (Figures 22 and 23)

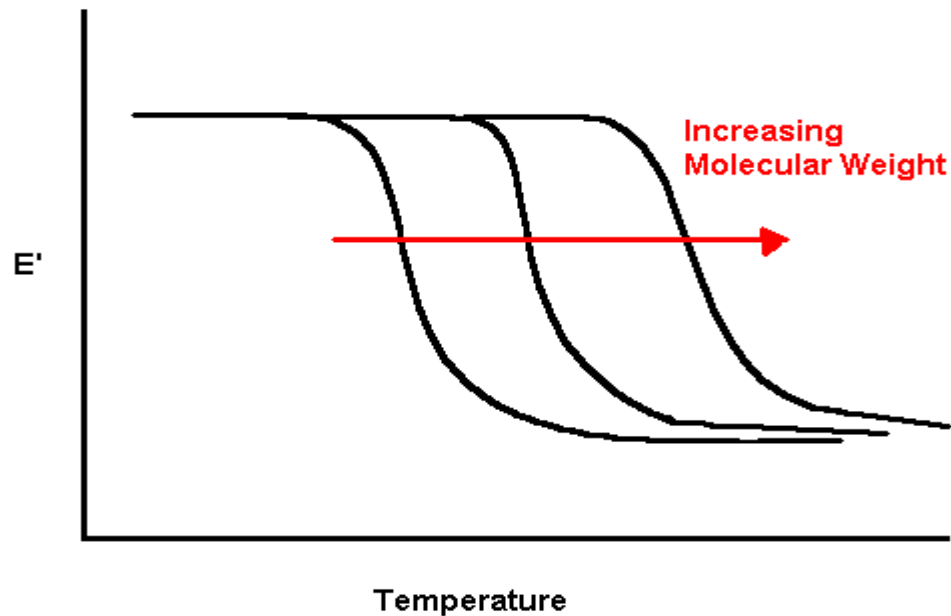


Fig 22:  $E'$  vs T for increased MW

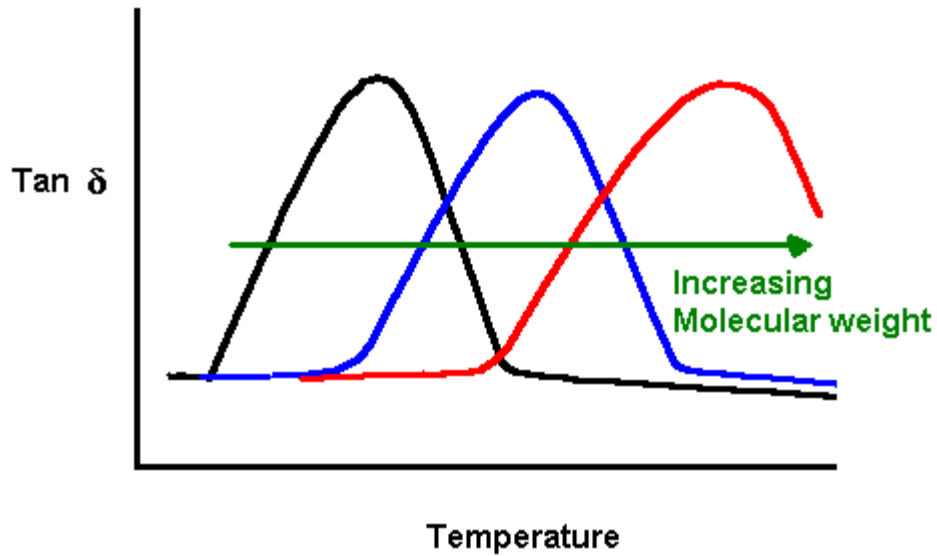


Fig 23: Tan delta vs T for increased MW

Molecular structure information can be determined by the frequency behavior of the material. For a quick comparison between materials, the cross over point between  $E'$  and  $\eta$  or  $E'$  and  $E''$  can be used and related to the molecular weight and molecular weight distribution through the use of the Doi-Edwards theory.

Time temperature superposition (TTS) is based on the Boltzmann superposition principle. It allows for the estimation of sample performance outside the instrument's capabilities or personnel time constraints. The Boltzmann superposition principle allows for an estimation to be made with many properties through the use of a master curve as discussed in the previous section.

Additionally creep and creep recovery tests can be performed on the DMA. Creep evaluates the materials response to a constant load while creep recovery evaluates the

materials recovery once that load is removed. A single step can be performed or multiple cycles can be utilized to simulate real world applications. For instance a gasket that is compressed it's entire life by a bolt could be represented by a single step. The initial load would be applied and held constant for any period of time. For the evaluation of a gasket in a door, a cyclic creep recovery test would be more accurate. For this the gasket would be placed under a load for a period of time. At the end of the time the load would be removed allowing the gasket to recover. After a recovery period, the load is applied again for a period of time. The amount of repetition is dependent upon the results desired. This second procedure is excellent in comparing materials' performance. These analyses can be performed at varying temperatures to match real world conditions. A generic creep recovery plot is seen in Fig 24.

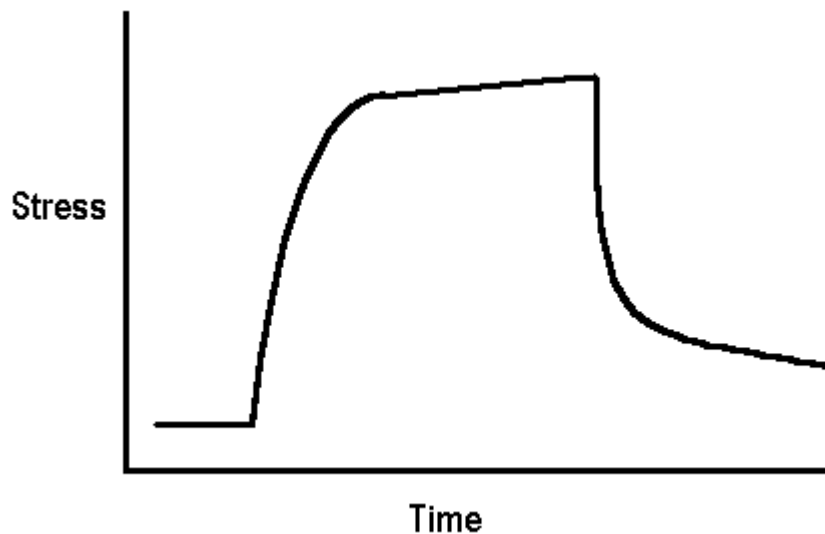


Fig 24: Creep recovery

### 2.3 Differential Scanning Calorimeter

Differential scanning calorimetry (DSC) is a technique that is used to evaluate changes in materials heat capacity and temperature associated with a materials transitions as a function of time and/or temperature. Qualitative and quantitative data on endothermic and exothermic processes of materials during physical transitions caused by phase change, melting, oxidation, and other heat related changes can be evaluated with a DSC. A DSC analysis of a polymer allows the determination of the glass transition( $T_g$ ), melting point( $T_m$ ), melting peak enthalpy, and heat capacity among other things. This information can be used to determine the appropriate processing temperature of the polymer, the identity of an unknown sample, and prove differences between dissimilar materials.

There are two basic types of DSC units on the market today. They are the Quantitative DTA(also called the Heat-flux DSC) and the Power Compensated DSC. The difference between these two types of DSC is in their heater, thermocouple, and the measured data.(4) In Heat-flux DSC, temperature difference between the sample and the reference is measured. Energy required to maintain equal temperatures between the sample and the reference is measured in the Power Compensated DSC. These will both be described next. It depends upon who you ask that determines which type is better. They both have a maximum sensitivity of  $35\mu\text{m}$ .(4) In the following evaluations, a Heat-flux DSC will be utilized.

The Heat-flux DSC is a term used to describe Quantitative Differential Thermal Analysis (DTA) instruments. Heat-flux DSC measures the temperature difference

between the sample and the reference at controlled temperature conditions. This difference in temperatures is proportional to heat flux. The evaluation can be performed as a function of temperature or time. Fig 25 shows a schematic of the Heat-flux DSC. The sample and the reference sit on a raised platform on the heat sensitive plate. This heat sensitive plate acts as the primary source of heat transfer between the furnace and the sample. Thermocouples are attached to both the sample and reference holder bases, furnace, and the heat sensitive plate. Generally, as the experiment is performed, the resultant differential heat flux to the sample and reference is monitored. During a transition, this difference in heat flux is measured between the temperature sensitive disc and the furnace.

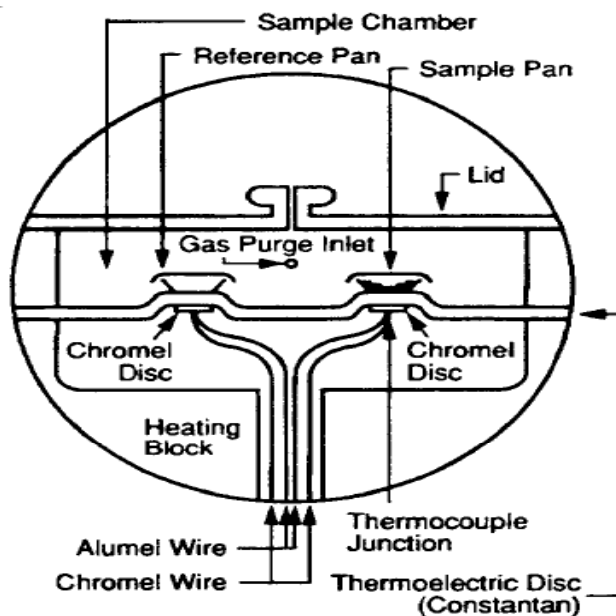


Fig 25: Heat flux DSC(Diagram Copied with permission of TA Instruments) (5)

Typically Heat-flux DSC instruments can be utilized up to 1000K. The maximum sensitivity of a Heat-flux DSC is 35 $\mu$ m. For maximum sensitivity, the sample evaluated

should be smaller than 10mg and be placed uniformly across the bottom of the sample vessel.

Power Compensated DSC instruments are slightly different and more expensive than the Heat-flux DSC instruments. In a Power Compensated DSC the energy input per unit time is measured as a function of temperature or time. This energy input per unit time is proportional to the heat capacity of the sample. The sample and reference holder each are equipped with a resistance sensor and a resistance heater. The heaters in the power compensated DSC are much smaller than that of a Heat-flux DSC. This allows the power compensated DSC to have a quicker temperature response than the Heat-flux DSC. Additionally the smaller furnace allows the instrument to have a higher scanning rate. Typically, a Power Compensated DSC can be utilized up to 1000K and have a sensitivity of 35 $\mu$ m.

Modulated DSC (MDSC) is a technique that can be utilized with both the Heat-flux DSC and the Power compensated DSC instruments. In MDSC, a sinusoidal temperature oscillation is overlaid on the conventional linear temperature ramp (as seen in Fig26). The modulated temperature ramp is sometimes faster and sometimes slower than the underlying linear temperature ramp. The actual variation in the modulated temperature ramp depends upon the amplitude of modulation and the frequency of modulation.

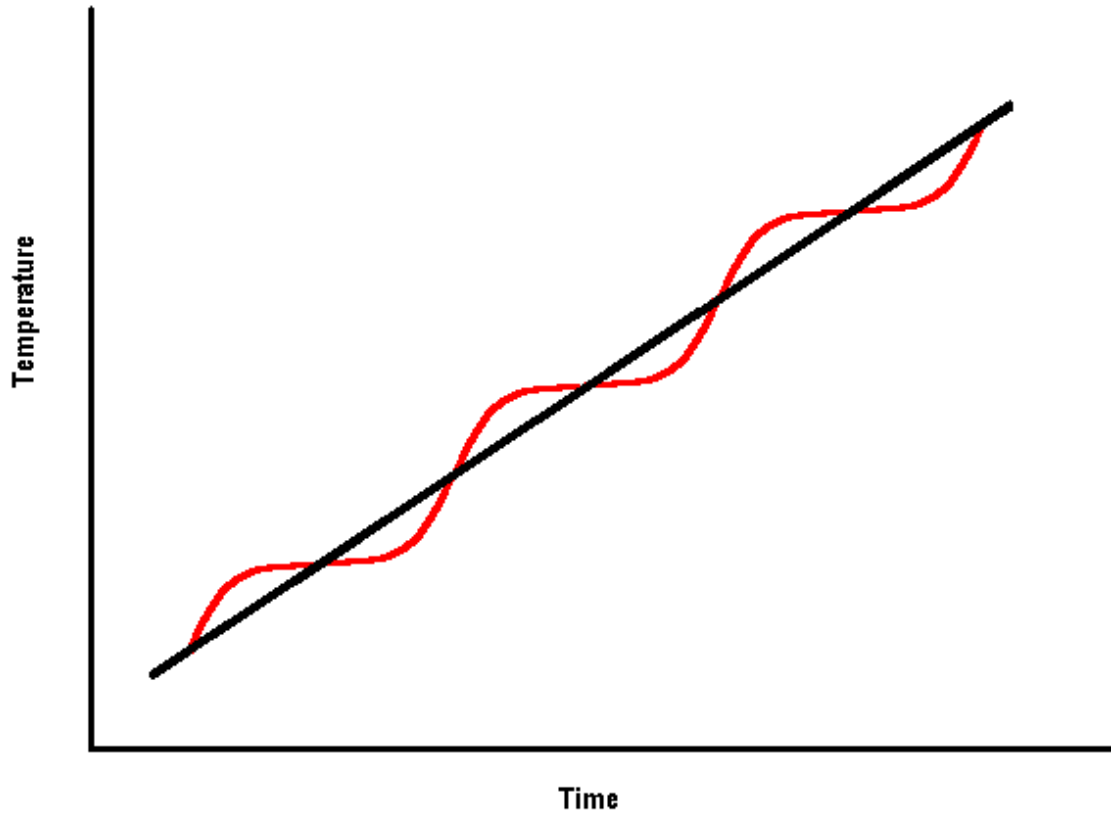


Fig 26: MDSC temperature ramp

To get a perspective on the impact the modulation creates in a Heat flux DSC the general equation describing calorimetric response needs to be evaluated. DSC heat flow can be represented as:

$$dQ/dt = C_p(dT/dt) + f(t,T)$$

(5) where:

$dQ/dt$  = Heat flow

$dT/dt$  = heating rate

$C_p$  = sample heat capacity

$t$  = time

$f(t,T)$  = a function of time and temperature which governs the kinetic response of any physical or chemical transition observed in DSC

This equation shows the total Heat-flux DSC heat flow is comprised of two components. The first one is heating rate dependent ( $C_p(dT/dt)$ ) while the second is only dependent upon absolute temperature ( $f(t,T)$ ). The heat capacity component follows the modulating heating rate thus showing the heat flow dependence of modulation. Most DSC instruments can perform MDSC; however, specific software is required to utilize this option. The limiting factor on the amount of modulation is the instrument design.

Typically the first DSC scan is representative of the quenched or processed state of the material and includes both macro(stress-induced or quenched) and micro(molecular) effects. A second DSC scan run on the same sample is representative of a stress relieved or annealed state which is a better indicator of the material “molecular state” where processing or macro-effects have been removed. If the evaluation is concerned with the state the material is in before the evaluation, the first run is of more interest. With this first run, molded in stresses, crystallinity, degradation, and compatibility of blended materials can be studied. The second run becomes of more interest when the materials properties without any outside effects are required. The properties desired could be as simple as the materials glass transition or melting temperature or it could be in depth like determining the component percentages in a blend.

A generic DSC curve of a semicrystalline material is shown in Fig 27. In this plot exothermic is in the up direction. As you can see because this is a semicrystalline material it has both amorphous (glass transition,  $T_g$ ) and the crystalline (melting point,  $T_m$ ) characteristics. In this plot, the glass transition midpoint is given as 92.78 °C. This

plot shows that this material has a peak melting point of 221.70 °C. Also, the melting enthalpy in this plot is 23.88 J/g. This plot only shows the heating portion of the plot.

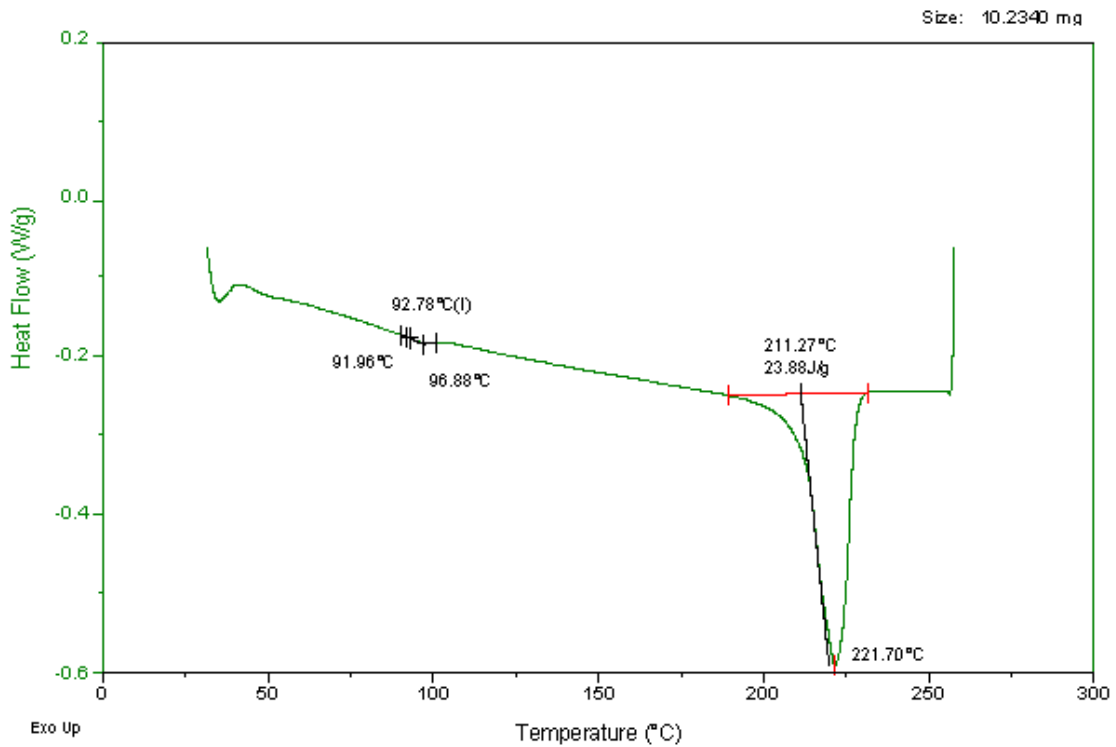


Fig 27: DSC plot of a semicrystalline material

There are many factors that affect a DSC evaluation, a few follow. Generally increasing the size of a sample will increase its transition temperature. This is due to increased temperature gradient created by increasing the sample size. Increasing the heating rate of a sample usually increases its observed transition temperature. This increase in transition temperature occurs because there is a temperature lag between the heater and the sample. The instrument is recording data at a temperature that is different than the sample temperature. Also, the height of the transition and the melting peak area

increase with increasing scanning rate. If the heating rate and the sample size is excessively large the sample can produce several transition temperatures for a single thermal process. Figures 28 and 29 represent these effects.

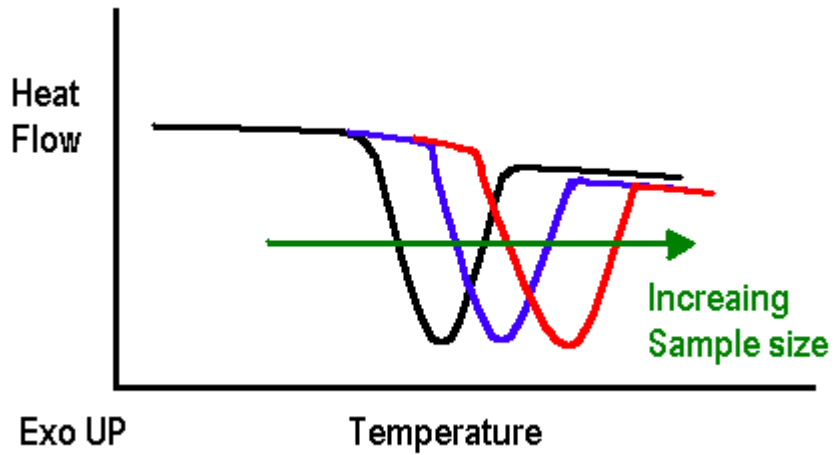


Fig 28: Effect of Sample size on transition temperature

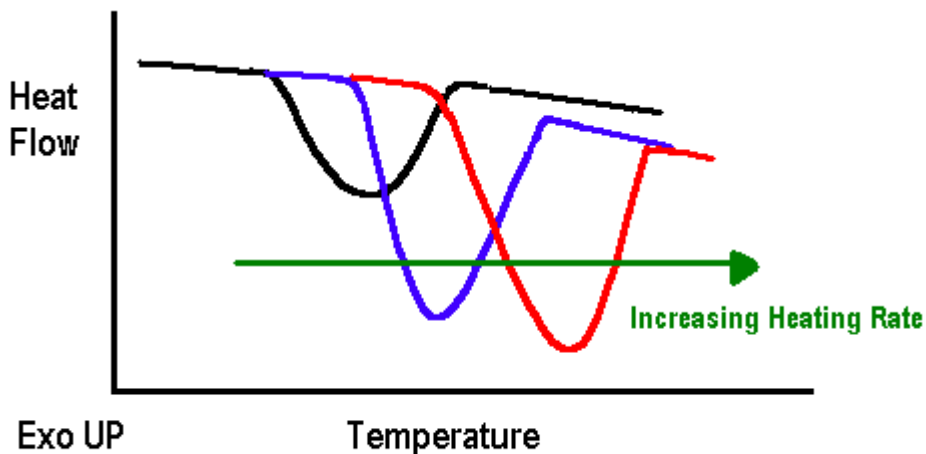


Fig29: Effects of heating rate on transition temperature

There are many uses of a DSC from incoming inspection to the use as a research tool. DSC scans can show the presence of impurities (different species melting points or Tg's), degree of cure, volatiles, material crystallinity, heat capacity, and many other characteristics. Combined with Fourier Transform Infrared Spectroscopy (described later) DSC can help identify a material's base polymer composition. For instance, DSC can aid in determining if a material is a blend or a copolymer. Thermoset curing can be evaluated on a DSC by following the heat flux through a temperature ramp or temperature step cure profile. This can be useful in determining the amount of cure in various curing profiles for optimization. The presence of volatiles can be seen through an endothermic baseline deviation of a sample's first run. This would be absent in the second run. The crystallinity of a polymer can be estimated using DSC analysis. The

crystallinity( $X_c$ ) of the polymer is the ratio of the polymers measured enthalpy of melting( $\Delta H$ ) to that same polymer at 100% crystallinity( $\Delta H_{100}$ ) as follows:

$$X_c = \Delta H / \Delta H_{100} \quad (4)$$

For most samples  $\Delta H_{100}$  is not available so it is replaced in the above formula by the enthalpy of fusion per mole of chemical repeating units ( $\Delta H_u$ ). (4) This enthalpy of fusion is calculated using Flory's relation for the equilibrium melting temperature ( $T_m^0$ ) depression due to low molecular mass diluent as follows:

$$1/T_m - 1/T_m^0 = (R / \Delta H_u) (V_u / V_1) (v_1 - x_1 v_1^2) \quad (4) \text{ where}$$

$T_m$  = melting temperature of the polymer–diluent system  
 $V_u$  = molar volume of the repeating unit  
 $V_1$  = molar volume of the diluent  
 $v_1$  = volume fraction of the diluent  
 $x_1$  = thermodynamic interaction parameter

The heat capacity of a polymer can be determined in both the heat flux DSC and the power compensated DSC instruments. An estimated heat capacity can be determined by comparing the samples baseline against the baseline of the DSC without any sample present. To estimate this the baseline of the DSC is obtained over the temperature range desired. The DSC must have a reference pan and an empty sample pan in place. Once this is completed, a 10 mg sample is placed in the empty sample pan previously used and it's baseline is obtained over the same temperature range. These two plots are overlaid

on a graph of Heat flow in mW on the Y-axis and Temperature in °C on the X-axis. The heat flow difference between the two baselines are taken(in mW) at a particular temperature and put into the following equation:

$$C_p = (60E/Hr)(\Delta H/m) \quad (5) \quad \text{where}$$

$C_p$  = heat capacity of the sample (J/g°C)  
 $E$  = cell calibration coefficient @ Temp. of interest  
 $Hr$  =heating rate of the two plots (°C/min)  
 $\Delta H$  = change in heat flow between the sample and blank baselines (mW)  
 $m$  = sample mass (mg)

The term (60E/Hr) is constant under a specific experimental conditions. This term converts the heat flow difference into units of J/g°C. To obtain a more accurate heat capacity measurement of a sample this term can be more accurately determined by running a reference material and using it's  $\Delta H$ ,  $m$ , and  $C_p$  to solve for (60E/Hr).

## 2.4 Thermomechanical Analysis

Thermomechanical analysis (TMA) measures the change in dimension of a material with respect to time and or temperature. The TMA instrument is similar to a precision caliper inside an accurate oven. Micrometer changes in dimensions can be evaluated throughout a TMA run. Typically a TMA evaluation is over a temperature range. The sample is placed in the TMA and heated at the required heating rate to the maximum temperature. Once the sample temperature reaches the maximum temperature, the sample is usually cooled at a preset cooling rate to the final temperature. Throughout

this entire cycle the materials dimensions are recorded. Usually a set of TMA scans consists of two heat up and two cool down portion. Each of these runs give different data to the operator. The first scan reveals any molded in stresses. The second scan will give a smoother curve representative of the molecular state effects. A cross cut section of a TMA is seen in Fig 30 Here the furnace, sample stage, thermocouple, and expansion probe can be seen. As the sample expands, the probe is pushed up and the dimension change is recorded with respect to time and/or temperature.

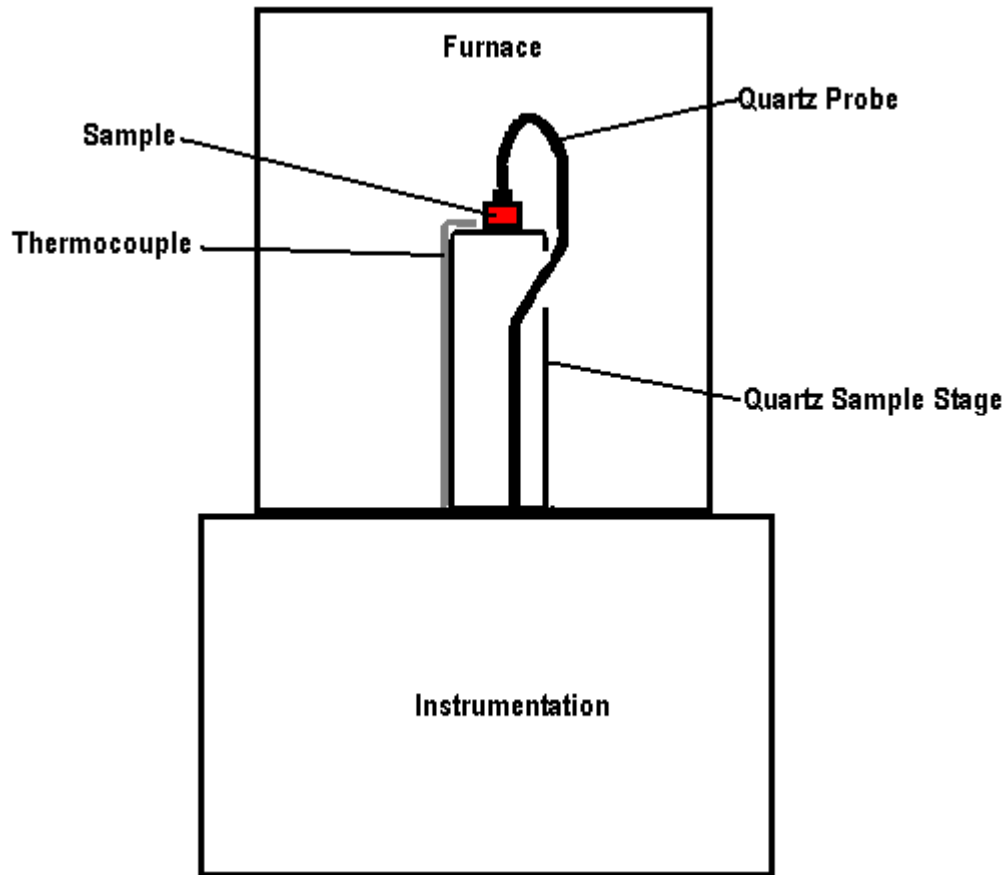


Fig 30: Diagram of TMA

The expansion of the material is caused by the increase in free volume of the sample. As the sample is heated the free volume within the sample expands. This rate of expansion is usually linear and is called the thermal expansivity. Once the temperature reaches the glass transition region there is a change in slope of thermal expansivity. After the glass transition there is a larger increase in free volume with respect to temperature and hence a larger chain mobility

TMA curves provide several different types of material properties. From a TMA curve, melting temperature, glass transition region, thermal expansivity, mold shrinkage, estimated percent filler, anisotropy index, and maximum useful temperature among other properties can be determined. Fig 31 is a TMA scan of the second heat of a thermoset material. In this figure, there are two distinct thermal expansivity values. The region of transition between these two slopes is the glass transition region. A glass transition, in TMA, is characterized by a change in slope, usually with the higher temperature slope being larger. The glass transition region in this figure is from 110 – 125 °C with a midpoint (usually called the glass transition) at 118 °C. The thermal expansivities of the upper and lower regions are 186 and 52  $\mu\text{m}/\text{m}^\circ\text{C}$  respectfully. The application of this thermoset is a rigid adhesive. From this TMA graph, it can be seen that the operational range of this material is below approximately 110°C.

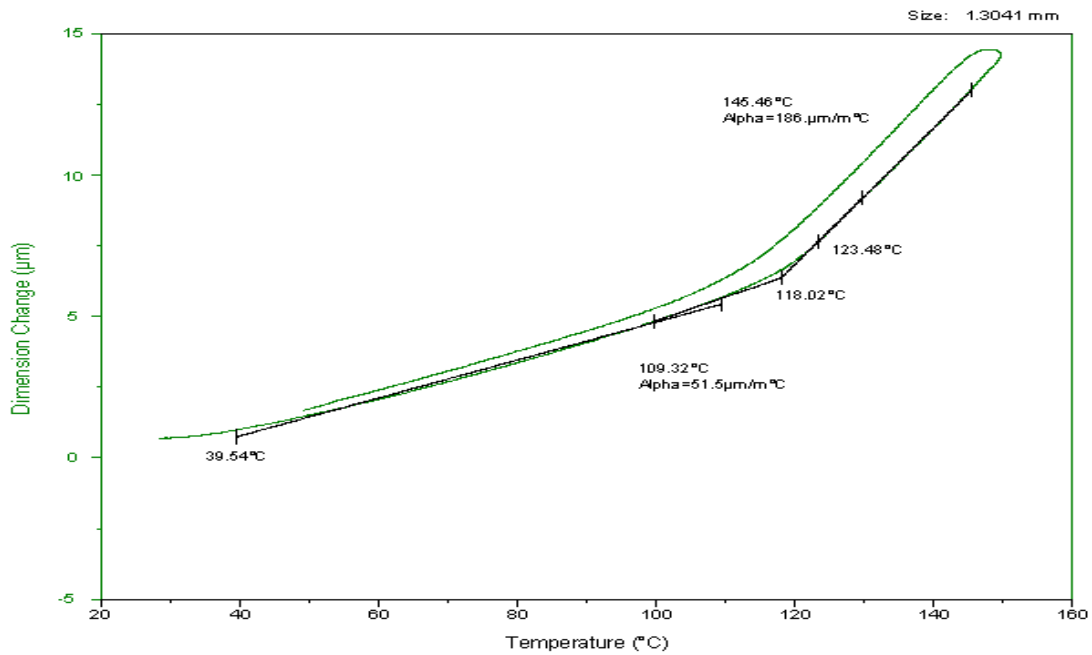


Fig31: TMA plot of a thermoset material

The melting temperature of a material can also be determined with a TMA; however, other methods are usually recommended due to the cleanup involved after melting a material in a TMA. A melting point, in a TMA, is characterized by a monotonic slope followed by a drastic decrease in sample dimension (usually to zero). Fig 32 is a scan of a melt represented on TMA. It can be seen that approximately 171°C is the onset of the melting temperature.

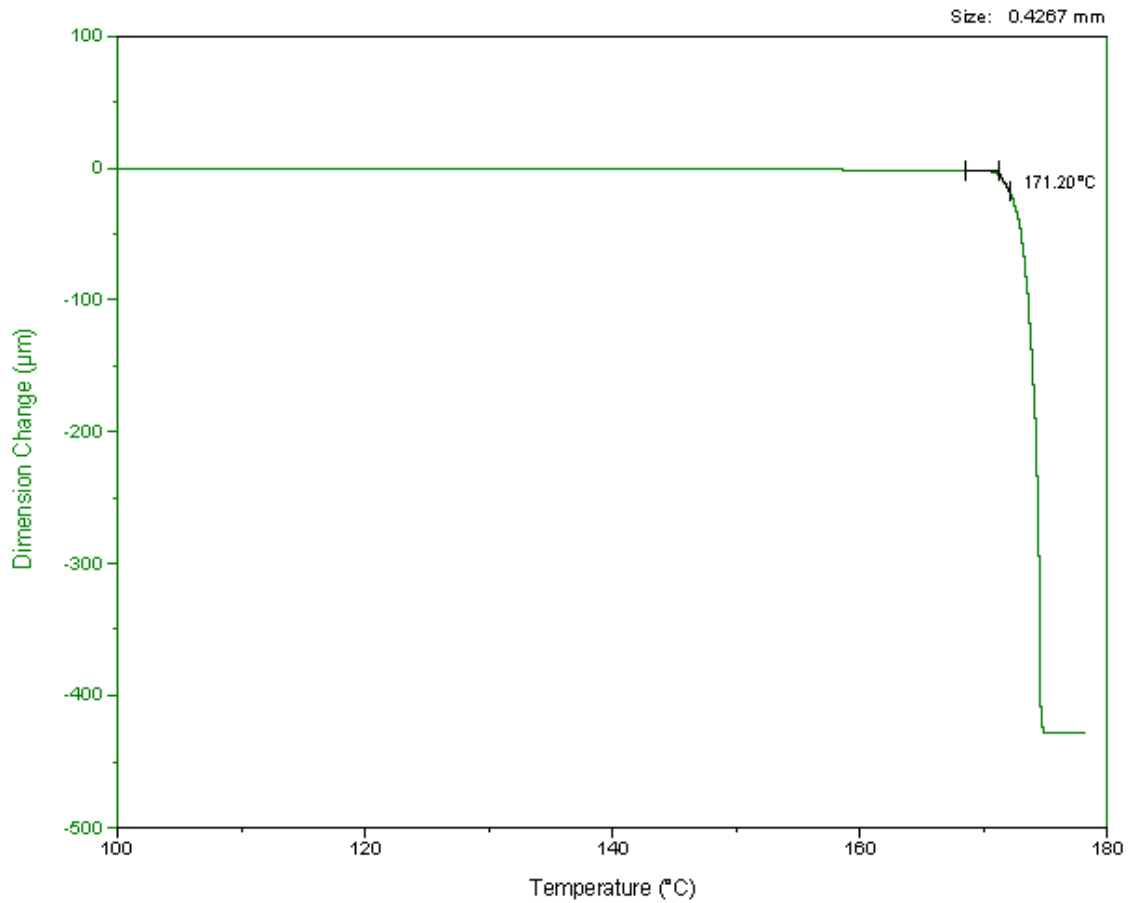


Fig 32: Melting point analysis on a TMA

The most widely used data obtained from a TMA is the material's thermal expansivity. Thermal expansivity is sometimes called coefficient of thermal expansion; however, this terminology is incorrect and the term thermal expansivity will be used.

Thermal expansivity( $\alpha$ ) is given by the following formula:

$$\alpha = (\Delta L / \Delta T)(1/L_0) \quad \text{where}$$

$\alpha$  = thermal expansivity  
 $\Delta L$  = change in linear dimension  
 $\Delta T$  = change in temperature  
 $L_0$  = initial dimension of the sample

This gives the linear thermal expansivity. Thermal expansivity can be used to see if materials will be compatible throughout a temperature range. The thermal expansivities become extremely important for compatibility in layers of a laminate.

The volumetric thermal expansivity ( $V\alpha$ ) can be calculated by adding the thermal expansivities of the three principle directions as follows:

$$V\alpha = \Sigma\alpha's$$

Using the linear and the volumetric thermal expansivity, the materials Anisotropy Index can be determined. The Anisotropy Index (AI) is a measure of the materials uniformity. Anisotropy Index is a ratio of the largest difference in thermal expansivities to the volumetric thermal expansivity as follows:

$$AI = (\alpha_{\max} - \alpha_{\min})/V\alpha$$

Where  $\alpha_{\max}$  is the maximum thermal expansivity and  $\alpha_{\min}$  is the minimum thermal expansivity. The closer the anisotropy index is to zero the more uniform the materials properties become.

The mold shrinkage of a material is the opposite of the thermal expansivity. Instead of expanding with increasing temperature, the sample is shrinking with decreasing temperature. For instance, the linear thermal expansivity of a material is  $30 \mu\text{m}/\text{m}^\circ\text{C}$ , this means that the sample will increase in linear direction  $30 \mu\text{m}$  per meter of sample thickness per degree C. So for this particular sample, this linear dimension would decrease  $30 \mu\text{m}$  per meter of sample thickness per degree C decreased.

An estimation of the percent of a known filler can also be performed utilizing a TMA. For this estimation the following formula is used:

$$P_1c_1 + P_2c_2 + P_3c_3 + \dots = \text{property}$$

In this formula P represents the property of the individual component and c represents the percentage of the component. Therefore, the sum of the properties times their percentages gives the property of the composite. For example, if we have a polymer composite with a thermal expansivity of  $40 \mu\text{m}/\mu\text{m}^\circ\text{C}$  and we know the base polymer has a thermal expansivity of  $70 \mu\text{m}/\mu\text{m}^\circ\text{C}$  and the filler is a glass with a thermal expansivity of  $10 \mu\text{m}/\mu\text{m}^\circ\text{C}$ . Then we know that there is 50% glass in our polymer.

$$P_1c_1 + P_2c_2 = 40 = 70(0.5) + 10(x)$$

Many factors affect the properties seen in a TMA graph. The percent and type of filler can have profound effects on the thermal expansivity of a material as seen in Fig 33.

Here the increasing glass filler percentage is decreasing the thermal expansivity of the composite.

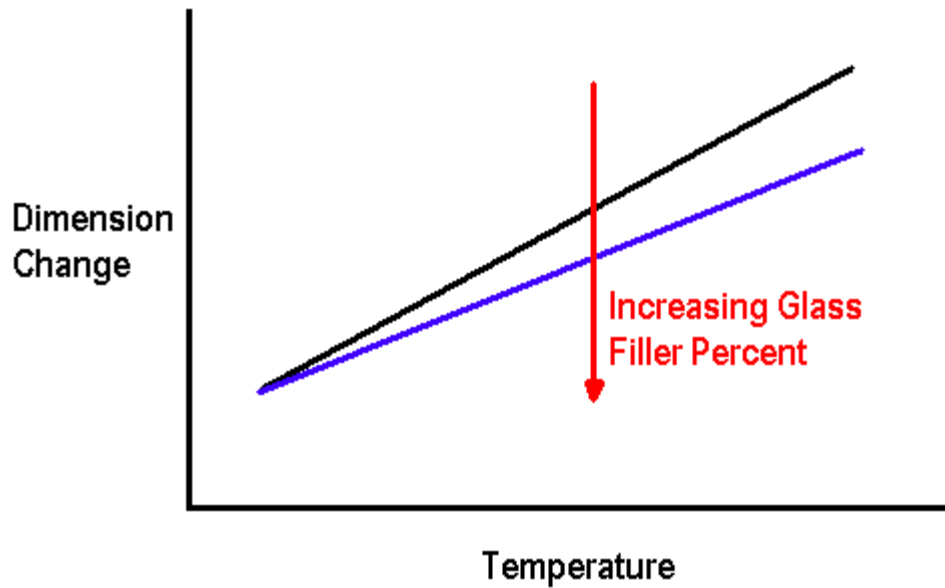


Fig 33: Increasing glass filler decreases a materials thermal expansivity

The percent cure of a thermoset can change both the thermal expansivity of the material and the glass transition midpoint. As the thermoset becomes more cured, the thermal expansivity decreases while the glass transition midpoint increases. This is due to the uncured thermoset being in the amorphous state while the cured thermoset is in the crystalline state. A crystalline material generally has a lower thermal expansivity than an amorphous material. This is because the structure of a crystalline material is more rigid than that of an amorphous material and there is a smaller increase in free volume with

increasing temperature. The glass transition midpoint increases because as the material becomes more crystalline it requires more energy for the glass transition to occur. These phenomenon can be seen in Fig 34.

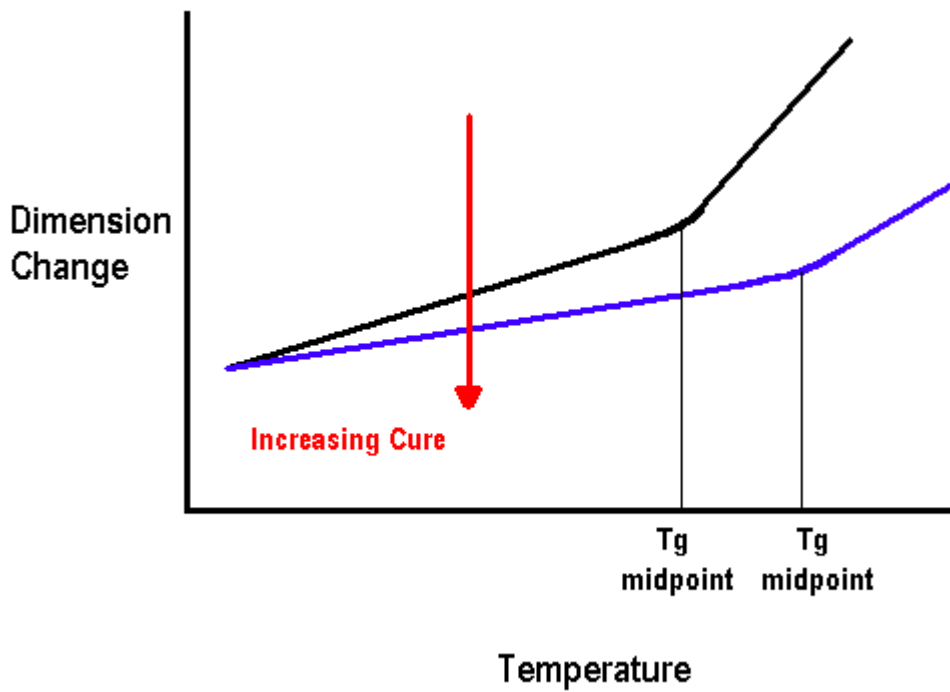


Fig 34: Effects of increasing a TS cure

The molecular weight of the base polymer has a large affect on the shape and position of the TMA curve. An increased molecular weight in a polymer requires more energy to cause a glass transition; therefore, an increase in molecular weight would increase the glass transition region. This molecular weight changes can be seen in Fig 35.

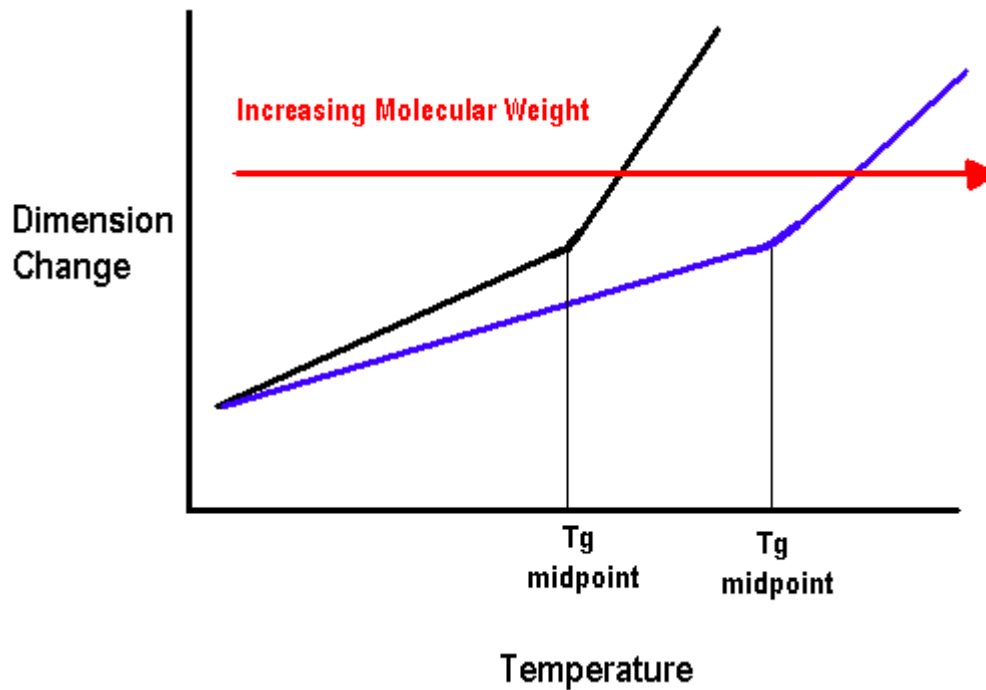


Fig35: MW effects on Tg

If we were to take linear and branched polyethylene (PE), we would see that below their melting points the branched polyethylene has a larger thermal expansivity. This is due to the free volume change in these materials. Linear PE is denser than branched PE, this causes the branched PE to have the larger thermal expansivity. Also, as the melting

temperature is passed the linear PE has a much narrower transition than the branched PE. The deviations in TMA results caused by the branching in the PE can be seen in Fig 36.

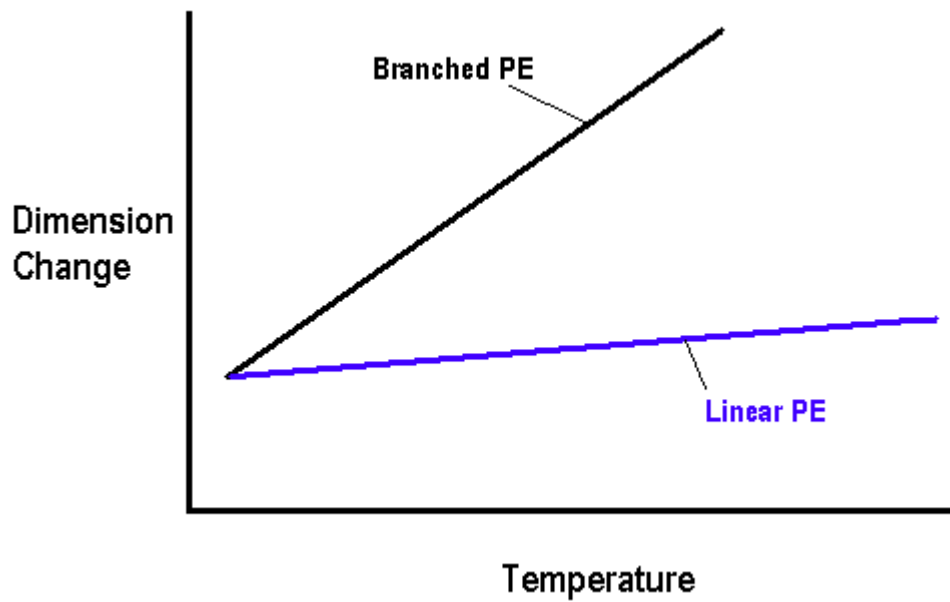


Fig 36: Linear and branched PE

## 2.5 Thermogravimetric Analysis

Thermogravimetric Analysis (TGA) gives you the ability to analyze a material's weight with respect to time and/or temperature. Using these features, the material's degradation kinetics, percent carbon, and percent inorganic filler contents can be evaluated. Generally, TGA can detect phase changes due to decomposition, oxidation, or dehydration. Utilizing different purge gasses can give the operator the ability to analyze the material in different environments.

The TGA is basically a micro-balance within a high precision furnace. A cross section of a TGA is given in Fig 37. In this figure, the heater core, water jacket, thermocouple, sample pan, hang-down wire, counter weights, and micro-balance electronics are seen. The heater core is the component that heats the sample. The heater core is made out of ceramic. The water jacket is used in combination with the heater to maintain a particular temperature and to heat-up and cool-down at the prescribed rates. The thermocouple determines the temperature inside the heater core. It is important that the thermocouple is in extreme close proximity with the sample to have an accurate sample temperature. The sample pan holds the sample during the evaluation. It must not be included with the sample weight or the results will be incorrect. Sample pans can be made of several different materials including aluminum, platinum, and ceramic. The sample pan used for an evaluation is primarily regulated by the maximum temperature of the evaluation. The sample pan is attached to the hang-down wire that is attached to the micro-balance electronics. In a balance the counter weights are used to offset the sample

weight. The counter weights are located on the opposite side of the electronics from the sample.

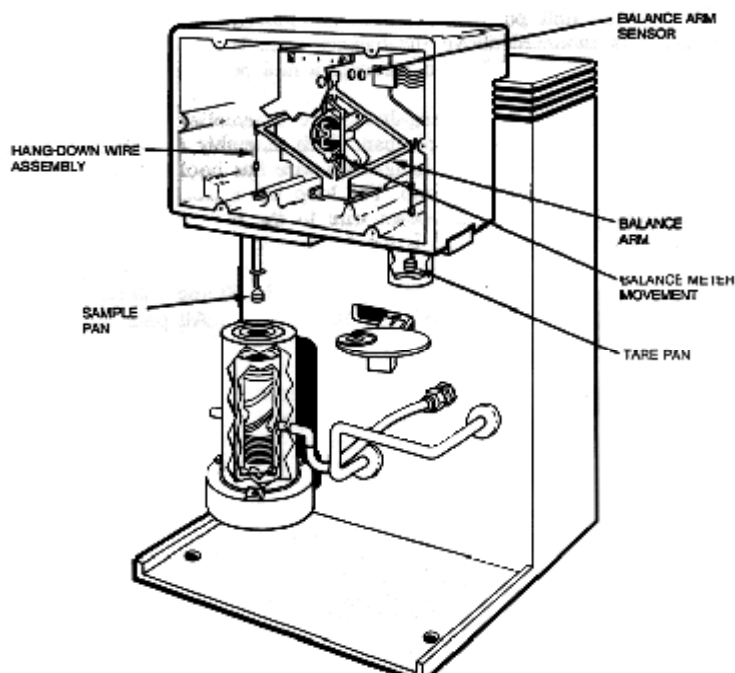


Fig 37: TGA cross section(Copied with permission of TA Instruments) (6)

TGA is extremely useful for evaluating a materials thermal decomposition. However, these thermal decompositions can be long and drawn out or they may overlap with other decompositions. Therefore, it is extremely important to have a TGA instrument capable of producing a high resolution plot of thermal decompositions to be able to distinguish between different transitions.

The TGA instruments have evolved to try to address the high resolution issue. There are four main types of methods that have been used for high resolution TGA

experiments. The first is the controlled heating rate. To increase the resolution of the data the heating rate is set at an extremely low heating rate. This type of experiment is extremely slow and can have adverse effects possibly oxidizing the sample. A second method is an increased heating rate with an isothermal period at the onset of decomposition. At the completion of the decomposition, the sample resumes the original heating rate until the next thermal decomposition is reached. This method has the same drawbacks as the first method. The experimental time is long and the sample can undergo changes at long times in high temperatures. The third method involves a controlled heating rate by maintaining a preselected reaction rate (% decomposition/min). This method can have very slow or even negative heating rates. The experimental time and the effects of long times at high temperature still are the major issues with this method. The fourth method addresses the issues with resolution and increased time. This method called Dynamic Rate TGA (DRTGA) has a heating rate that is dynamically and continuously modified in response to the rate of decomposition to maximize the resolution of the sample weight change. This method allows for a higher heating rate while avoiding transition overshooting. It also avoids the effect of long times at high temperatures. This method is basically a combination of the second and third methods above. It involves an increased heating rate with a dynamically controlled heating rate to maintain the preselected reaction rate (% decomposition/min) at transition regions. In this method, as the reaction rate increases the heating rate decreases and vice-versa. These heating rates can be seen in Fig 38. Plot 1 represents the constant heating rate of 5°C/min, plot 2 represents the increased heating rate (50°C/min) with isothermal periods,

plot 3 represents the controlled heating rate by preselected a reaction rate, and plot 4 represents the DRTGA with a heating rate of (50°C/min).

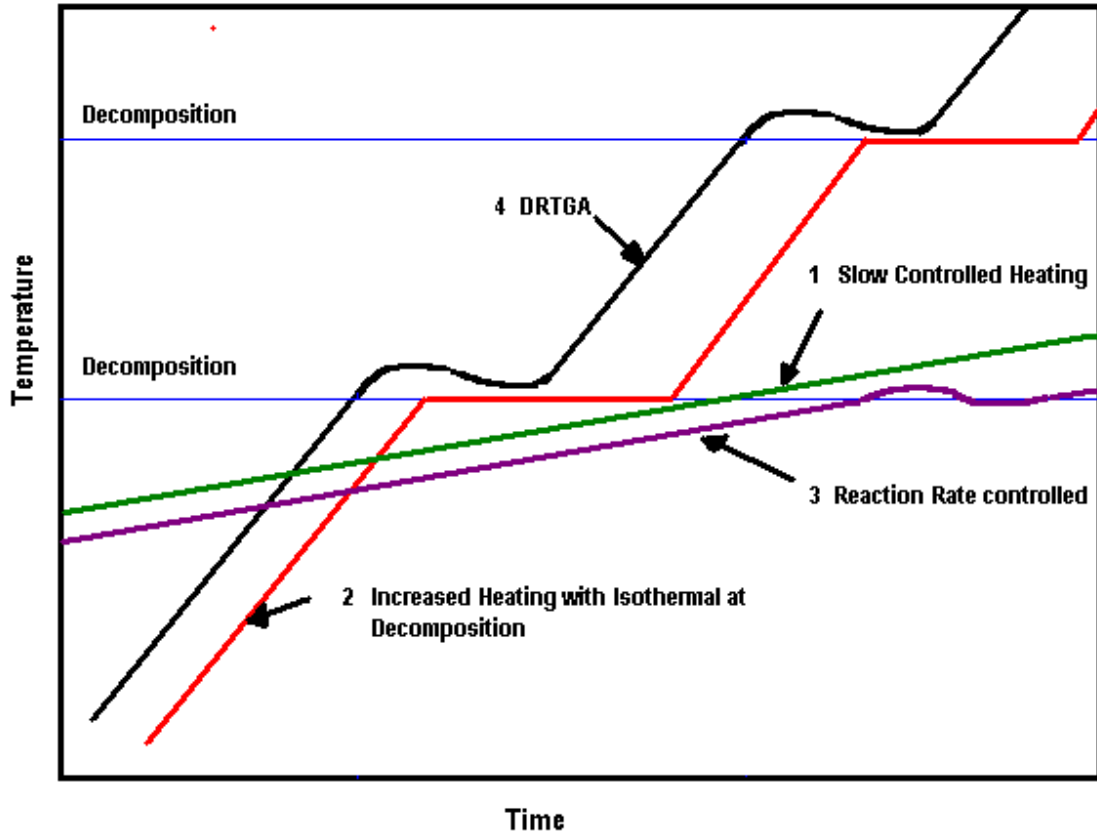


Fig 38: Types of TGA heating rates

Purge gasses are important in a TGA instrument. There are two purge gasses on a TGA. The first purge gas is in the micro-balance compartment. This purge is usually an inert dry gas that is used to protect the micro-balance. The second purge flows into the sample compartment. This gas can vary depending upon the application. Typically a dry air purge gas is utilized to simulate normal processing conditions or to determine the

percent inorganic filler. Other gasses used in the sample compartment purge include nitrogen, argon, and oxygen. The purge gas flow should remain constant during an experiment and should always be constant with the calibrated flow. A change in the flow of the purge gas can change the convection currents and change the sample heating rate.

A typical TGA curve is shown in Fig 39. This curve was created in an air environment. This graph can be used to determine the initial degradation temperature, hence the maximum operating temperature for this material, and the percent inorganic filler. In this graph, it can be seen that the maximum manufacturing temperature is approximately 260°C. It can also be seen that there is approximately 20% inorganic filler in the sample. This is seen in the 80% weight loss. After the analysis, the residue can be evaluated to determine it's composition.

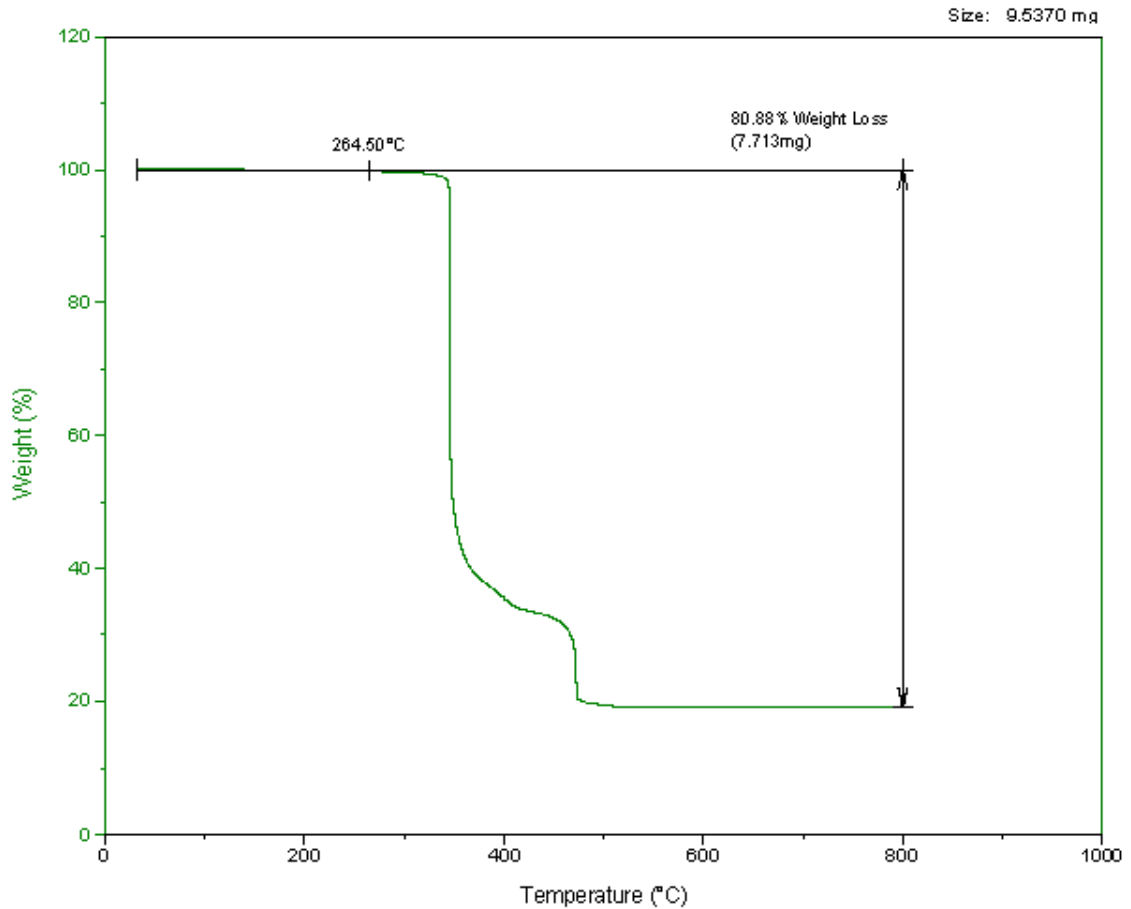


Fig 39: Typical TGA plot in air

This sample could have also been analyzed in a different manner by taking the sample to a set temperature and evaluating its weight change at that temperature vs time. This method is used to determine residence time effects on injection molded and extruded polymers and to determine the percent outgassing at processing temperatures. A typical residence time experiment is given in Fig 40. It should be noted that this plot is weight vs time and not weight vs temperature like in the previous plot. This evaluation was performed in air.

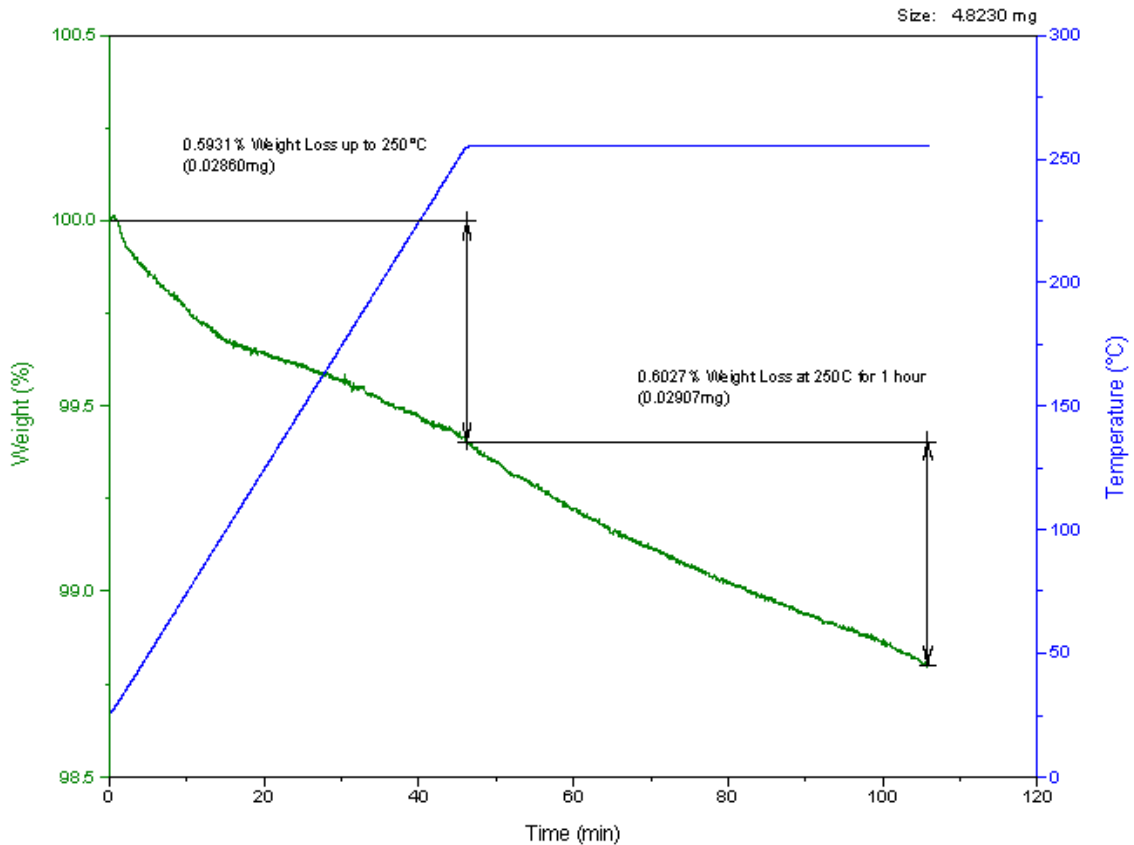


Fig 40: Resonance time effects in TGA

Some TGA evaluations may require the sample purge gas to be changed during the experiment. There are many reasons for this including composition ratio determination and curve characteristic comparisons. These gas switching experiments generally involve heating the sample to a temperature destination in one gas and once this temperature is reached and the weight has equilibrated the purge gas is changed to the second gas. There are two ways to analyze these plots. They can be analyzed on a

weight vs temperature or a weight vs time scale. To get the most information out of one of these plots the weight vs time scale should be used. This plot will give you a distinct break in between the two different gasses. A plot of a gas switched TGA experiment is seen in Fig 41. The upper portion of this plot was performed in nitrogen and the lower portion was performed in air. The gas switch was performed at 800°C. It is important during the gas switch that the gas flow remain constant to minimize the change in convection currents.

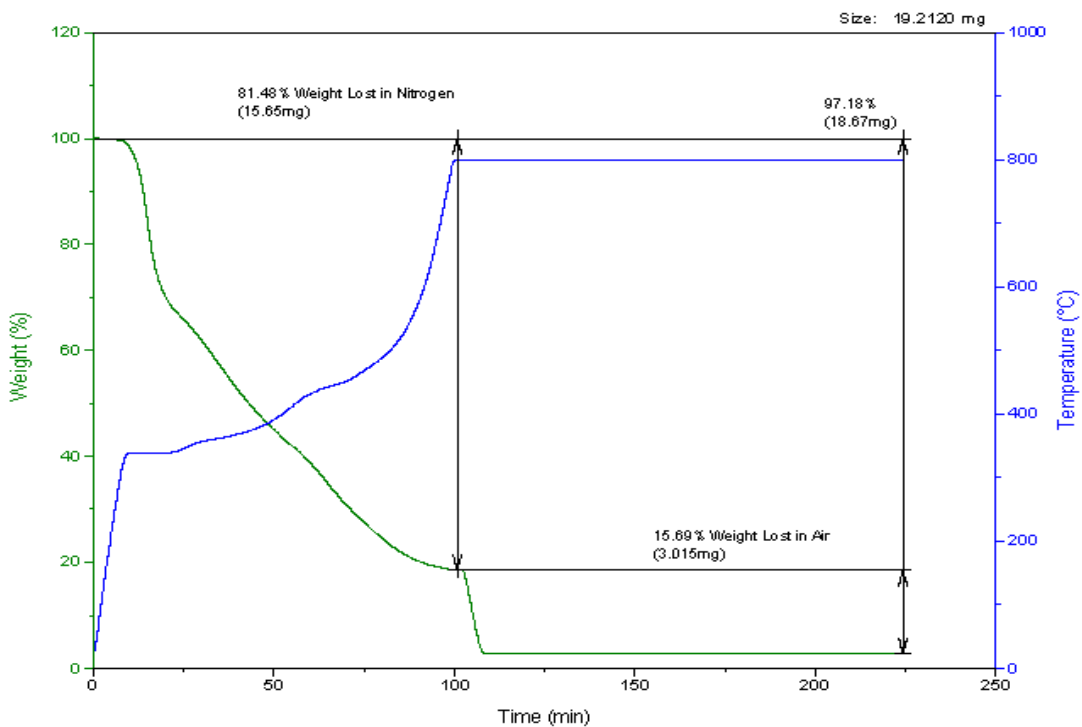


Fig 41: TGA gas switch (N<sub>2</sub>- Air)

There are many factors that effect the results and data obtained from a TGA evaluation. The method used in the experiment must correlate with the calibration methods used. The portions of the method that have the largest impact on the results are

the purge gas flow, heating rate, sample size, and the buoyancy effect. If the purge gas and the purge gas flow rate are not constant and not the same as the calibration settings there can be errors in the results obtained by the TGA. These errors are caused by the change in the convection currents within the furnace caused by changing the purge gas or the purge gas flow rate. The error could be a positive or negative deviation in the sample weight and/or the sample temperature. The heating rate and sample size must be similar to the calibration parameters to ensure uniform sample heating throughout the sample evaluation. If the sample is too large or the heating rate is too fast there may be a temperature gradient through the sample which will broaden the temperature decomposition region. These will also lower the percent weight loss at a particular temperature. The buoyancy effect can be caused by the sample or the purge gas. Buoyancy effects are caused by variations in the behavior of the furnace atmosphere under different experimental conditions. If the sample changes volume during an experiment, it is susceptible to buoyancy effects. Common purge gasses have different densities caused by the instantaneous temperature and the pressure. Changing the purge gas during an experiment can change the furnace gas density and cause a deviation in sample mass.

There are many uses of TGA including incoming inspection, material processing, and sample characterization. Incoming inspection evaluations could be set up to monitor the percent glass filler in a thermoplastic resin. This is generally a straight forward experiment that involves placing the sample in an air environment, taking the initial weight, ashing the sample, and then taking the final weight. The percent inorganic filler is the weight percent left in the ash. For material processing, the TGA can be run in

isothermal mode at elevated temperatures to simulate degradation kinetics during processing. This technique is useful for simulating residence time effects during extrusion or injection molding processing. Also, the minimum degradation temperature can be determined through a thermogravimetric experiment in a dry air environment. TGA can also help to evaluate the effect of processing temperatures on different materials. This type of evaluation is commonly called “Percent Outgassing”. This is the amount of volatiles that are given off at a particular temperature. It is basically the percent weight loss at a particular temperature. These experiments are generally the same as the residence time effect experiments, but at lower temperatures. These experiments are used to determine what the effect of an epoxy curing temperature would have on a polymer substrate while residence time effect experiments are interested in the polymer processing temperature and the polymer molten state.

An additional experiment commonly performed on a TGA involves oxidizing metals to determine metal-scale adhesion and estimate Pilling-Bedworth ratios (PBR). The PBR is the ratio of the volume of the metal oxide to the volume of the metal. This is performed by acquiring a sample and determining its mass and surface area. The sample is then suspended from the micro-balance inside the TGA furnace. The sample has a purge gas over it that allows for the oxidation of the sample. The sample is heated and cooled and a plot of the change in mass per unit area versus time is produced. The general oxidation plot is seen in Fig 42. In this plot the linear region of the oxidation is dominated by the kinetics of the reaction. Once this plot deviates from the linear region the oxidation is dominated by the kinetics of diffusion.

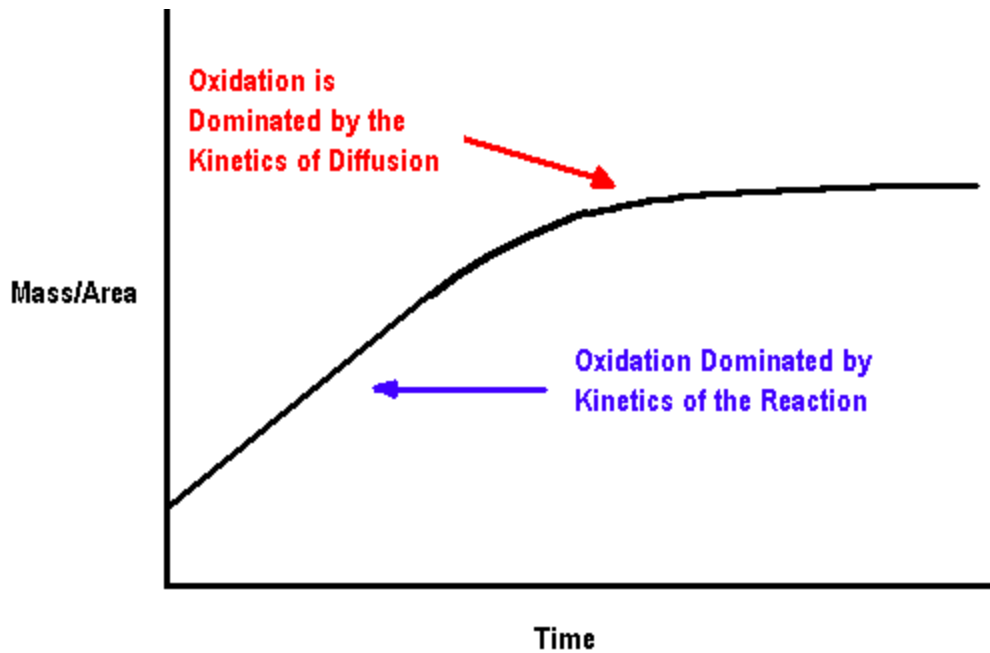


Fig 42: General oxidation plot.

To estimate if the sample has a good PBR, the sample is thermally cycled. The sample is heated to a specific temperature then cooled and then repeated several times. If the PBR is between 1 and 1.75 the plot will look like the previous plot. The plot will level off and then remain constant. However, a PBR of less than 1 will have tensile stresses that cause cracking and the oxide will spall off.(7) If the PBR is larger than 1.75, the compressive stresses will cause the scale to fail (crack).(7) These two types of scale failure and PBR estimations can be seen in Figures 43 and 44.

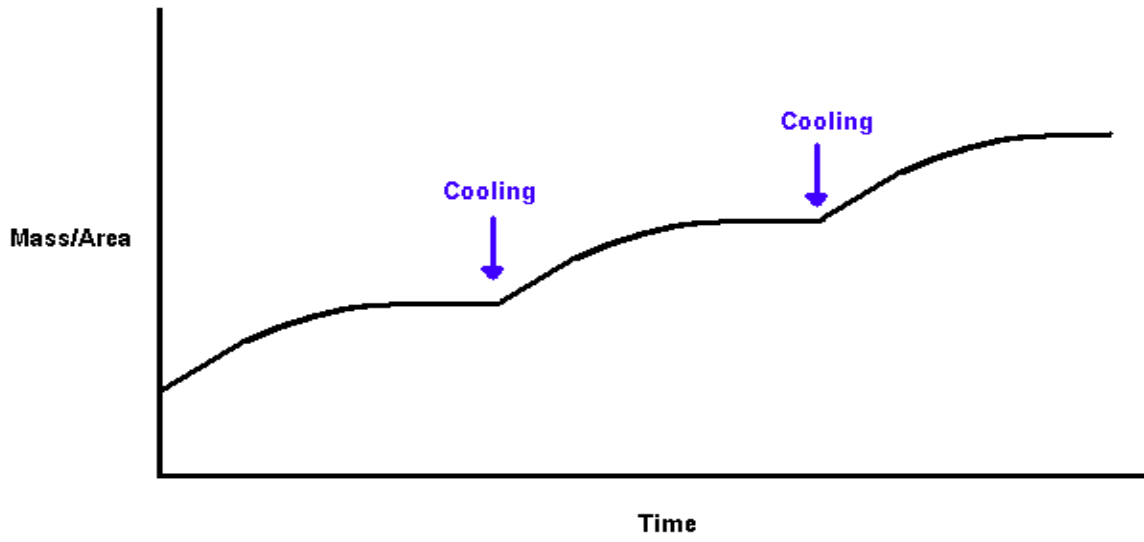


Fig 43:  $PBR > 1.75$  – scale cracking

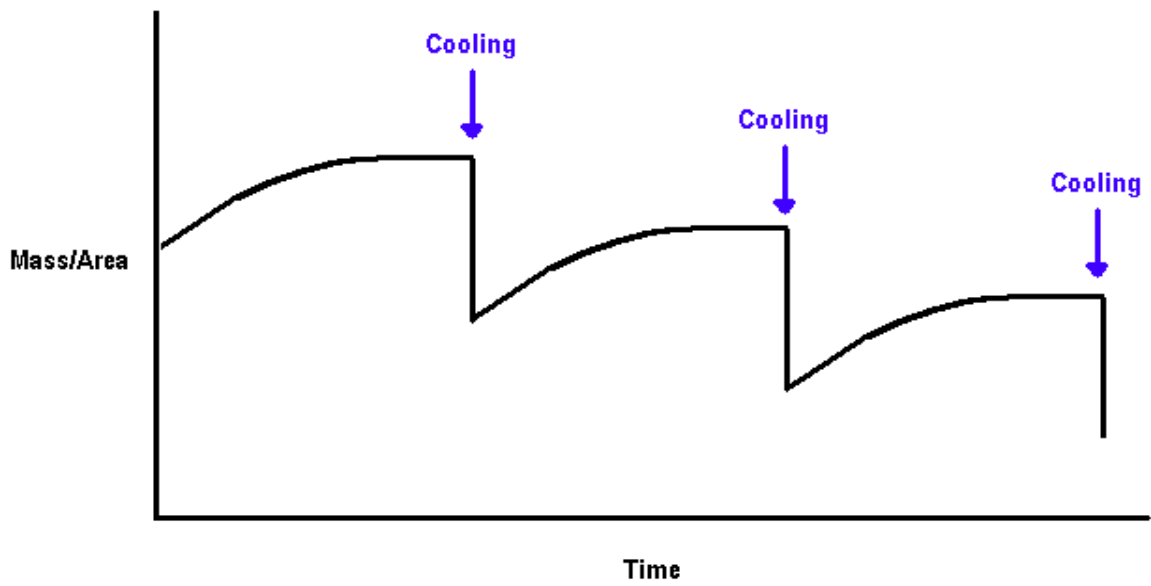


Fig 44:  $PBR < 1$  – scale spalling off

It can be seen in the first figure that upon cooling the scale cracked and remained on the sample surface. This causes the additional increase in weight change per unit area after the sample is heated for the second and third time. This material could be estimated to have a PBR of greater than 1.75.

The second figure shows a material with a PBR of less than 1. This can be seen in the negative weight change per unit area upon cooling of the sample. This is the scale spalling off. Upon heating for a second time, the sample again follows the original oxidation plot.

## 2.6 Dielectric Analysis

Dielectric Analysis (DEA) measures the capacitive and conductive components of a material as a function of time, temperature, and frequency. The capacitive component represents the materials ability to store electrical charge. The conductive ability of the material is the ability to transfer the electrical charge. With this capability, the DEA can analyze the electrical properties of a solid material, determine which material is better suited for an ultrasonic welding application, or optimize a thermoset's cure profile.

There are two basic types of DEA setups. The first, and most commonly used, is the parallel plate capacitor setup. This setup evaluates solid materials electrical permittivity and dissipation. This setup is based on a parallel plate capacitor, as the name implies. The sample setup involves placing a sample of 2.54 cm in diameter in between two platinum and gold conductive plates. The sample is placed in an inert purge gas and the temperature can be ramped or maintained isothermally as the experiment requires.

The testing frequency can also be changed. The second setup is designed for liquid samples. In this setup the liquid sample is placed on a ceramic, gold, and platinum plate and an aluminum plate is pushed down on to the liquid to form a uniform sample thickness. The sample is also placed in an inert environment while the temperature is ramped or maintained isothermally as required. The frequency in this setup can also be changed. Fig 45 is a diagram of the parallel plate setup for DEA. In Fig 46 a diagram of the single plate setup is shown. In this figure, the left diagram is the ram head that presses down on the sample. The right diagram is the liquid sample holder. These two diagrams are not to scale.

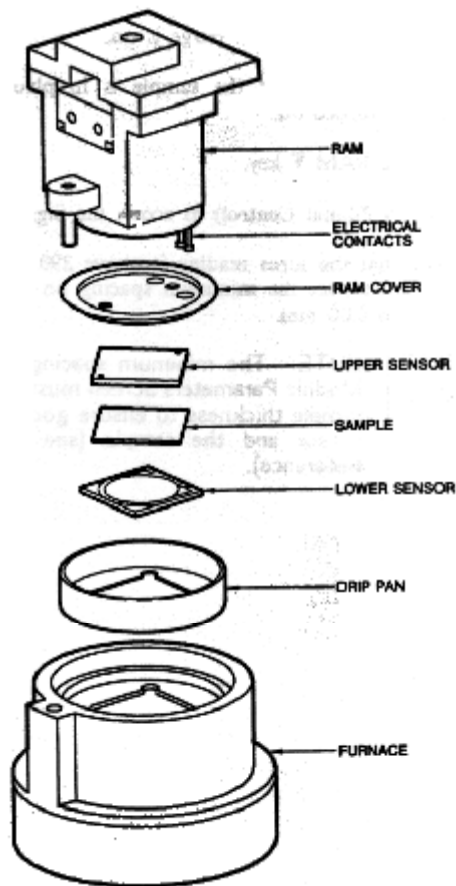


Fig 45: Parallel Plate capacitor of DEA(Copied with permission of TA Instruments) (8)

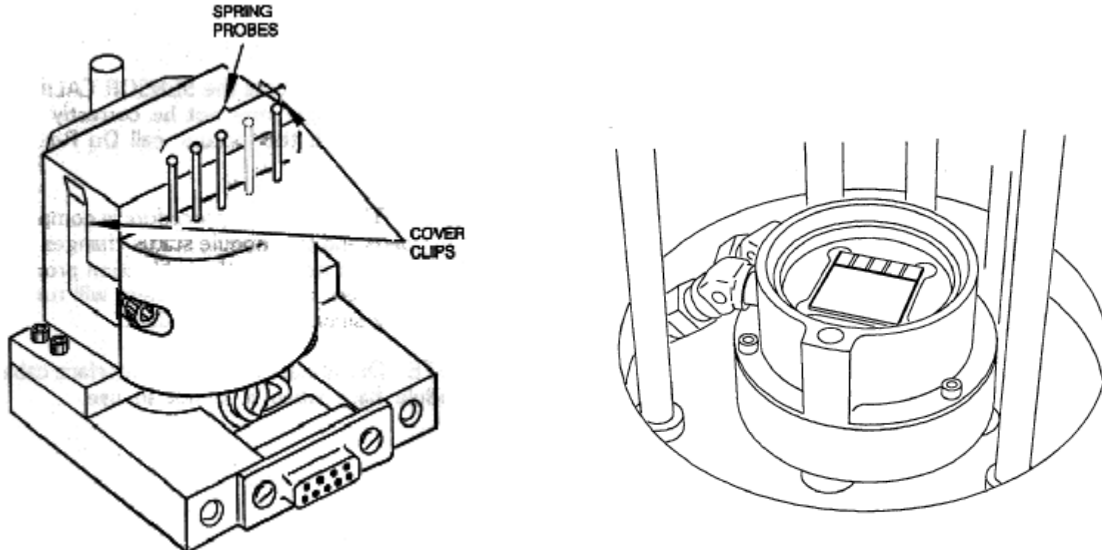


Fig 46: Single Plate of DEA(Copied with permission of TA Instruments) (8)

In DEA, a sinusoidal voltage is applied to the sample creating an alternating electric field. This imposed alternating electric field produces polarization of the same, alternating frequency as the electric field within the sample. The measured current is the sum of the capacitive and conductive components. The capacitance(C) and conductance(1/R) can be calculated as follows:

$$C(\text{farads}) = (I_m/V_a) * (\sin \theta/2\pi f) \quad \text{and} \\ 1/R (\text{mhos}) = (I_m/V_a) * \cos \theta \quad (8)$$

where:

- C = Capacitance
- (1/R) = Conductance
- R = resistance (ohms)
- I<sub>m</sub> = measured current
- I<sub>a</sub> = applied voltage
- f = applied frequency (Hz)
- θ = phase angle shift

The dielectric constant or permittivity ( $\epsilon'$ ) is a measure of the reversibly stored charge of the material. The dissipation or loss tangent ( $\epsilon''$ ) is a measure of the conductive or irreversible component of the complex dielectric parameter. Similar to viscoelastic parameters,  $\tan \delta$  is  $\epsilon''/\epsilon'$ . Permittivity and dissipation can be calculated as follows:

$$\begin{aligned} \epsilon' &= (Cd/\epsilon_0A) & \text{and} \\ \epsilon'' &= (d/RA2\pi f\epsilon_0) & (8) \end{aligned} \quad \begin{aligned} &\text{where} \\ \epsilon' &= \text{permittivity} \\ \epsilon'' &= \text{dissipation or loss factor} \\ C &= \text{capacitance (farads)} \\ R &= \text{resistance (ohms)} \\ A &= \text{electrode plate area} \\ d &= \text{plate spacing} \\ f &= \text{frequency (Hz)} \\ \epsilon_0 &= \text{absolute permittivity of free space} \\ &\quad (8.85 \times 10^{-12} \text{ F/m}) \end{aligned}$$

Ionic conductivity ( $\sigma$ ) is related to the viscosity of a material. This is because it is a measure of the ease of migration of ionic species through a fluid sample. Ionic conductivity can be used to monitor viscosity changes associated with thermoplastic or thermoset curing. The dissipation factor ( $\epsilon''$ ) can be used, above the materials glass transition region, to calculate the bulk ionic conductivity as follows:

$$\sigma = \epsilon''2\pi f\epsilon_0 \quad (8)$$

A generic plot of permittivity versus temperature is given in Fig 47. It can be seen in this figure that the glass transition region for this material runs between 50°C and 100° C. This can be seen in the increased slope through that region. This DEA evaluation was performed with the parallel plate setup.

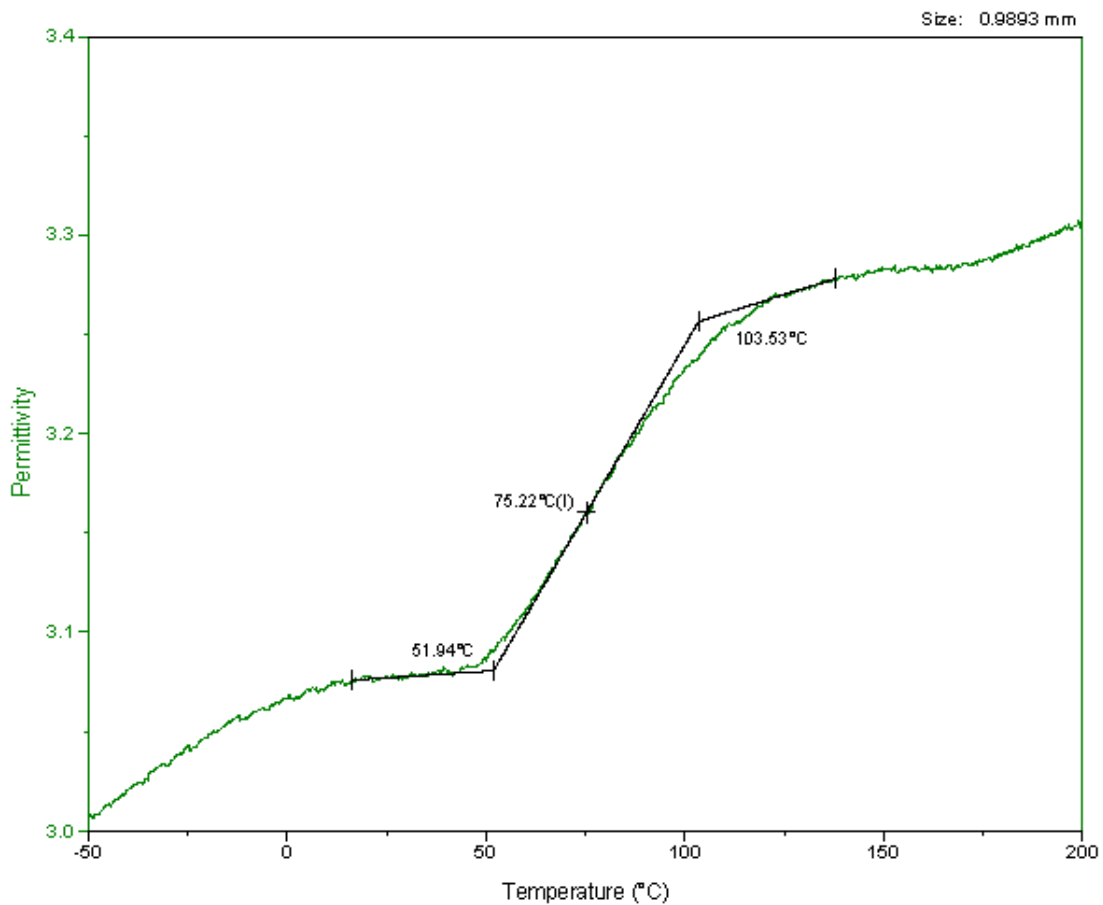


Fig 47: General permittivity vs temperature plot

Typically, an increase in permittivity decreases the materials ability to ultrasonically weld. This is because an increasing amount of polar plasticizer increases the permittivity of the material and decreases it's weldability. Comparisons can be made within a group

of similar base chemistry polymers to determine which of the group is most suitable for the ultrasonic welding process. Fig 48 compares the permittivities of three similarly based polymers. In this plot it can be seen that there is a difference in their permittivities. This difference was directly related to the experimental results related to the materials ultrasonic weldability. The material with the highest permittivity values had the hardest time being ultrasonic welded, while the material with the lowest values had the easiest time being ultrasonic welded.

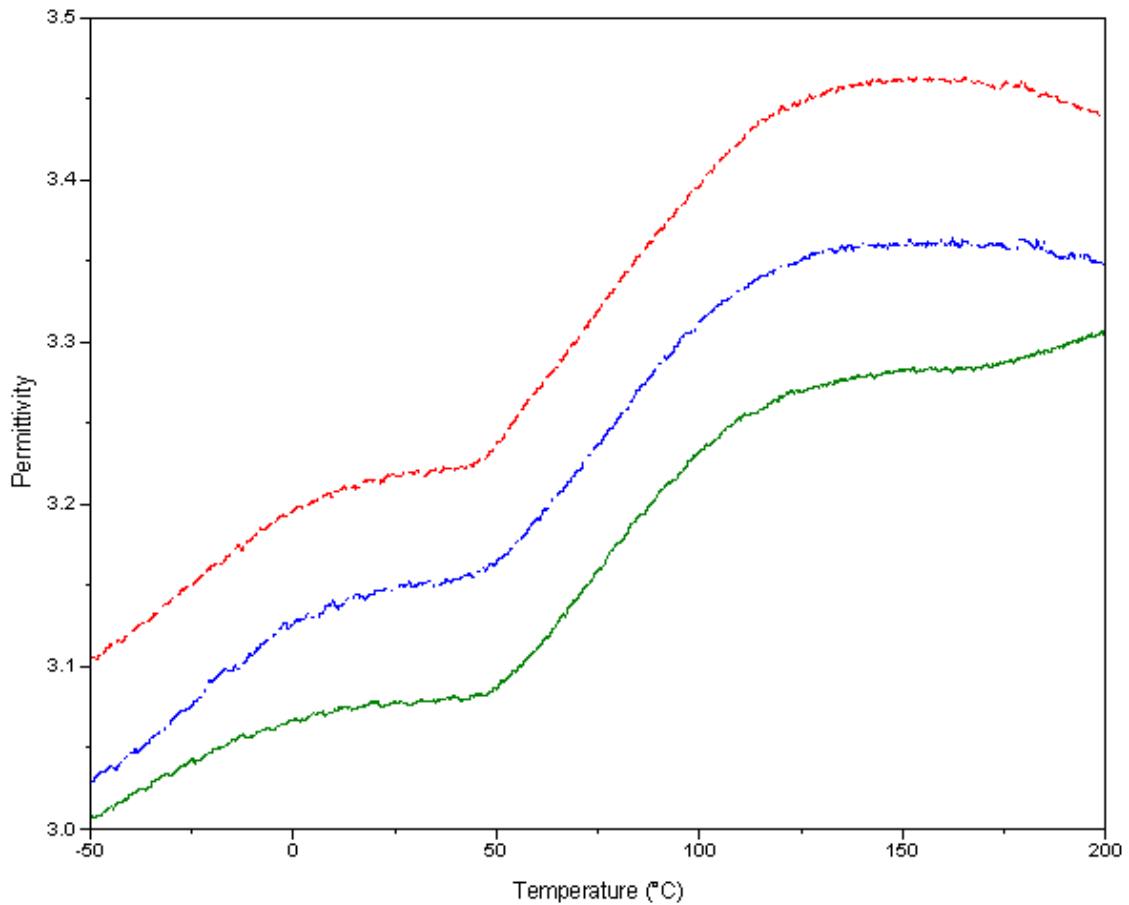


Fig 48: Permittivity comparison

The single plate setup is usually used for liquids, gels, and pastes. The most common use of the single plate is the cure optimization of thermoset materials. Fig 49 shows the cure of an epoxy from room temperature to 200°C. This is a plot of ionic conductivity versus temperature. This plot has frequencies of 1000, 3000, 10000, and 30000 Hz. In this plot the ionic conductivity before the epoxy is cured is relatively frequency independent. However, upon curing the ionic conductivity drops and becomes frequency dependent. In this region, as the frequency is increased the ionic conductivity is increased. This is seen in the plot with the top line representing the 30000 Hz and the bottom line representing the 1000 Hz.

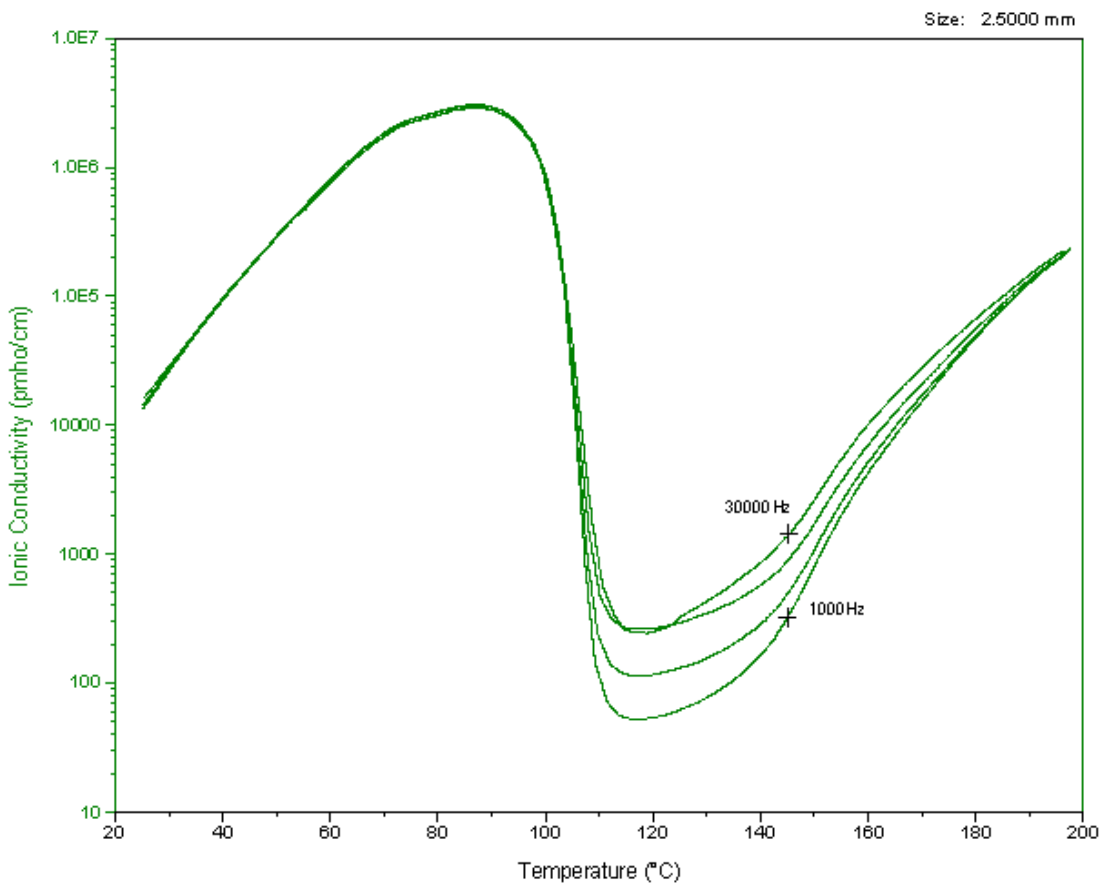


Fig 49: Single plate DEA of High Temperature Epoxy

There are many factors that effect the results obtained with DEA. The factors that cause the most error in the results are moisture and ionic contaminants. As long as the instrument is properly calibrated and maintained, these are the main problems to be concerned with. Frequency also plays a role in the data obtained from a DEA. With respect to permittivity, as the frequency increases the permittivity decreases. This is the opposite effect seen with ionic conductivity. As frequency is increased, ionic conductivity is increased.

## 2.7 Fourier Transform Infrared Spectrometer

“The goal of infrared spectroscopic applications is to determine the chemical functional groups contained in a particular material. Each functional group uniquely absorbs characteristic frequencies of infrared radiation. Thus, a plot of radiation intensity versus frequency (the infrared spectrum) fingerprints the identifiable chemical groups in the unknown.” (9) Infrared spectra show absorption bands with energies corresponding to the various motions(vibrations) of the atoms which make up the material of interest. Infrared radiation is light from 12800 – 10  $\text{cm}^{-1}$ . There are three divisions of the IR spectrum: Near, Mid, and Far IR ; Near IR (12800 – 4000  $\text{cm}^{-1}$ ) consists of mostly combination and overtone bands; Mid IR (4000-400 $\text{cm}^{-1}$ ) consists of mostly fundamental normal modes; Far IR (400-10 $\text{cm}^{-1}$ ) consists of mostly pure rotational modes (between the subdivisions of a particular energy band). This analysis only

involves the mid-infrared region from 4000 – 400cm<sup>-1</sup>. The IR spectrum is unique for every unique molecule, which is called it's fingerprint. There are two basic groups of frequencies: "functional" frequencies and "fingerprint" frequencies. The functional frequencies consist of frequencies from 4000 to 1500 cm<sup>-1</sup> while fingerprint frequencies consist of frequencies from 1500 to 400cm<sup>-1</sup>.(9) The functional frequencies consist of stretching of bonds while the fingerprint region consists of bending bonds. Fingerprint frequencies are highly characteristic of the molecule. They indicate the environment of the present functional groups.

There are several vibrations which are localized and very characteristic of specific functional groups. In the fingerprint region, if a band appears at the frequency characteristic of a specific functional group, that group may or may not be present. For this, the interpretation of the peaks in the fingerprint region must be characterized by intensity and/or shape. Here it is usually more reliable for a peak to be absent than present. The best way to interpret IR spectra is to gain knowledge at the high frequencies(above 1500cm<sup>-1</sup>) and verify your conclusions in the fingerprint region (below 1500 cm<sup>-1</sup>). A functional group must always be found in the spectra of molecules which contain that group. It also must always occur in the same narrow range of frequencies. The frequency must generally have the same reliable shape for each molecule containing the group. Only optical isomers absorb in exactly the same way. This data generated by FTIR must be combined with other information such as sample history (what is possible), physical properties(Mw, Tm, Tc, etc.), additional analysis, ect to be 100% sure of the identity.

“The frequency of the absorbed radiation is the molecular vibrational frequency actually responsible for the absorption process.”(10) “In order to absorb infrared radiation, a molecule must undergo a net change in dipole moment as a consequence of its vibrational or rotational motion.”(10) Therefore absorption of IR is only allowed in molecular species with small energy changes within their molecular motions. “If the frequency of the radiation exactly matches a natural vibrational frequency of the molecule, a net transfer of energy takes place that results in a change in the amplitude of the molecular vibration; absorption of the radiation is the consequence. Similarly, the rotation of asymmetric molecules around their centers of mass results in a periodic dipole fluctuation that can interact with radiation.”(10) Homonuclear species such as O<sub>2</sub>, N<sub>2</sub>, and Cl<sub>2</sub> have no net change in their dipole moment during their vibration or rotation; therefore, homonuclear species can not absorb in the IR spectra. There are several stretching and bending motions. A stretching motion is characterized by a continuous change in the bond length between the two atoms. There are symmetric and asymmetric stretches. A bending motion is characterized by the change in bond angle between the two bonds. There are four types of bending motions: Twisting, Rocking, Scissoring, and Wagging as seen in Fig 50.

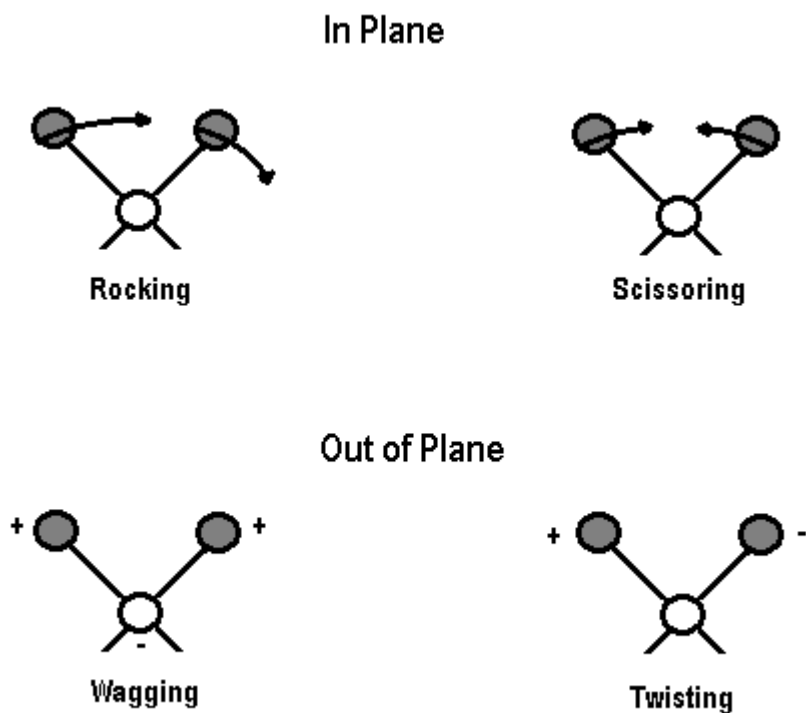


Fig 50: Bending motions

Fewer numbers of vibrations are present when: symmetry restricts the change in dipole moment from a particular vibration, there are identical or nearly identical energies of two or more vibrations, the intensity of the absorption is too weak for detection, or the absorbed frequency is out of the instruments range.(9) Additional peaks are sometimes present in spectra. These can be caused by overtones or resonance structures of the absorbing group.

To correctly and accurately identify an IR spectrum, it is important to follow these four steps.

1. Start at 4000cm<sup>-1</sup> and try to determine the functionality of the compound
2. Work your way form 4000cm<sup>-1</sup> to the lower frequencies to confirm your findings.
3. Look at the shape, location, and appearance. Do your ideas make sense?
4. Draw example structures and then search appropriate libraries.

The number one error in identifying an IR scan is peak picking. This is where you make your conclusion based on only a few peaks without working your way completely through the spectrum. In the following figure, IR spectra will be identified.

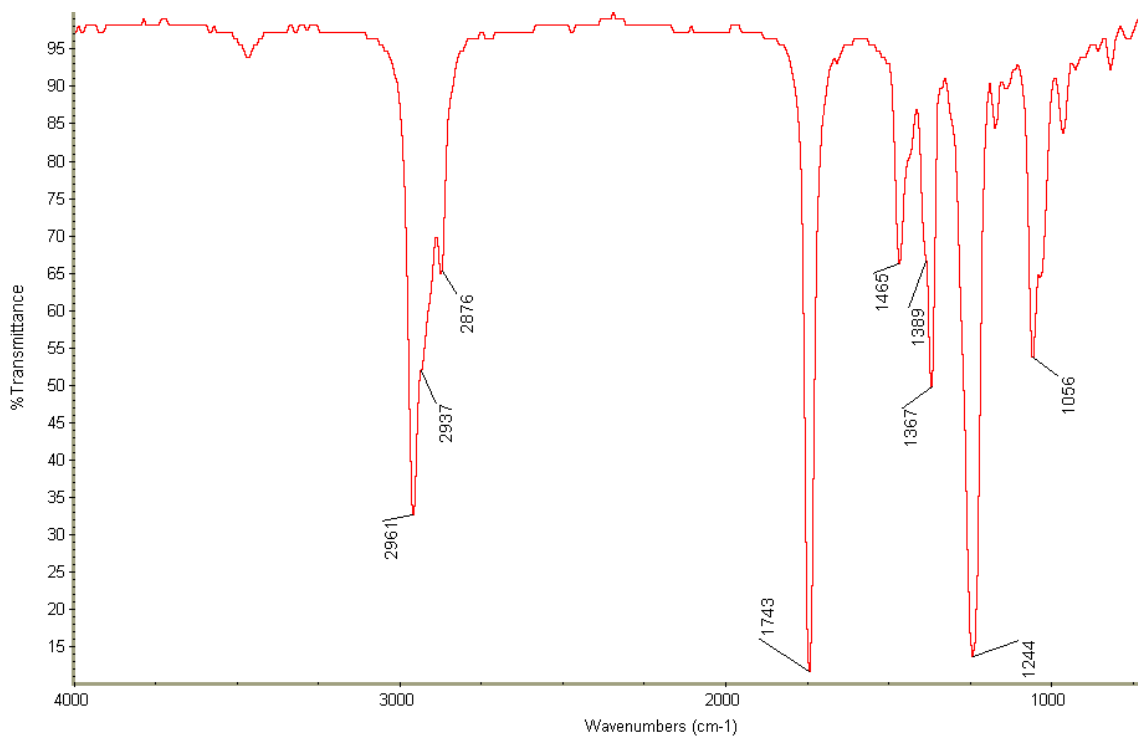
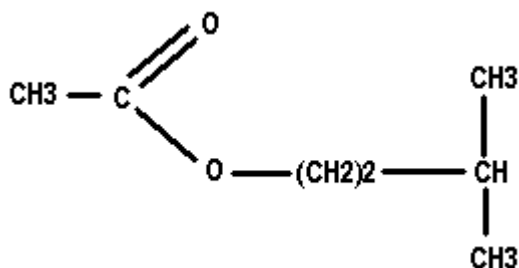


Fig 51: Examples of basic characteristic peaks

The above IR spectra is of Isoamyl acetate. It has the general structure of



In the spectra, the methyl groups produce an asymmetric stretch near  $2960\text{ cm}^{-1}$  and a symmetric stretch near  $2875\text{ cm}^{-1}$ . The peak at  $2937\text{ cm}^{-1}$  is caused by an asymmetric stretch of the methylene groups. The methylene groups also has a symmetric stretch around  $2860\text{ cm}^{-1}$ , but it is masked by the surrounding peaks. Working toward lower wavenumbers, a peak at  $1743\text{ cm}^{-1}$  is encountered. This peak is characteristic of a carbonyl stretch. Determining that there is a carbonyl group present in the structure, the possibility of an ester should be evaluated. Ester groups produce large broad peaks, known as the “Ester Sisters”, near  $1050$  and  $1250\text{ cm}^{-1}$ . These peaks are present in this structure, signifying an ester in the structure. Methyl and methylene bending motions are represented in this spectra with the peak at  $1465\text{ cm}^{-1}$ . The split of the  $1379\text{ cm}^{-1}$  peak is caused by only methyl bending motions and represents either an isopropyl or geminal dimethyl grouping. These two peak are utilized to confirm the findings between  $2875$  and  $2965\text{ cm}^{-1}$  and their ratios can be used to estimate the ratio of methyl to methylene in the structure. The other important features of this spectrum is the lack of peaks. This spectra does not have double or triple bond peaks and it doesn't have a peak for long methylene chain rocking. In IR interpretation, the absence of peaks is sometimes more useful than the presence of peaks.

There are many important IR peaks that can be evaluated. Their position in the spectrum is determined by their surroundings on the structure. The position of a peak can be altered by many structures including conjugated bonds, large side groups, halogenated elements, and many other circumstances. The following is a small list of average peak positions of non-altered peaks.

<b>Structure</b>	<b>Position (cm<sup>-1</sup>)</b>
Methyl asymmetric stretch	2960
Methylene asymmetric stretch	2926
Methyl symmetric stretch	2874
Methylene symmetric stretch	2861
Methyl bend	1460 and 1379
Methylene bend	1460
Methylene long chain rocking	726
Vinyl stretch	3080-3030
C-C triple bond	3300
C-C triple bond stretch	2100
Nitrile	2200
Conjugated C-C double bond	1598
Cumulative C-C double bond	1965
Aromatic ring CH stretch	3000

Ketone	1750
Ester	1740, 1050, and 1250
Ether	1100
Anhydride	1050
Alcohol OH stretch	3350
Amides	1690-1625
Amines	3400-3200

Table of Infrared Peaks (9)

This is an incomplete list and many of the structures listed have additional peaks, but this can be used as a simple reference. Many more complex references are available.

The Beer-Lambert Law gives the absorbance intensity:

$$A = abC \quad \text{where}$$

$A = \text{absorbance} = -\log T$   
 $T = I_{\text{sample}} / I_{\text{background}}$   
 $a = \text{absorption coefficient (extinction coefficient)}$   
 $b = \text{pathlength}$   
 $C = \text{concentration}$

The absorption coefficient is a property of the material and describes how easily the material absorbs IR energy and is wavelength dependent. This is the basis of all quantitative analysis using IR spectroscopy; however, it is not necessary for qualitative analysis where characteristic peaks and frequencies are used. A linear wavenumber scale gives a direct proportionality between the absorbing components quantity and both energy and frequency.

Classical Model: Consider a diatomic molecule for simplicity. It only has one possible vibration. The vibration of the bond between the two atoms of a diatomic is given by Hooke's Law:  $\text{freq.}(\text{cm}^{-1}) = (0.5\pi c)(k/\mu)^{0.5}$  (9); where  $k$  = force constant ;  $\mu$  = reduced mass =  $(m_1 \times m_2)/(m_1 + m_2)$  ; and  $c$  = speed of light. This is the formula of a simple harmonic oscillator. In order for absorption of radiation to occur, the frequency of light must be exactly equal to the natural frequency of vibration of the molecule. To absorb in the IR region, the molecule is not required to have a permanent dipole; however, the vibrations must create a change in the dipole moment of the molecule. The intensity of the absorption is proportional to the amount of change in the dipole moment during the vibration as follows:  $I = (\pi/3c)(\delta\mu/\delta Q)^2$  (9); where :  $c$  = speed of light ;  $\mu$  = electric dipole moment ; and  $Q$  = normal coordinate (description of the vibration). If  $I = 0$  then  $\mu$  does not change during the vibration and the vibration does not absorb. It is considered IR "forbidden". If  $\delta\mu/\delta Q$  is large, then the band is intense. Large changes occur in the stretching of polar bonds. Different electronegativities give rise to large dipole moments while similar electronegativities produce small changes in dipole moments and weak bands. Also, out of plane wagging produces a large change in the dipole moment.

"The normal frequencies of vibration in a molecule can not be predicted by considering all stretching modes as simple harmonic oscillators (predicted by Hooke's Law). There may be coupling occurring which results in bands appearing at theoretically unexpected frequencies."(9) For example, usually a single absorption peak would be present for a particular vibration that absorbs exactly one frequency; however, relatively broad bands are seen instead. This is due to the change in potential energy as the bond

oscillates back and forth. An absorption corresponds to a jump in energy levels. . As seen in the graph of potential energy vs bond length. Fig 52.

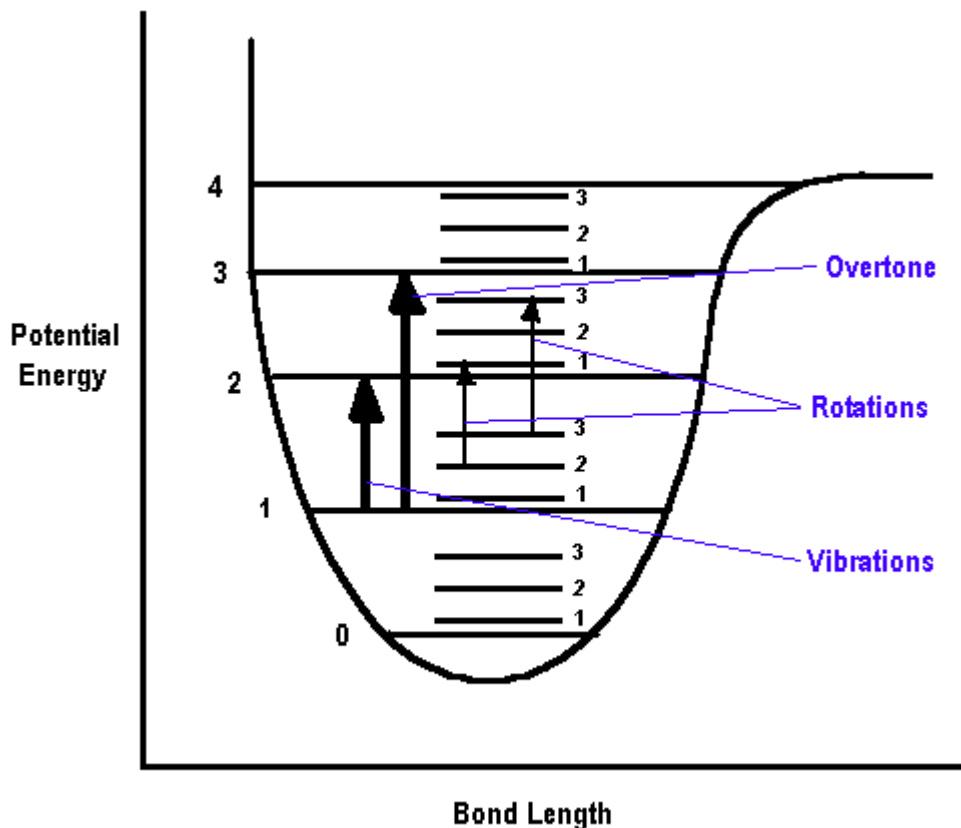


Fig 52: Potential Energy/ Bond Length

The energy levels are broken down in to sublevels which are characterized by rotation of the molecules. These combined make the exact energies slightly different. An overtone is characterized by a jump to the second or third energy levels. These are weaker absorption peaks and rare.

The FTIR utilizes the Fourier transform technique. Advantages of the FTIR over the old type include: only one moving part (mirror), increased speed and sensitivity, greater optical throughput, and the use of an internal laser reference.

The FT-IR spectrometer has three basic parts: the IR source, a Michelson interferometer, and a detector. (Fig 53)

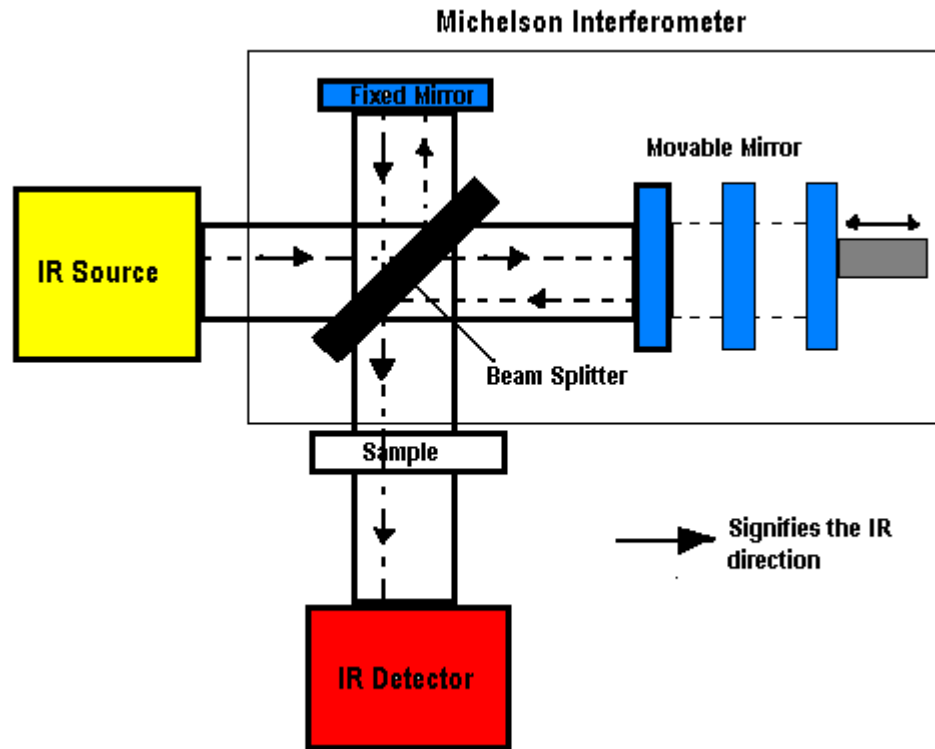


Fig 53: Three basic parts of a FTIR

The Michelson interferometer consists of a beamsplitter, moving mirror, and a fixed mirror. IR radiation from the source is directed into the interferometer. In the interferometer, the beam contacts the beamsplitter where the beam is split into two beams of approximately the same energy and is directed to the two mirrors (signified by the arrows). The two beams are reflected off the mirrors and meet back at the beam splitter. Constructive and destructive interference, due to the position of the moving mirror, occur

at the beam splitter. This resulting beam passes through the sample and to the detector. The scan in FTIR is the mechanical displacement of the moving mirror assembly. The resolution of the FTIR is determined by the distance the moving mirror can move past the fixed mirror. A laser is used for alignment in the FTIR. Each data point of the interferogram represents the summation of components from each modulated frequency.

## CHAPTER 3

### Experimental

#### 3.1 Sample 1

##### 3.1a Equipment

- Fourier Transform Infrared Spectrometer (Nicolet Magna 560)
- Thermal Analysis Instrument
  - Differential Scanning Calorimeter (TA Inst. MDSC 2910)
  - Dynamic Mechanical Analyzer (TA Inst. DMA 2980)
  - Thermomechanical Analyzer (TA Inst. TMA 2940)
  - Dielectric Analyzer (TA Inst. DEA 2970)
  - Thermogravimetric Analyzer (TA Inst. TGA 2950)
- Parallel Plate Torsion Rheometer (Rheometrics Ares)
- Capillary Extrusion Rheometer (Rosand)

##### 3.1b Procedures

The experimental procedure for this type of evaluation is more complicated than most experimental procedures. Some of these experiments must be run in series rather than parallel due to the fact that the procedures of some instruments rely on the data obtained from other instruments. Also these experiments should be run in series because some experiments are destructive while others are not and sometimes small quantities of samples are supplied for these evaluations.

The experimental procedure for Sample 1 requires some experiments run in series as described above. Initially in all evaluations of this type, FTIR is performed to determine the base chemistry of the material. FTIR is a non-destructive test and the sample can be reused in other instruments such as the TGA or for rheology. This information obtained by the FTIR can guide the remainder of the experiments. With the base chemistry of the polymer known information about this material can be researched including the melting temperature and glass transition where appropriate. These temperatures can be used as guidelines for the DSC which is usually run second. Running the DSC second confirms your results about the base chemistry of the sample. The third, fourth, and fifth tests (DMA, TMA, and DEA) are interchangeable and only require the materials melting and/or glass transition temperature to proceed. These temperatures can be used as guidelines which should be carefully considered so not to melt a material in any of these instrument. All these tests are non-destructible tests and the samples can be reused in the TGA or either of the rheometers. The sixth test is the TGA. It is performed later in the evaluation because it can use previously evaluated samples. It's initial degradation temperature is used in the rheology experiments as an upper temperature limit. The seventh test performed is the parallel plate rheometer. This test can utilize previously analyzed sample and requires the TGA and DSC data to proceed. This test should be performed before the capillary rheometer because if the temperature is incorrect there is less sample lost per run than in the capillary rheometer. The final test (#8) is the capillary extrusion rheometer. This is performed last because of the quantity of sample and other experimental results that are required. Each experiment described above is further described below.

## Fourier Transform Infrared Spectrometer

Compositional non-destructive evaluation of the sample was performed using mid-infrared spectroscopy between 4000 and 675 wavenumbers ( $4000^{\text{cm}^{-1}}$ - $675^{\text{cm}^{-1}}$ ). Mid-infrared goes down to  $200^{\text{cm}^{-1}}$ , but the crystal used was Germanium. Germanium absorbs IR radiation below  $650^{\text{cm}^{-1}}$  and the signal can not be distinguished from the Germanium spectrum easily. The analysis was performed in a Fourier Transform Infrared Spectrometer (FTIR) manufactured by Nicolet using an Attenuated Total Reflectance (ATR) accessory for solid materials. Sixty four scans of each sample was performed. These scans were averaged by the software to give the sample spectrum. The aperture was originally set at 75, the movable mirror velocity was originally set at 0.9494 cm/s, and the gain was originally set on autogain. The spectral resolution was originally set at 4 which correlates to a data spacing of  $1.928^{\text{cm}^{-1}}$ . These settings were utilized for the first trial; however, they were slightly altered during the analysis to improve signal to noise ratio.

## Differential Scanning Calorimeter

The DSC evaluations on Sample 1 was a two part experiment. The first part evaluated the sample between room temperature and  $300^{\circ}\text{C}$  to determine if there are any constituents in the material that were not seen by the FTIR. The second evaluation was performed between  $30^{\circ}\text{C}$  and  $250^{\circ}\text{C}$ . The initial sample weight was kept between 10

and 20 mg. Two complete heat-up and cool-down cycles were run. The samples were heated at 10°C/min and cooled at 5°C/min. The samples were held at 82.20°C for 15 minutes on the cool down cycle to enhance crystallinity development. The heat flow of the sample was monitored and the presence of glass transitions and melting points was determined. The average of three sample sets were obtained to determine the range of the data acquired. This testing was performed in a dry nitrogen environment with a flow rate of 30cm<sup>3</sup>/min.

#### Dynamic Mechanical Analysis

The DMA sample evaluations were performed in the single cantilever mode. For each sample, only a single heating run was performed. This testing was performed on 1/8"t x 1/2"w samples. Each sample was cooled down to -50°C and then heated at 5°C/min to 150°C. Each sample was of a rectangular geometry. The results required from this evaluation were the glass transition region reported from the loss modulus on a linear scale. The air bearing on the DMA is dry air with a constant pressure of 80psi.

#### Thermomechanical Analysis

The TMA evaluations were performed between 30°C and 85°C. The samples were heated and then cooled in dry nitrogen at 5°C/min. This regimen was performed

twice consecutively on each sample. The dimensional changes of the sample were monitored continuously and this information in combination with the original sample dimension allows estimation of the thermal expansivity of the material. The dry nitrogen was held at 10 psi throughout the experiment. TMA analyses were performed for the three principle directions of each sample: length (flow), width (transverse), and thickness. Three measurements of each sample were taken and averaged to give the range of results.

#### Dielectric Analysis

Three samples were evaluated on the DEA from  $-50^{\circ}\text{C}$  to  $200^{\circ}\text{C}$ . The sample geometry used was a one inch diameter disk approximately one millimeter in thickness. The samples were dried at  $70^{\circ}\text{C}$  for one day under a dry nitrogen blanket prior to the analysis. The samples were initially cooled to  $-50^{\circ}\text{C}$  in the DEA using liquid nitrogen. Once the sample reached this initial temperature, the test was conducted using a heating rate of  $5^{\circ}\text{C}/\text{min}$  to  $200^{\circ}\text{C}$  under a frequency of 20kHz. The test was performed in a dry nitrogen environment with a flow rate of  $50\text{cm}^3/\text{min}$ .

#### Thermogravimetric Analysis

This TGA evaluation was performed between  $30^{\circ}\text{C}$  and  $800^{\circ}\text{C}$  in a dry air environment. The sample weights were held near 10 mg. The samples were heated with

a DRTGA at 50°C/min. Once the sample reached 800°C, the temperature was held isothermal for 120 minutes and the weight change of the sample was continuously monitored. The end results of this evaluation gave the upper temperature processing range and the percent inorganic filler. This inorganic filler was evaluated with the optical microscope to help identify its composition. Three samples were evaluated and the results were averaged to get the range of results. These evaluations were performed with a nitrogen flow rate in the mechanical chamber of 30 cm<sup>3</sup>/min and the air flow rate in the sample chamber of 50cm<sup>3</sup>/min.

#### Parallel Plate Torsion Rheometer

The parallel plate rheology experiments were based on a frequency sweep, 0.1 – 100 Hz with 5 points per decade, at 255°C. This temperature was chosen based on the polymer base chemistry and the data obtained from the DSC. Materials analyzed on this instrument were reground parts. To use this regrind, the regrind must be melted and mixed without any residual air in the melt. The rheological data was obtained in oscillatory parallel plate mode. The plates utilized were 25mm in diameter and 1% strain was maintained throughout the experiment. Three runs were evaluated to determine the validity of the data through reproducibility. Prior to analyzing, the regrind was dried in a vacuum oven at 110°C for four hours.

## Capillary Extrusion Rheometer

The capillary extrusion rheological experiments were based on a shear rate sweep (100 – 20000s<sup>-1</sup>) at 255°C. The temperatures chosen for each material was the same as the parallel plate rheometer. Three runs of each condition were run to determine the validity of the data through reproducibility. The die measurements are: length = 9.17 mm, diameter = 0.989 mm, and an entrance angle of 90°. The barrel of the rheometer has three thermocouples, evenly spaced down the barrel, and one pressure transducer near the die. The measurements were taken at each shear rate once it came to equilibrium and was converted to viscosity. The regrind was dried at 110°C for four hours before rheology experiments could be performed. The samples for this test were in regrind form. The extrusion rheometer was run in the steady shear mode.

### 3.2 Sample 2

#### 3.2a *Equipment*

- Fourier Transform Infrared Spectrometer (Nicolet Magna 560)
- Thermal Analysis Instrument
  - Differential Scanning Calorimeter (TA Inst. MDSC 2910)
  - Dynamic Mechanical Analyzer (TA Inst. DMA 2980)
  - Thermogravimetric Analyzer (TA Inst. TGA 2950)
- Parallel Plate Torsion Rheometer (Rheometrics Ares)
- Capillary Extrusion Rheometer (Rosand)

### 3.2b *Procedures*

The experimental procedure for Sample 2 requires some experiments run in series as described above. Initially in all evaluations of this type, FTIR is performed to determine the base chemistry of the material. FTIR is a non-destructive test and the sample can be reused in other instruments such as the TGA or for rheology. This information obtained by the FTIR can guide the remainder of the experiments. With the base chemistry of the polymer known information about this material can be researched including the melting temperature and glass transition where appropriate. These temperatures can be used as guidelines for the DSC which is usually run second. Running the DSC second confirms or refutes your results about the base chemistry of the sample through the acquired or lack of melting point and/or glass transition. The third test was the DMA. The DMA requires the material's melting and/or glass transition temperature to proceed. These temperatures can be used as guidelines which should be carefully considered so not to melt a material in the instrument. This test can be performed as a non-destructible test and the samples can be reused in the TGA or for rheology. The fourth test is the TGA. It is performed later in the evaluation because it usually can use previously evaluated samples. It's initial degradation temperature is used in the rheology experiments as an upper temperature limit. The fifth test performed is the parallel plate rheometer. This test can usually utilize previously analyzed sample and requires the TGA and DSC data to proceed. This test should be performed before the capillary rheometer because if the evaluation temperature is incorrect there is less sample lost per run than in the capillary

rheometer. The final test (#6) is the capillary extrusion rheometer. This is performed last because of the quantity of sample and other experimental results that are required. Each experiment described above is further described below.

#### Fourier Transform Infrared Spectrometer

Compositional non-destructive evaluation of the sample was performed using mid-infrared spectroscopy between 4000 and 675 wavenumbers ( $4000^{\text{cm}^{-1}}$  -  $675^{\text{cm}^{-1}}$ ). Mid-infrared goes down to  $200^{\text{cm}^{-1}}$ , but the crystal used was Germanium. Germanium absorbs IR radiation below  $650^{\text{cm}^{-1}}$  and the signal can not be distinguished from the Germanium spectrum easily. The analysis was performed in a Fourier Transform Infrared Spectrometer (FTIR) manufactured by Nicolet using an Attenuated Total Reflectance (ATR) accessory for solid materials. Sixty four scans of each sample was performed. These scans were averaged by the software to give the sample spectrum. The aperture was originally set at 75, the movable mirror velocity was originally set at 0.9494 cm/s, and the gain was originally set on autogain. The spectral resolution was originally set at 4 which correlates to a data spacing of  $1.928^{\text{cm}^{-1}}$ . These settings were utilized for the first trial; however, they were slightly altered during the analysis to improve signal to noise ratio.

## Differential Scanning Calorimeter

The DSC evaluations on Sample 2 was a two part experiment. The first part evaluated the sample between room temperature and 300°C to determine if there are any constituents in the material that were not seen by the FTIR. The second part was performed between 30°C and 200°C. The initial sample weight was kept between 10 and 20 mg. Two complete heat-up and cool-down cycles were run. The samples were heated at 10°C/min and cooled at 5°C/min. The heat flow of the sample was monitored and the presence of glass transitions and melting points was determined. The average of three sample sets were obtained to determine the range of the data acquired. This testing was performed in a dry nitrogen environment with a flow rate of 30cm<sup>3</sup>/min.

## Dynamic Mechanical Analysis

There were two types of evaluations performed on the DMA. The first evaluation was the sample's viscoelastic property verse temperature evaluation. This evaluation was performed between 0 and 165°C at 10 Hz. The second evaluation was also performed between 0 and 165°C, but it was a frequency sweep of 0.1 to 100 Hz with 5 points per decade. This evaluation was combined with one of the evaluations performed on the parallel plate to create a master curve. These DMA sample evaluations were performed in the single cantilever mode. For each sample, only a single heating run was performed. This testing was performed on ~2mm x ~4mm samples with an amplitude of 10µm.

Each sample was cooled down to 0°C and then heated at 5°C/min to 165°C. Each sample was of a rectangular geometry. The results required from this evaluation were the glass transition region reported from the loss modulus on a linear scale, the viscoelastic properties versus temperature profile, and the master curve evaluation for storage and loss modulus. The air bearing on the DMA is dry air with a constant pressure of 80psi.

### Thermogravimetric Analysis

This TGA evaluation was performed between 30°C and 800 °C in a dry air environment. The sample weights were held near 10 mg. The samples were heated with a DRTGA at 50°C/min. Once the sample reached 800°C, the temperature was held isothermal for 120 minutes and the weight change of the sample was continuously monitored. The end results of this evaluation gave the upper temperature processing range and the percent inorganic filler. This inorganic filler was evaluated with the optical microscope to help identify its composition. Three samples were evaluated and the results were averaged to get the range of results. These evaluations were performed with a nitrogen flow rate in the mechanical chamber of 30 cm<sup>3</sup>/min and the air flow rate in the sample chamber of 50cm<sup>3</sup>/min.

## Parallel Plate Torsion Rheometer

Three types of evaluations were performed on the parallel plate rheometer. The first evaluation was the creation of a master curve of this material along with the data obtained from the DMA. The second evaluation used some of the data from this first evaluation and combined it with data from the capillary rheometer to predict the temperature dependence of this material near the assumed processing temperature. The third evaluation took this same data from the parallel plate and the capillary rheometer that was used in the temperature dependence and created a cross model prediction for the material.

The parallel plate rheology experiments were based on a frequency sweep, 0.1 – 100 Hz with 5 points per decade, every 10 degrees between 225 and 295°C. The master curve utilized all the data from this temperature range while the temperature dependence and the cross model used only the data at 275, 285, and 295°C. These temperatures were chosen based on the polymer base chemistry and the data obtained from the DSC as the assumed processing temperature range for this material. Materials analyzed on this instrument were regrind parts. To use this regrind, the regrind must be melted and mixed without any residual air in the melt. The rheological data was obtained in oscillatory parallel plate mode. The plates utilized were 25mm in diameter and 1% strain was maintained throughout the experiment. Three runs were analyzed to determine the validity of the data through reproducibility. Prior to analyzing, the regrind was dried in a vacuum oven at 121°C for three hours as recommended for this type of material.

## Capillary Extrusion Rheometer

The capillary extrusion rheological experiments were based on a shear rate sweep ( $100 - 20000\text{s}^{-1}$ ) at 275, 285, and 295°C for the use in the cross model prediction and the temperature dependence prediction. The temperatures chosen for each material were the same as the parallel plate rheometer. Three runs of each condition were run to determine the validity of the data through reproducibility. The die measurements are: length = 9.17 mm, diameter = 0.989 mm, and an entrance angle of 90°. The barrel of the rheometer has three thermocouples, evenly spaced down the barrel, and one pressure transducer near the die. The measurements were taken at each shear rate once it came to equilibrium and was converted to viscosity. The samples for this test were in regrind form. The regrind was dried at 121°C for three hours before rheology experiments could be performed. The extrusion rheometer was run in the steady shear mode.

### 3.3 Sample 3

#### 3.3a Equipment

- Fourier Transform Infrared Spectrometer (Nicolet Magna 560)
- Thermal Analysis Instrument
  - Differential Scanning Calorimeter (TA Inst. MDSC 2910)
  - Thermomechanical Analyzer (TA Inst. TMA 2940)
  - Dynamic Mechanical Analyzer (TA Inst. DMA 2980)
- Thermogravimetric Analyzer (TA Inst. TGA 2950)
- Parallel Plate Torsion Rheometer (Rheometrics Ares)

### 3.3b Procedures

This program was performed on a single fiber optic boot. Additional material was not available so the experiments had to be performed extremely carefully. The total weight of the sample used for all experiments was approximately 750mg.

The experimental procedure for Sample 3 requires some experiments run in series as described above. Initially in all evaluations of this type, FTIR is performed to determine the base chemistry of the material. FTIR is a non-destructive test and the sample can be reused in other instruments such as the TGA or rheology. This information obtained by the FTIR can guide the remainder of the experiments. With the base chemistry of the polymer known information about this material can be researched including the melting temperature and glass transition where appropriate. These temperatures can be used as guidelines for the DSC which is usually run second. Running the DSC second confirms or refutes your results about the base chemistry of the sample through the presence or absence of melting points and/or glass transitions. The third test performed was the TMA. The TMA requires the material's melting and/or glass transition temperature to proceed. These temperatures can be used as guidelines which should be carefully considered so not to melt a material in any of these instrument. This test is a non-destructible tests and the samples can be reused in the TGA or for rheology. The fourth test is the DMA. This test was performed after the DSC and the TMA because this material was soft and melting it in the instrument was a concern. The fifth characterization performed was the TGA. It was performed later in the evaluation because it can use previously evaluated samples and the sample quantity was limited. The

material's initial degradation temperature is used in the rheology experiments as an upper temperature limit and is obtained through the TGA. The sixth test performed was the parallel plate rheology. This test utilized previously analyzed sample and requires the TGA and DSC data to proceed. Other similar materials were also evaluated on the parallel plate rheometer to ensure the secondary use of the material did not alter the results. This evaluation did not use the capillary extrusion rheometer. The sample quantity obtained was an insufficient quantity for this characterization to be involved.

#### Fourier Transform Infrared Spectrometer

Compositional non-destructive evaluation of the sample was performed using mid-infrared spectroscopy between 4000 and 675 wavenumbers ( $4000^{\text{cm}^{-1}}$ - $675^{\text{cm}^{-1}}$ ). Mid-infrared goes down to  $200^{\text{cm}^{-1}}$ , but the crystal used was Germanium. Germanium absorbs IR radiation below  $650^{\text{cm}^{-1}}$  and the signal can not be distinguished from the Germanium spectrum easily. The analysis was performed in a Fourier Transform Infrared Spectrometer (FTIR) manufactured by Nicolet using an Attenuated Total Reflectance (ATR) accessory for solid materials. Sixty four scans of each sample was performed. These scans were averaged by the software to give the sample spectrum. The aperture was originally set at 75, the movable mirror velocity was originally set at 0.9494 cm/s, and the gain was originally set on autogain. The spectral resolution was originally set at 4 which correlates to a data spacing of  $1.928^{\text{cm}^{-1}}$ . These settings were

utilized for the first trial; however, they were slightly altered during the analysis to improve signal to noise ratio.

### Differential Scanning Calorimeter

The DSC evaluations on Sample 3 was a two part experiment. The first part evaluated the sample between room temperature and 300°C to determine if there are any constituents in the material that were not seen by the FTIR. The second evaluation was performed between 30°C and 200°C. The initial sample weight was kept between 10 and 20 mg. Two complete heat-up and cool-down cycles were run. The samples were heated at 10°C/min and cooled at 5°C/min. The heat flow of the sample was monitored and the presence of glass transitions and melting points was determined. The average of three sample sets were obtained to determine the range of the data acquired. This testing was performed in a dry nitrogen environment with a flow rate of 30cm<sup>3</sup>/min.

### Thermomechanical Analysis

The TMA evaluations were performed between 30°C and 100°C. The samples were heated and then cooled in dry nitrogen at 5°C/min. This regimen was performed twice consecutively on each sample. The dimensional changes of the sample were monitored continuously and this information in combination with the original sample

dimension allows estimation of the thermal expansivity of the material. The dry nitrogen was held at 10 psi throughout the experiment. TMA analyses were performed on a disk made on a carver press. There was only one direction thick enough to evaluate on the TMA. Three measurements of the sample were taken and averaged to give the range of results.

### Dynamic Mechanical Analysis

The DMA sample evaluations were performed in the film and fiber mode. For each sample, only a single heating run was performed. This testing was performed on approximately 16.5mm x 8.0mm x 0.135mm samples. Each sample was heated at 5°C/min to 140°C. Each sample was of a rectangular geometry. The results required from this evaluation was the modulus verse temperature profile. The air bearing on the DMA is dry air with a constant pressure of 80psi.

### Thermogravimetric Analysis

This TGA evaluation was performed between 30°C and 800 °C in a dry air environment. The sample weights were held near 10 mg. The samples were heated with a DRTGA at 50°C/min. Once the sample reached 800°C, the temperature was held isothermal for 120 minutes and the weight change of the sample was continuously

monitored. The end results of this evaluation gave the upper temperature processing range and the percent inorganic filler. This inorganic filler was evaluated with the optical microscope to help identify its composition. Three samples were evaluated and the results were averaged to get the range of results. These evaluations were performed with a nitrogen flow rate in the mechanical chamber of 30 cm<sup>3</sup>/min and the air flow rate in the sample chamber of 50cm<sup>3</sup>/min.

#### Parallel Plate Torsion Rheometer

The parallel plate rheology experiments were based on a frequency sweep, 0.1 – 100 Hz with 5 points per decade, at 200°C. This temperature was chosen based on the polymer base chemistry and the data obtained from the DSC. Materials analyzed on this instrument was a regrind part. To use this regrind, the regrind must be melted and mixed without any residual air in the melt. The rheological data was obtained in oscillatory parallel plate mode. The plates utilized were 25mm in diameter and 1% strain was maintained throughout the experiments. Three runs were evaluated to determine the validity of the data through reproducibility. The sample was not dried before the evaluation because it was determined to be hydrophobic.

## CHAPTER 4

### Results

#### 4.1 SAMPLE 1

Sample 1 is used as an outdoor enclosure for telecommunication products. It's operation exposes it to UV radiation, extreme thermal cycling, rain, ice, and generally any other element possible in the continental United States. Sample 1 was evaluated to find an improved material for replacement in similar enclosures. Initial compositional analysis was performed using Fourier Transform Infrared Spectroscopy (FTIR). The FTIR allows for the identification of chemical species, which can be combined to determine the identity of the unknown material. Through peak identification, it was determined that the base material composition of Sample 1 was a Polycarbonate-Poly(butylene terephthalate) blend. Additionally, comparisons were made between the material's spectra, the Hummel Polymer and Additives library, and various known materials spectra to verify these results. The corresponding IR spectra can be seen in Figures 54, 55, and 56.

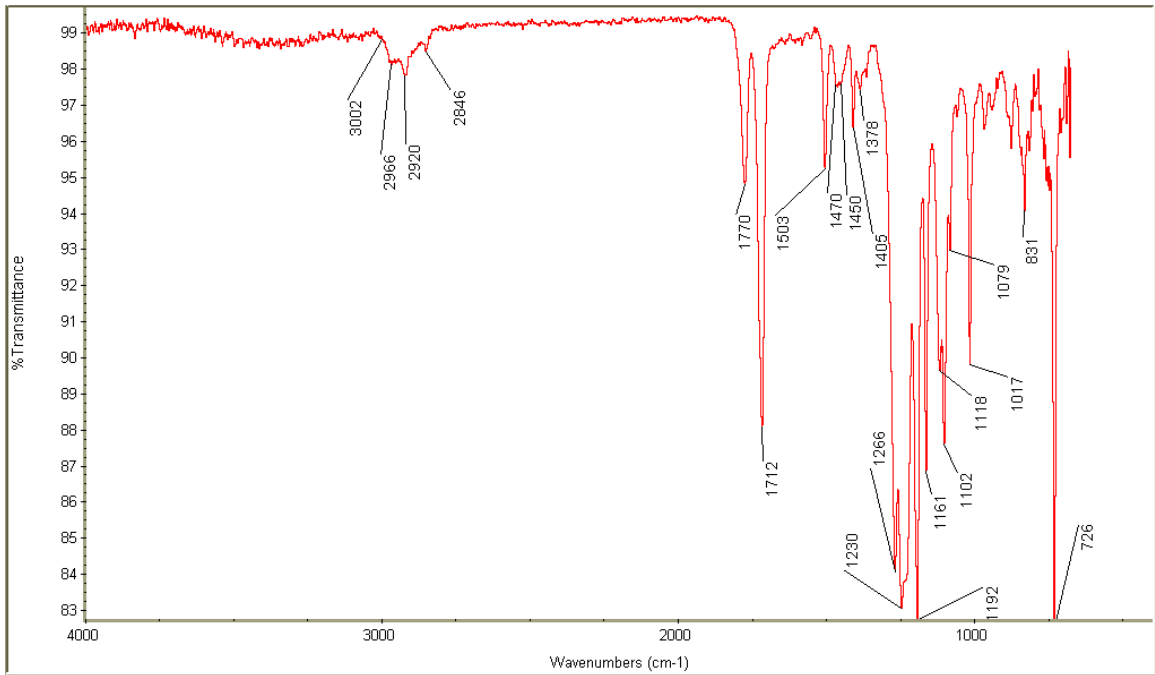


Fig 54: Analyzed Sample 1 IR spectra

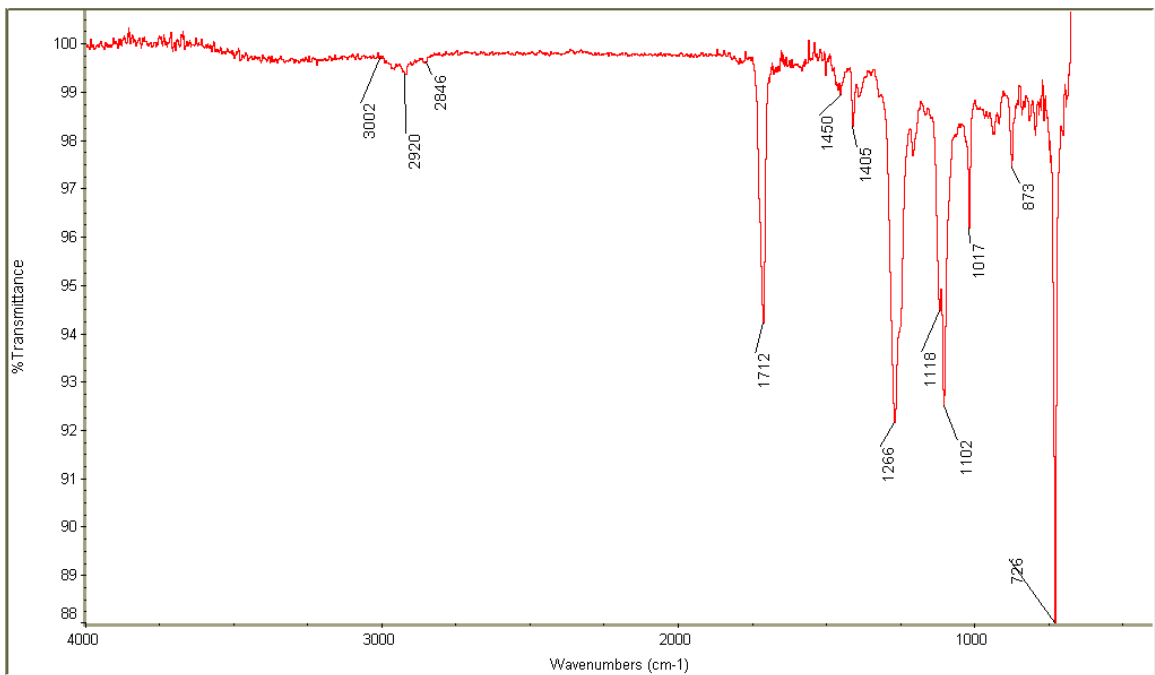


Fig 55: Referenced Polybutylene terephthalate

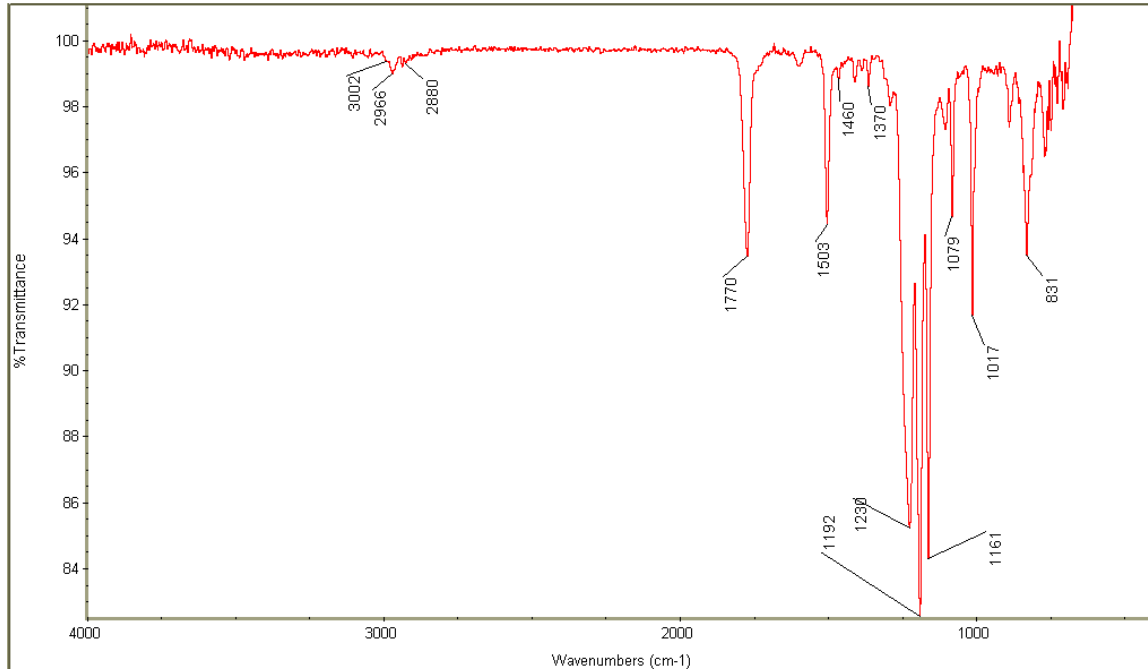


Fig 56: Referenced Polycarbonate

From the spectral of Sample1, it was determined that the spectra was a blend of PC and PBT. Therefore, the analysis will be performed which will include the cause of the peak and also which component is responsible for the peak. These peaks can be coordinated against the reference peaks for PBT and PC above.

The spectra begins with a peak at  $3002\text{ cm}^{-1}$ . This peak is caused by the C-H stretching on an aromatic ring. Both PC and PBT have an aromatic ring in their structures and are responsible for this peak. Following this peak is an overlap of peaks between  $2966$  and  $2846\text{ cm}^{-1}$ . These peaks are caused by the asymmetric and symmetric stretching of the methyl and methylene groups. These groups are present in both the PC

and PBT materials. The next major peak present is the  $1770\text{ cm}^{-1}$  peak. This peak is caused by the carbonyl group stretch of the ester present in the PC. The next peak at  $1712\text{ cm}^{-1}$  is an additional carbonyl group stretch of an ester, but this one is caused by the PBT. This peak is at a lower wavenumber because it is next to an aromatic ring in the PBT structure.  $1503\text{ cm}^{-1}$  is a peak caused by aromatic ring breathing in the PC. The peak at  $1460\text{ cm}^{-1}$  is split into a double at  $1450$  and  $1470\text{ cm}^{-1}$ . These peaks are caused by the methyl and methylene bending in the relevant materials. Ring breathing modes are captured for the PBT at  $1405\text{ cm}^{-1}$ . Methyl groups are only present in the PC and additional methyl stretches are seen at  $1378\text{ cm}^{-1}$ . Because the esters are in different environments within each material their characteristic “ester sisters” are slightly shifted. PBT has ester sisters present at  $1266$  and  $1017\text{ cm}^{-1}$ , while PC has its ester sisters present at  $1230$  and  $1017\text{ cm}^{-1}$ . The presence of an unsaturated ether is seen at  $1192\text{ cm}^{-1}$  and is caused by the PC. The position of the carbonyl group in the PC gives rise to the peak at  $1161\text{ cm}^{-1}$ . Conjugated ethers in the PBT cause a splitting of the  $1115\text{ cm}^{-1}$  peak into  $1118$  and  $1102\text{ cm}^{-1}$  peaks. The previous set of peaks has a shoulder at  $1079\text{ cm}^{-1}$  which is caused by the ester of the PC.  $831\text{ cm}^{-1}$  is a characteristic para-substituted aromatic ring. This is present in both the PC and the PBT. The final peak at  $726\text{ cm}^{-1}$  is caused by the four simultaneous methylene groups present in the PBT material. These peaks are consistent with the references for both PC and PBT.

The DSC measures the thermal transitions of the sample with respect to time and temperature. Utilizing the DSC, the glass transitions and melting points of the unknown material can be determined. This data is useful in identifying the unknown material and verifying the results of the FTIR. From the FTIR interpretation, initial composition of the

polymer determined it was a Polycarbonate-Poly(butylene terephthalate) blend. With this initial identification the thermal transition temperature ranges were determined. Polycarbonate (PC) is an amorphous material with a glass transition ( $T_g$ ) near 145 - 155°C. Poly(butylene terephthalate) (PBT) is a semicrystalline material with a glass transition region at approximately 40-60°C and a melting point ( $T_m$ ) near 200 - 220°C. Blends of these materials will manifest thermal behaviors dependent upon the ratio of the PC to PBT and the developed crystallinity of the PBT phase.

Sample 1 has thermal properties consistent with a PC-PBT blend. The PC glass transition portion of the blend is seen in the glass transition region of 140 - 150°C. The PBT thermal properties seen in the analysis included a glass transition region of 85 - 95°C and a melting region between 210 and 230°C. This glass transition is higher than the pure PBT glass transition and is caused by the blending with PC. A DSC plot of Sample 1 can be seen in Fig 57.

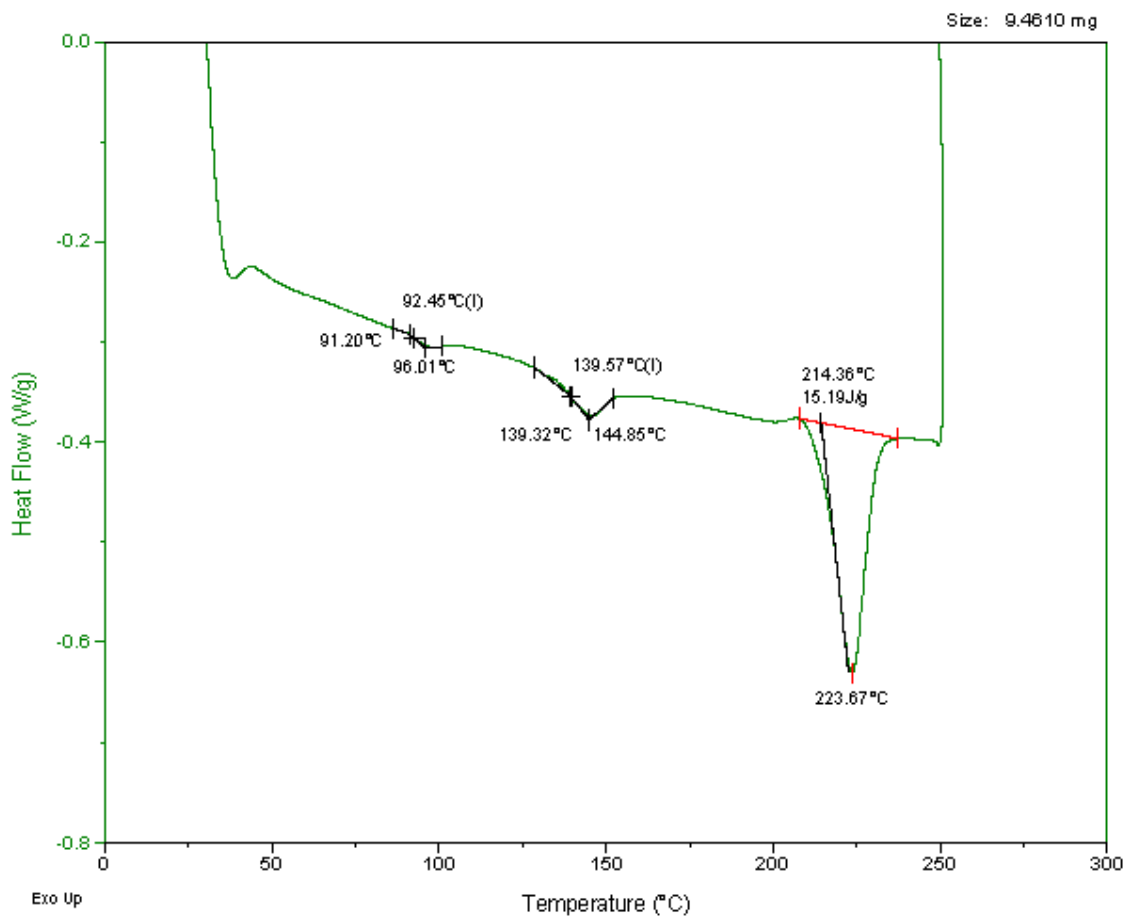


Fig 57: DSC plot of Sample 1

Thermal properties obtained from the DSC include:

Sample	PC Tg	PBT Tg	PBT Tm
Polycarbonate	145 – 155 °C	---	---
Poly(butylene terephthalate)	---	40 – 60 °C	200 – 220 °C
Sample 1	140 – 150 °C	85 – 90 °C	210 – 230 °C

These results confirm the FTIR initial determination of the composition of Sample 1 being a PC-PBT blend.

Dynamic Mechanical Analysis measures viscoelastic properties of a material as a function of time, temperature, and frequency. The previous evaluation on the DSC provided an upper evaluation temperature for Sample 1 on the DMA. If the melting temperature is reached, the sample will melt into the instrument causing future dilemmas; therefore, the sample was evaluated up to 225°C. Storage Modulus, Loss Modulus, and  $\tan \delta$  were evaluated on the DMA. Storage Modulus ( $E'$ ) is the ability of the material to return or store energy, it is the elastic portion of the material. Loss Modulus ( $E''$ ) is the ability of the material to lose energy due to friction and internal motion, it is also considered the materials inelastic portion.  $\tan \delta$ , also called damping, is the ratio of Loss Modulus ( $E''$ ) to Storage Modulus ( $E'$ ) and is relate to the materials ability to absorb a vibration or shock. These properties were characterized to determine Sample 1's viscoelastic property temperature dependence.

In Fig 58 it can be seen that Sample 1 goes through a set of  $\alpha$  and  $\beta$  glass transitions. The  $\alpha$ -transition is represented in the storage modulus as the drop from approximately 1300 MPa at 50°C to roughly 100 MPa at 150°C. Also the storage modulus shows a  $\beta$ -transition between -20 and -10 °C. These same glass transitions are seen in both the Loss Modulus and the  $\tan \delta$ . The Loss Modulus divides the  $\alpha$ -transition into a double transition with the first occurring between 90 – 100 °C and the second occurring between 125 – 135 °C. The  $\beta$ -transition is represented by the peak between -15

and  $-10^{\circ}\text{C}$ . The  $\text{Tan } \delta$  also separates the  $\alpha$ -transition into two different  $\alpha$ -transitions. This can be seen with the first occurring as the shoulder near  $100^{\circ}\text{C}$  on the main peak. The second  $\alpha$ -transition occurs approximately  $140$ - $150^{\circ}\text{C}$ . The  $\beta$ -transition is seen on the  $\text{Tan } \delta$  plot between  $-15$  and  $-10^{\circ}\text{C}$ .

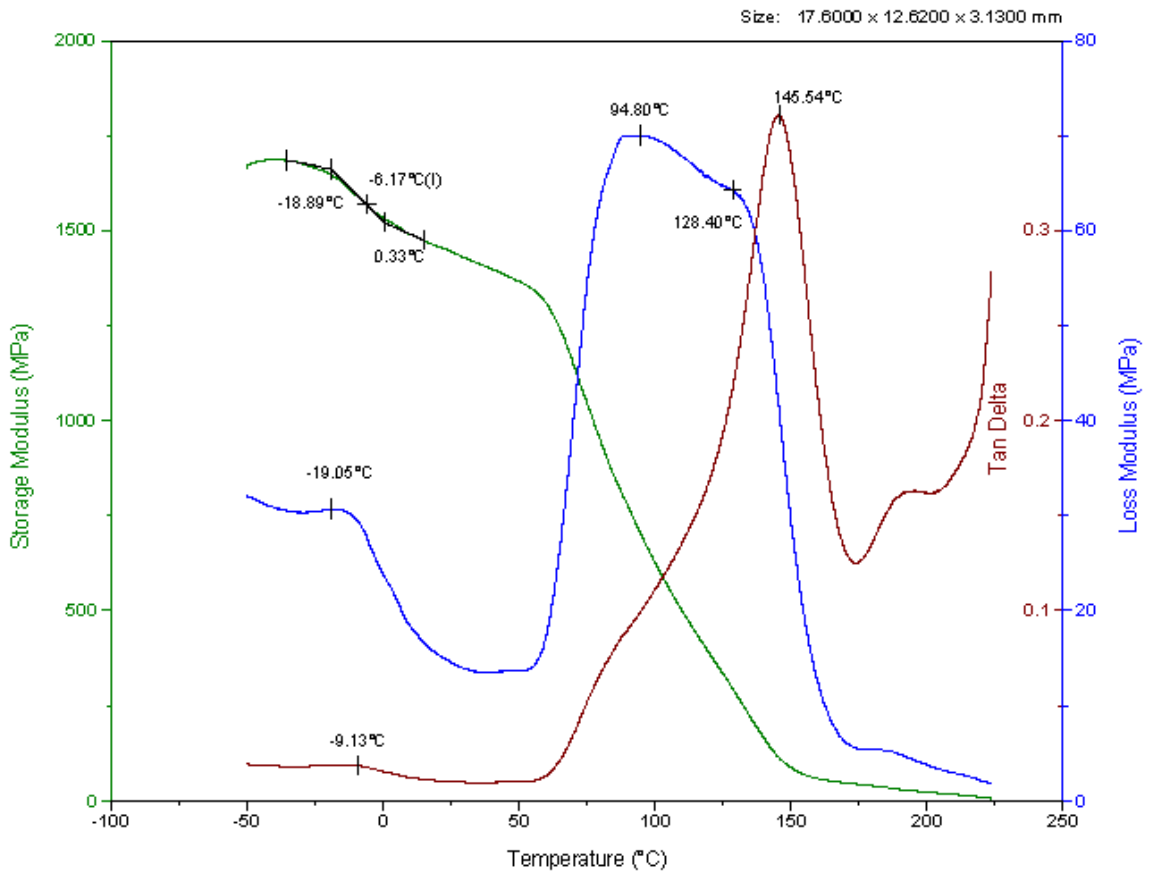


Fig 58: DMA plot of Sample 1

Thermomechanical analysis (TMA) measures the change in dimension of a material with respect to time and or temperature. Obtaining the sample's thermal expansivity was the main goal of the TMA experiments. The upper temperature of the evaluation was at the lower end of the first glass transition which was determined in previous experiments. The molded part was studied to determine flow patterns and two directions were chosen with respect to this discovered flow (flow direction and cross flow direction). These directions can be used to determine sample anisotropy. The thermal expansivities of the these directions overlapped between 130 – 138  $\mu\text{m}/\text{m}^\circ\text{C}$ . This leads to minimal or no anisotropy. This lack of anisotropy also signifies the absence of fiber reinforcement in the sample which will be determined in the TGA evaluation. A TMA plot of Sample 1 is seen in Fig 59.

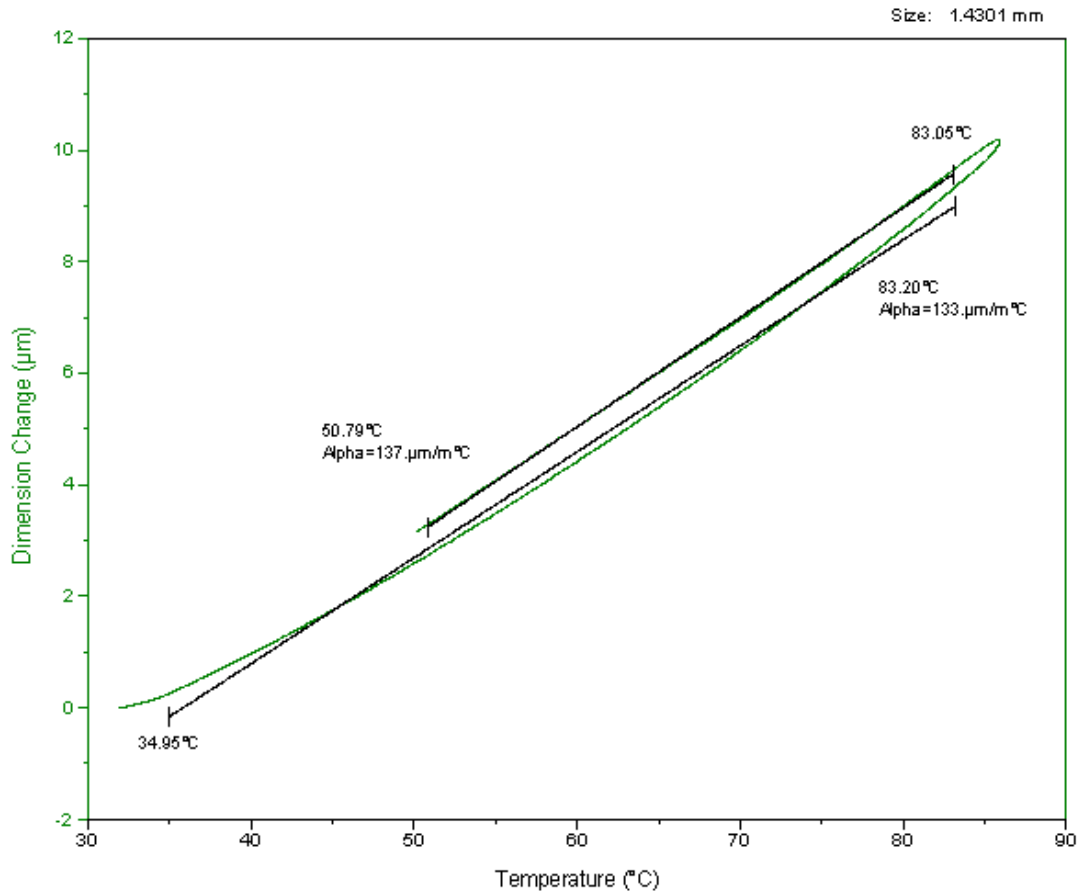


Fig 59: TMA of Sample 1

Dielectric Analysis measures the capacitive and conductive components of a material as a function of time, temperature, and frequency. Permittivity, loss factor, and ionic conductivity were all evaluated on Sample 1. The permittivity of Sample 1 is related to the molecular mobility of the material. The molecular mobility is related to the sample temperature and presence of glass transitions and melting temperatures. In Fig 60 the glass transitions of Sample 1 can be seen between 80 – 140 °C as an increase in molecular mobility and consequently an increase in permittivity. Ionic conductivity and loss factor also note the presence of the glass transitions with a steep positive slope through this region.

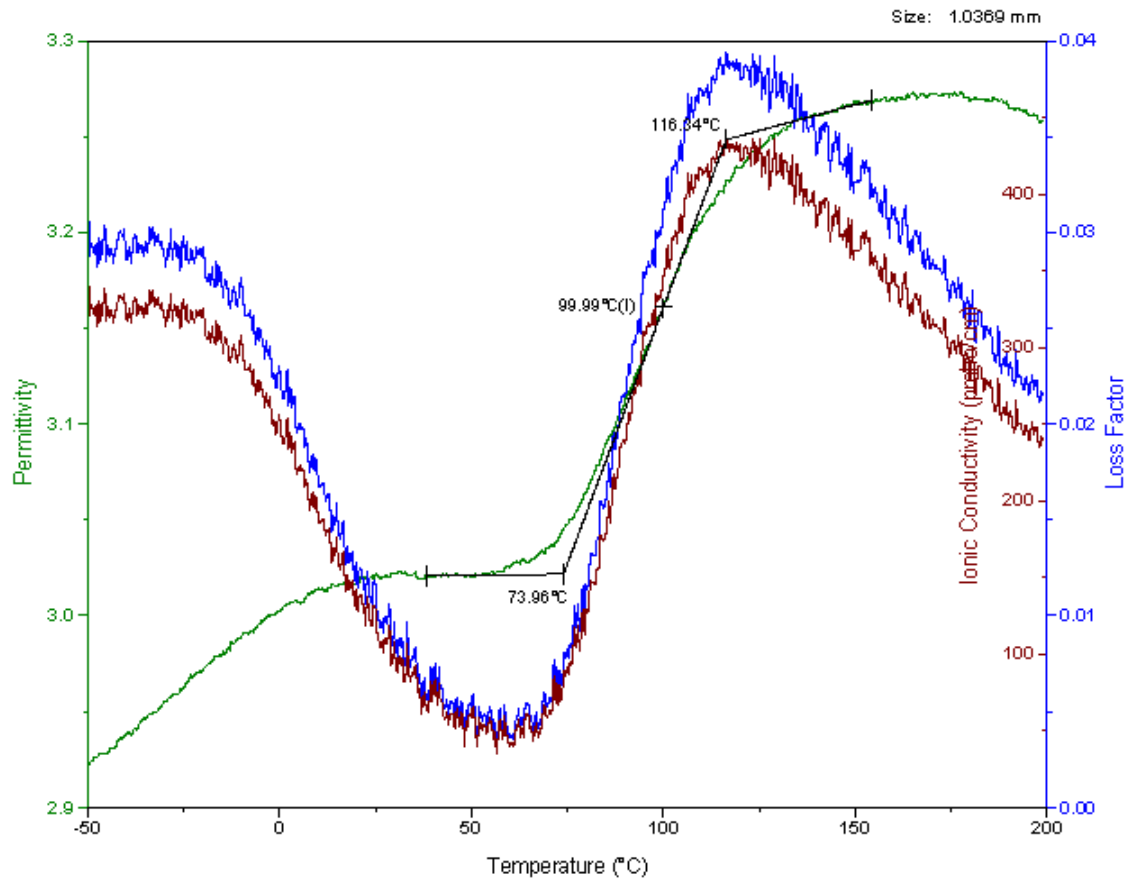


Fig 60: DEA of Sample 1

TGA measures weight change as a function of temperature and or time. In the TGA analysis, the minimum degradation temperature and the percent inorganic filler are of interest. The minimum degradation temperature is utilized in subsequent evaluations. The remaining percent ash allows for the determination of inorganic fillers, including glass fiber reinforcement, in the polymer. In Fig 61, Sample 1 has been determined to have a minimum degradation temperature of 305 – 310 °C in air. This TGA plot also concludes that there is approximately 2-3% inorganic filler. This inorganic residue was

further analyzed determining there was no glass fiber reinforcement, which was consistent with the previous TMA evaluation. This low percent of inorganic filler is probably either a mineral used for colorant or flame retardancy.

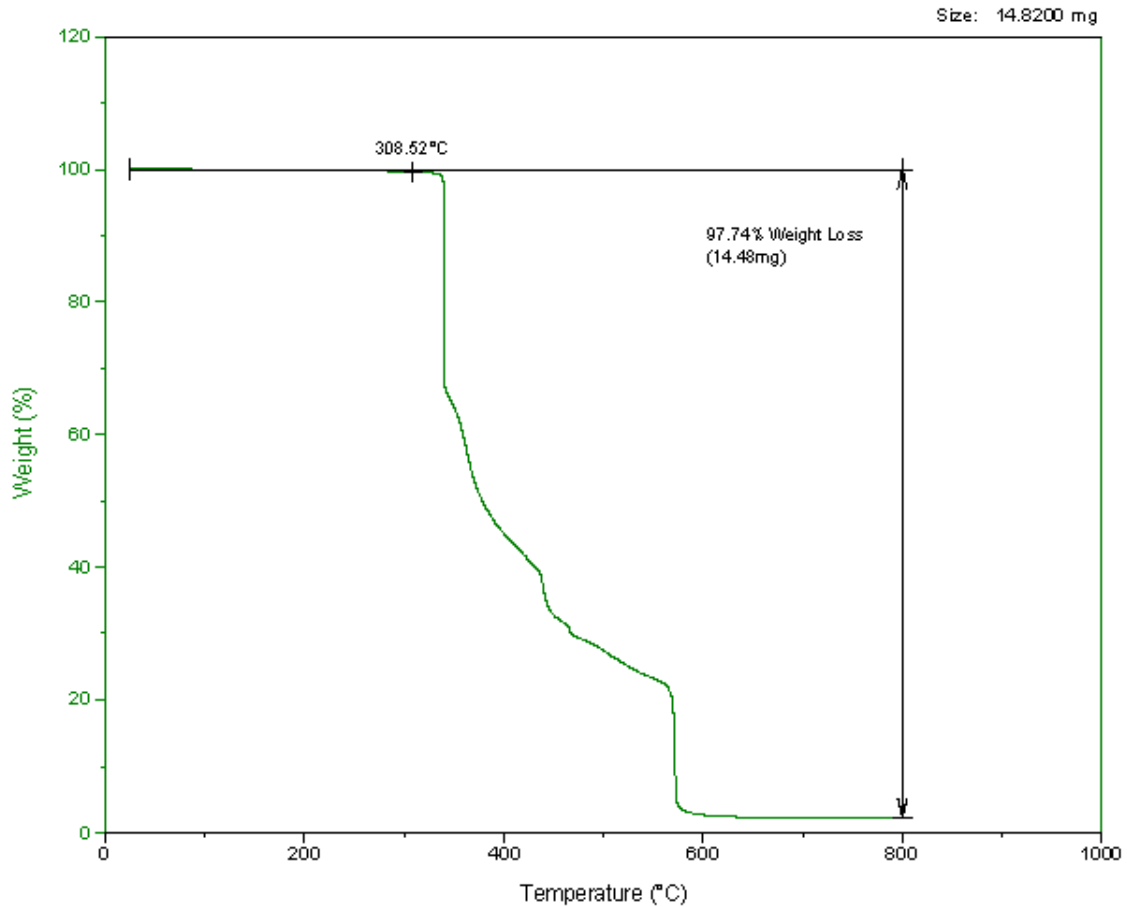


Fig 61: TGA of Sample 1

Through the combined extrusion and parallel plate rheology, an evaluation can be performed to predict important information about a polymer. Data collected on the extrusion rheometer and the parallel plate are fitted to a cross model through the use of the Cox-Mertz Rule. Application of the Cox-Mertz rule permits superposition of capillary and parallel plate data on a single shear rate-viscosity plot to yield a broader range of

shear rate-viscosity data. The Cox-Merz rule states that for rheologically simple materials the complex viscosity from dynamic measurements at a given frequency is equivalent to the steady shear viscosity at the same numerical value of shear rate. Thus the combined parallel plate-capillary rheometer plot for a polymer melt can cover a shear rate range of 0.1 to 20,000s<sup>-1</sup>. This method involves combining higher shear rate viscosity data from capillary rheometer with lower shear rate data from the parallel plate rheometer. By fitting this data to an appropriate steady shear viscosity model such as the “Cross” model critical parameters including the Newtonian plateau viscosity ( $\eta_0$ ), an indication of MWD ( $\tau^*$ ), and a power law or shear thinning index (n) are generated.  $\eta_0$  is related to  $M_w$  and thus to the critical part end-use properties.  $k$  is an indicator of the breadth of the molecular weight distribution of the sample. As  $k$  increases, the MWD decreases. In addition  $\eta_0$ ,  $\tau^*$ , and  $n$  are direct indicators of extrusion or injection molding melt processability. Once these parameters are established for a given polymeric raw material (resin) they can be used to assess lot-to-lot consistency as well as possible polymer degradation during extrusion or injection molding processing. This latter feature can be clarified by comparing the generated viscosity curves from the initial unprocessed (virgin) plastic resin and the corresponding extruded or injection molded part. Typically a significant downward shift in the viscosity curve for the processed part relative to the virgin resin is indicative of substantial thermal or mechanical degradation during melt processing; however, some polymers crosslink upon degradation and develop an increase in the viscosity curve upon degradation. The cross model evaluation at 255°C can be seen for Sample 1 in Fig 62.

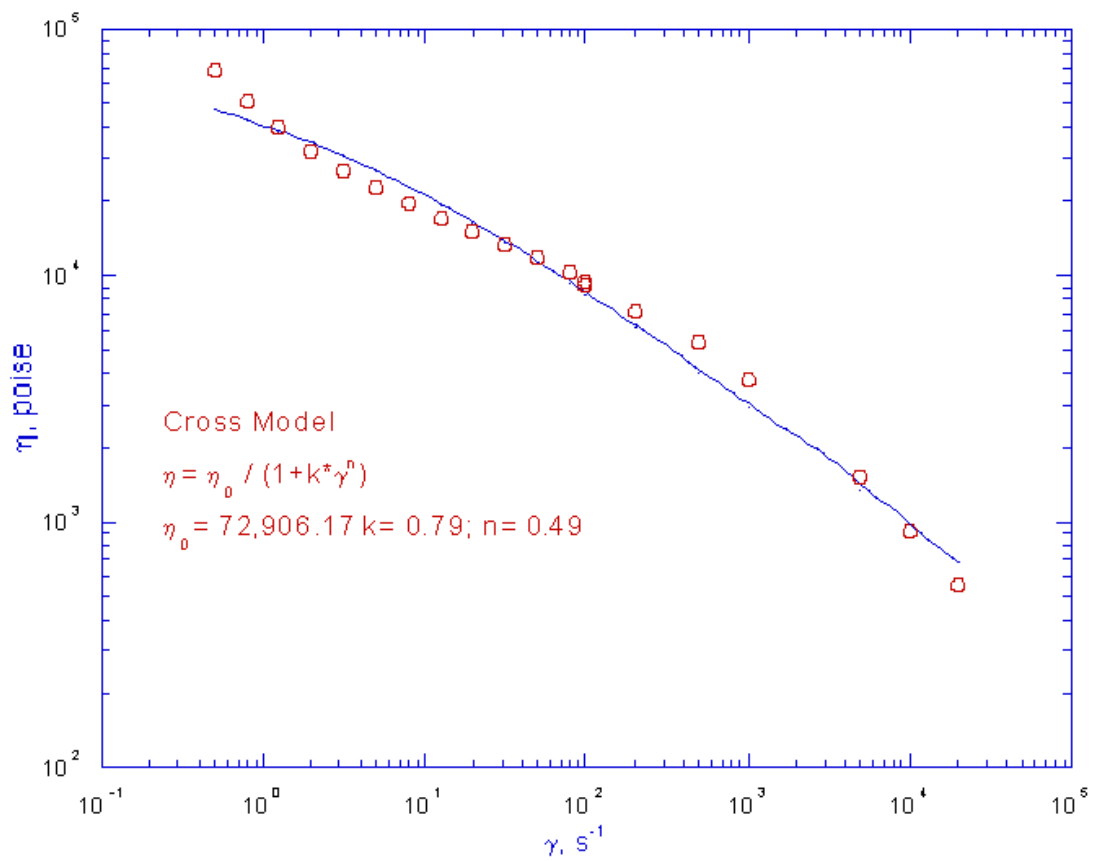


Fig 62: Cross model for sample 1 at 255°C

## 4.2 SAMPLE 2

Sample 2 is used in telecommunication connectors. This sample is a part of main components and is used in indoor applications. Throughout normal use, it is exposed to moderate temperatures. Sample 2 was characterized to determine the identity of this component. Initial compositional analysis was performed using FTIR analysis. The FTIR allows for the identification of chemical species, which can be combined to determine the identity of the unknown material. Through peak identification, it was determined that the base material composition of Sample 2 was polycarbonate. Additionally, comparisons were made between the material's spectra, the Hummel Polymer and Additives library, and various known materials spectra to verify these results. The corresponding IR spectra can be seen in Fig 63.

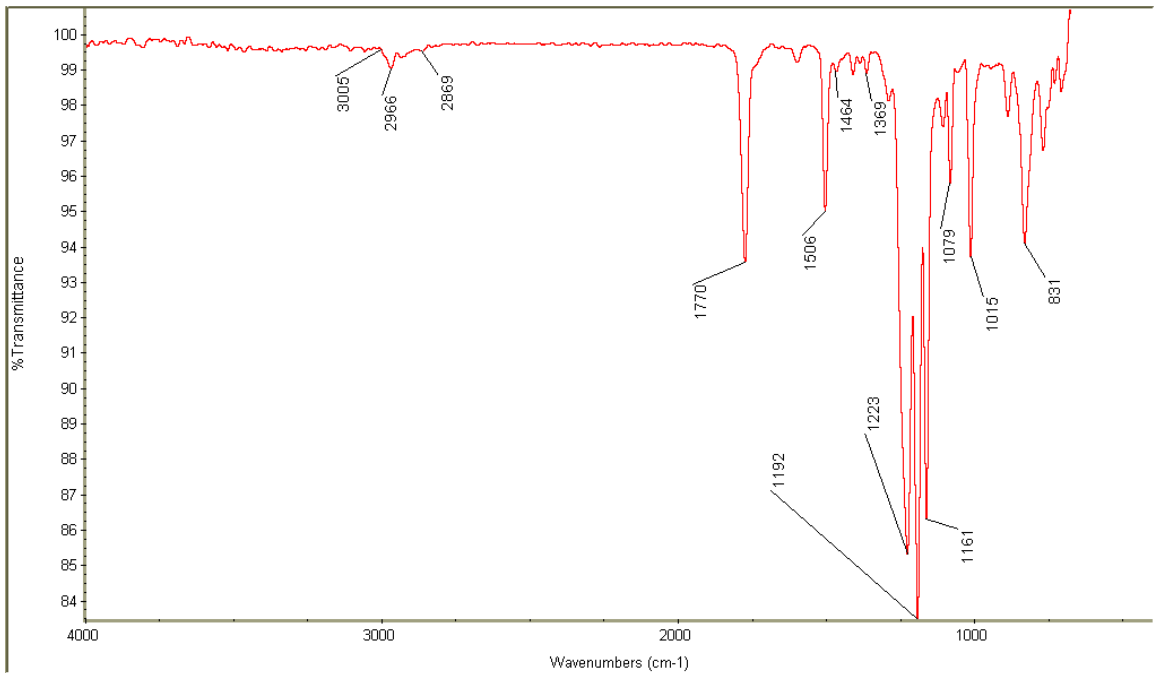


Fig 63: Sample 2 FTIR

The IR interpretation of Sample 2 begins at the higher wavenumbers and proceeds to the lower wavenumbers. The first peak encountered is at  $3005\text{ cm}^{-1}$ . This peak is caused by the C-H stretching on an aromatic ring structure. At slightly lower wavenumbers, there are peaks at  $2966$  and  $2869\text{ cm}^{-1}$ . These peaks are caused by the asymmetric and symmetric stretching of methyl groups. At  $1770\text{ cm}^{-1}$  there is a major peak caused by the carbonyl group stretch of the ester group present in the material. Aromatic ring breathing causes the peak at  $1506\text{ cm}^{-1}$ . Peaks caused by the methyl groups present in the material are seen at  $1464\text{ cm}^{-1}$ . These peaks are caused by the bending modes of the C-H bond in the methyl groups. Additionally, methyl bending motions are seen at  $1369\text{ cm}^{-1}$ . Sample 2 has an ester present as seen through the ester sisters at  $1233$  and  $1015\text{ cm}^{-1}$ . These peaks go along with the carbonyl peak at  $1770\text{ cm}^{-1}$ . There is the presence of unsaturated ether at  $1192\text{ cm}^{-1}$ . The surroundings of the carbonyl group in the structure gives rise to the peak at  $1161\text{ cm}^{-1}$ . At  $1079\text{ cm}^{-1}$ , there is an additional peak caused by the ester. And the final peak at  $831\text{ cm}^{-1}$  is the characteristic peak for a para-substituted aromatic ring. Through the combination of these peaks and experience it was determined that Sample 2 had a base polymer composed of Polycarbonate. This was verified through spectral libraries.

The DSC measures the thermal transitions of the sample with respect to time and temperature. Utilizing the DSC, the glass transition region of the unknown material can be determined. This data is useful in identifying the unknown material and verifying the results of the FTIR. From the FTIR interpretation, initial composition of the polymer determined it was polycarbonate. With this initial identification the thermal transition temperature ranges were determined. Polycarbonate (PC) has a glass transition ( $T_g$ )

region near 145 – 155 °C. Sample 2 has a glass transition region consistent with polycarbonate. Sample 2 has its glass transition region between 144 – 149°C. A DSC plot of Sample 2 can be seen in Fig 64.

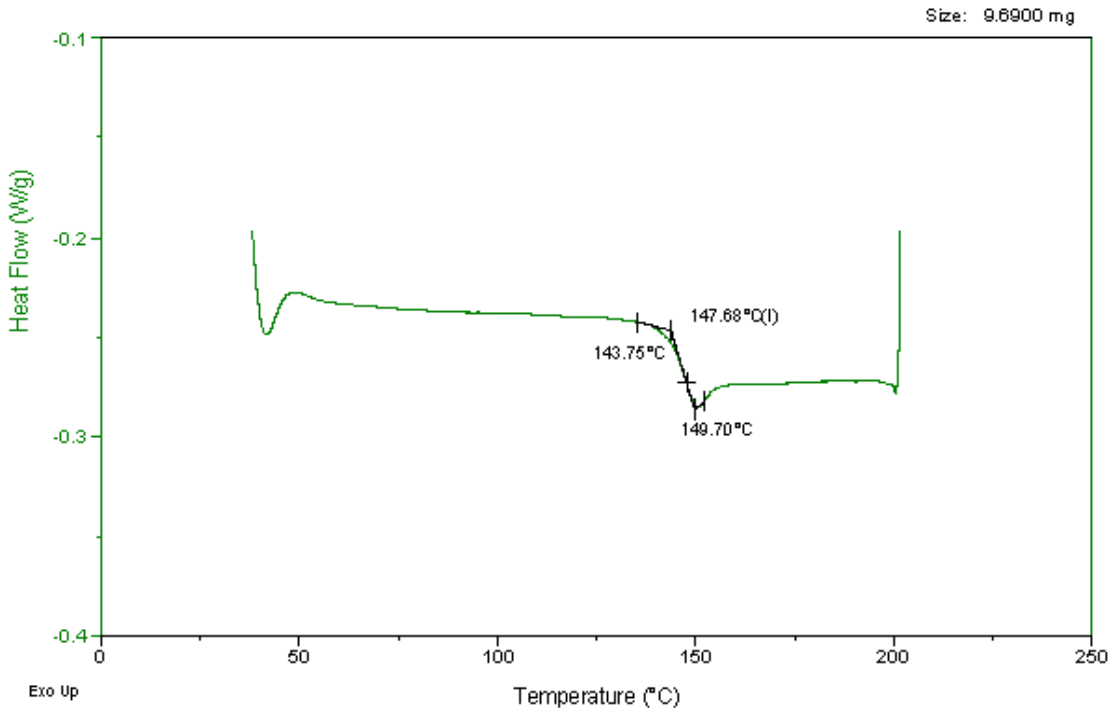


Fig 64: DSC plot of Sample 2

TGA measures weight change as a function of temperature and or time. In the TGA analysis, the minimum degradation temperature and the percent inorganic filler are of interest. The minimum degradation temperature is utilized in subsequent evaluations. The remaining percent ash allows for the determination of inorganic fillers, including glass fiber reinforcement, in the polymer. In Fig 65, Sample 2 has been determined to have a minimum degradation temperature of 420 – 430 °C in air. This TGA plot also

concludes that there is no inorganic filler in the material. This is determined by the 100% weight loss upon heating to 800°C.

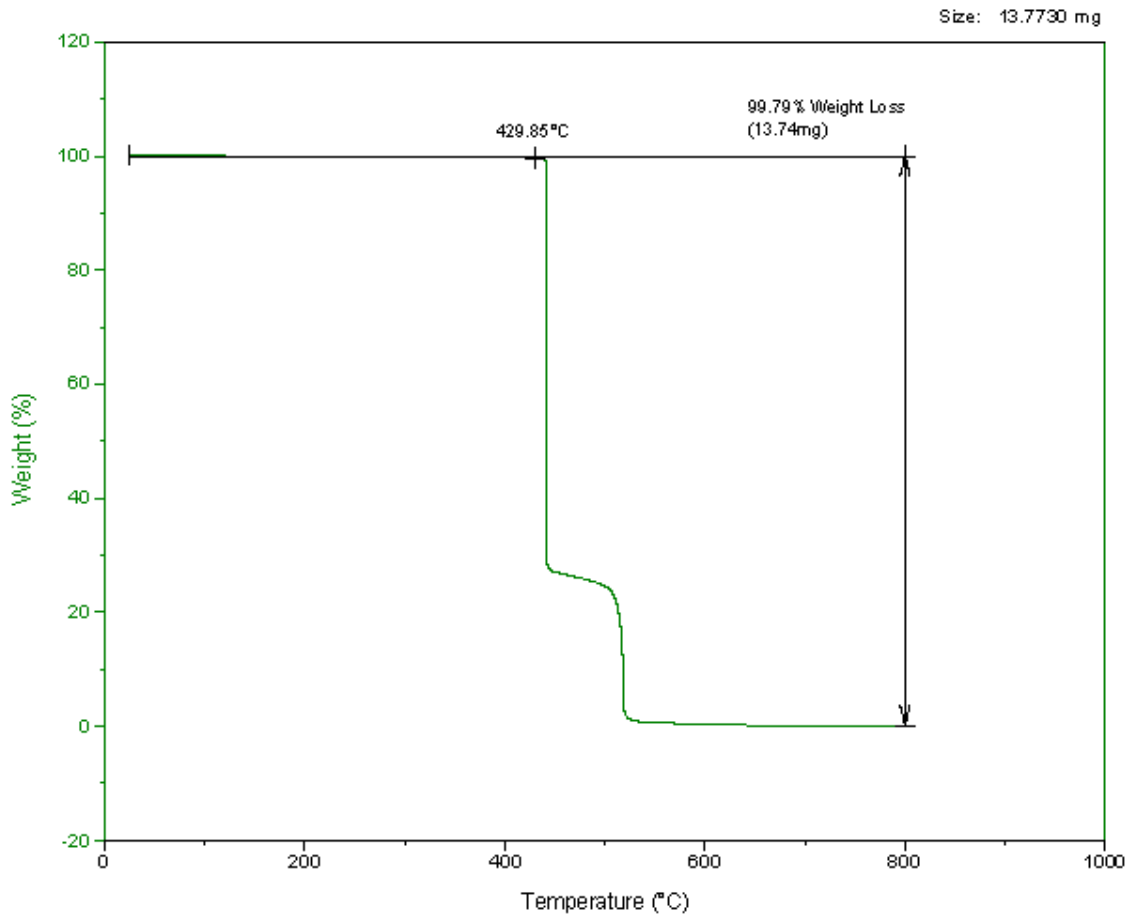


Fig 65: TGA analysis of Sample 2

Dynamic Mechanical Analysis measures viscoelastic properties of a material as a function of time, temperature, and frequency. The previous evaluation on the DSC provided an upper evaluation temperature for Sample 2 with the DMA. If the DMA

evaluation temperature is taken too much above the glass transition of the material, then the sample could flow into the instrument causing damage; therefore, the sample was evaluated up to 165°C. Storage Modulus, Loss Modulus, and Tan  $\delta$  were evaluated on the DMA. These properties were characterized to determine the materials viscoelastic property/temperature dependence.

Fig 66 is the DMA plot of Sample 2 analyzed between 0 – 165 °C at 10 Hz. In this plot, it can be seen that Sample 2 goes through a glass transitions between 140 and 150°C as determined by the peak of the loss modulus. This glass transition is consistent with a sharp decrease in the storage modulus of the sample. No  $\beta$  –glass transitions or melting points are seen for Sample 2 between 0 – 165°C.

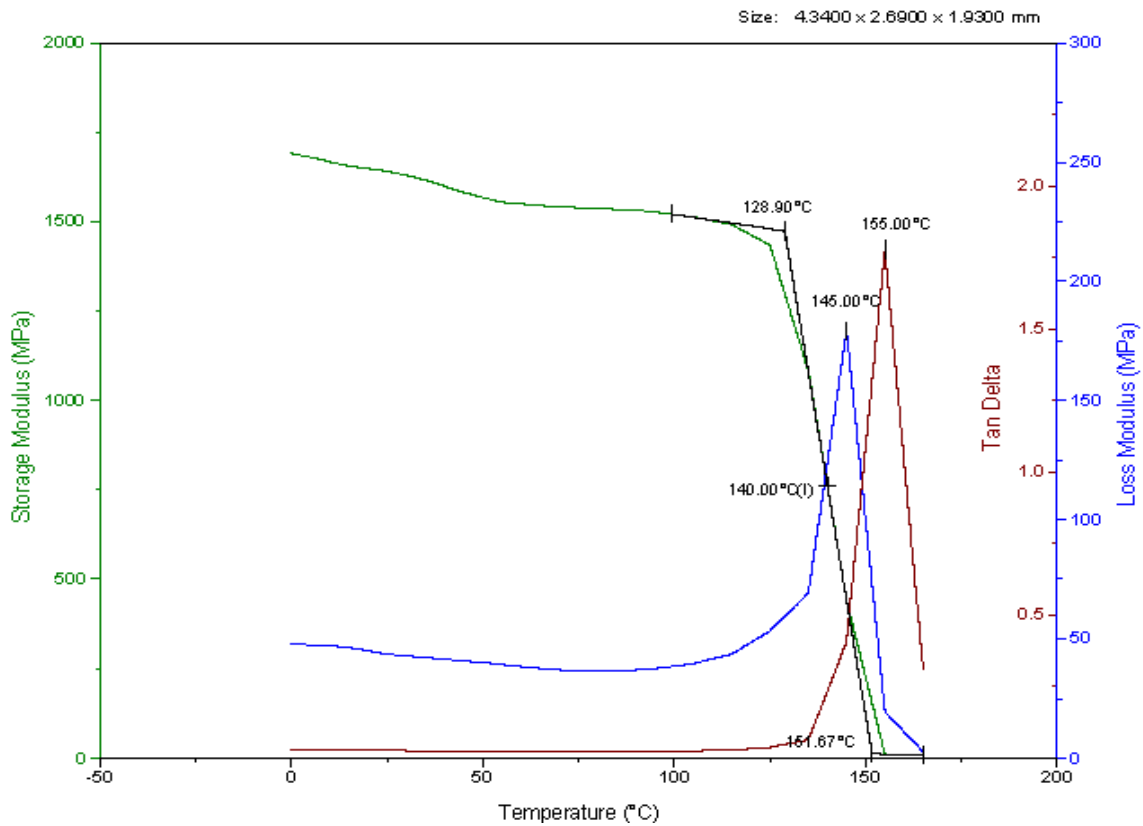


Fig 66: DMA analysis of Sample 2 at 10 Hz

The remaining rheological experiments consisted of several evaluations on several instruments. These evaluations required more than one instrument to perform the task. Through the combined extrusion and parallel plate rheology, an evaluation was performed to predict important information about Sample 2. By fitting this data to an appropriate steady shear viscosity model such as the “Cross” model critical parameters including the Newtonian plateau viscosity ( $\eta_0$ ), an indication of MWD ( $\tau^*$ ), and a power

law or shear thinning index ( $n$ ), an indicator of the breadth of the molecular weight distribution ( $k$ ) are generated. The cross model analysis can be seen for Sample 2 in Fig 67.

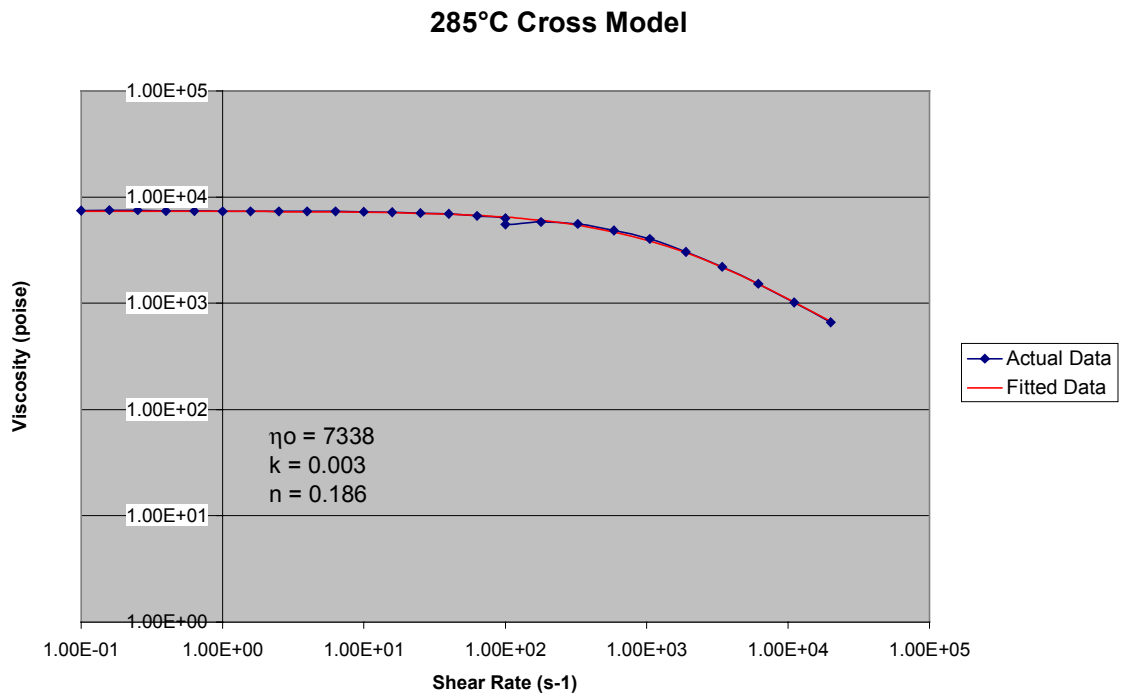


Fig 67: Cross Model of Sample 2

The combined parallel plate rheological and DMA data allow for the formation of a master curve of the data to predict storage ( $G'$ ) and loss ( $G''$ ) moduli at long times without having to test for long times. Modulus is a function of time as well as temperature which leads to the principle of Time Temperature Superposition (TTS).

Through the use of TTS a master curve can be generated that predicts moduli-time behavior at constant temperature. To be able to plot both the parallel plate and the DMA data on the same graph the DMA data needed to be converted to parallel plate data ( $E' \rightarrow G'$  and  $E'' \rightarrow G''$ ). This can be performed from the equation  $E = 2G(1 + \nu)$ ; where  $\nu$  is the Poisson's ratio of the material. The Poisson's ratio for Sample 2(PC) it is 0.42.

The Sample 2 master curve is given in Fig 68. The materials  $T_g = 145^\circ \text{C}$  was used for the  $T_r$  for this evaluation. In the master curve for Sample 2, the data has a discontinuity between the temperatures of  $140\text{-}135^\circ\text{C}$  and  $135\text{-}130^\circ\text{C}$ . The data was rerun and the same phenomenon occurred. This is because this material is not rheologically simple in this region.

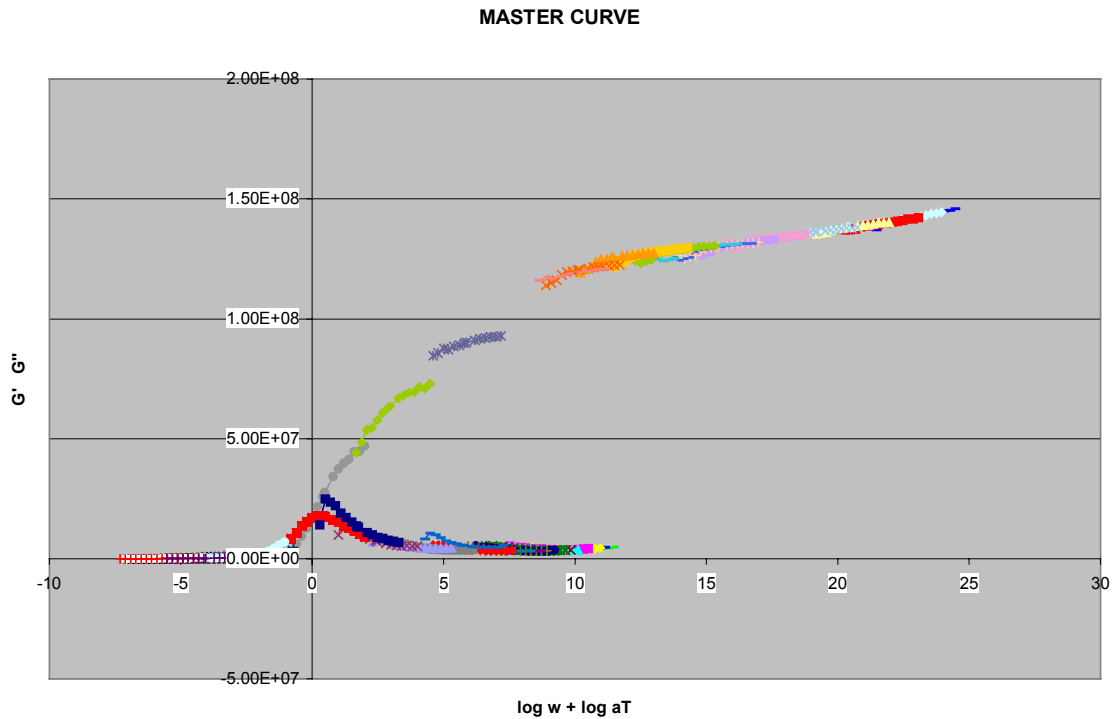


Fig 68: Master Curve of Sample 2

The final analysis involved DMA and parallel plate data, at 1Hz, being overlaid to create a complete  $G'$  and  $G''$  vs Temp graph. Sample 2's graph is represented in Fig 69 . The data up to 200°C represents the point where the DMA data ends and the parallel plate data begins. Again in this evaluation the DMA flex modulii (E) needed to be converted to shear modulii (G).

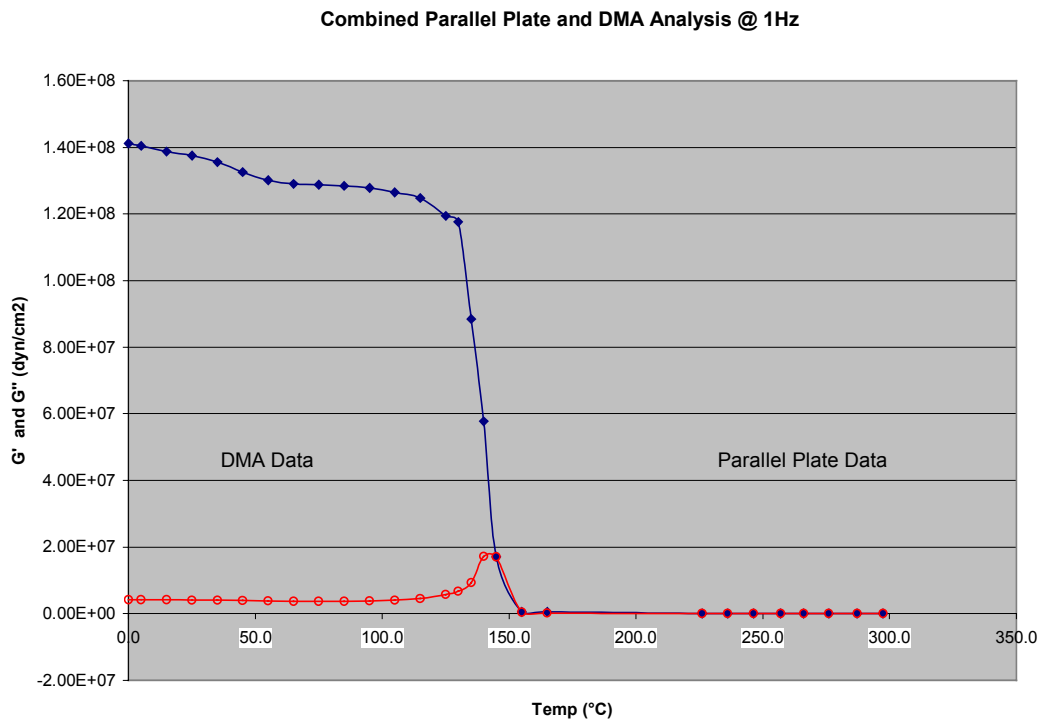


Fig 69: DMA/Parallel plate overlay at 1Hz of Sample 2

### 4.3 SAMPLE 3

Sample 3 is a fiber optic boot. It is the soft cone shaped polymer that surrounds the fiber optic cable just behind a fiber optic plug. The boot is used to avoid the fiber from becoming pulled too far to either side and being broken. This material is a total indoor application. The elements it will face include small temperature variations (less than 20°C) and very low or no UV radiation. Sample 3 was characterized to develop a base technology for these soft polymers and as a base for new material development. Initial compositional analysis was performed using FTIR analysis. The FTIR allows for the identification of chemical species, which can be combined to determine the identity of the unknown material. Through peak identification, it was determined that the base material composition of Sample 3 was a polyolefin.

The spectral analysis begins with the quartet of peaks between 2960 and 2835  $\text{cm}^{-1}$ . These peaks are characteristic of methyl and methylene symmetric and asymmetric stretching. An additional peak caused by these methyl and methylene groups is the peak at 1456  $\text{cm}^{-1}$  which is caused by the bending motions of these groups. Methyl groups have another peak at 1378  $\text{cm}^{-1}$  which is caused by a different bending motion in the group. The final important peak in determining the identity of the material is the peak at 722  $\text{cm}^{-1}$ . This peak is caused by long chain wagging of the methylene groups. Groups such as the 804 and 679  $\text{cm}^{-1}$  are filler peaks which match that of halogenated flame retardants. The presence of large amounts of CH<sub>2</sub> and CH<sub>3</sub> along with the presence of a long chain polymer peak and absence of unsaturated peaks leads to the assumption that

the polyolefin present consists of Polyethylene and Polypropylene. Additionally, comparisons were made between the material's spectra, the Hummel Polymer and Additives library, and various known materials spectra to verify these results. The corresponding IR spectra can be seen in Fig 70.

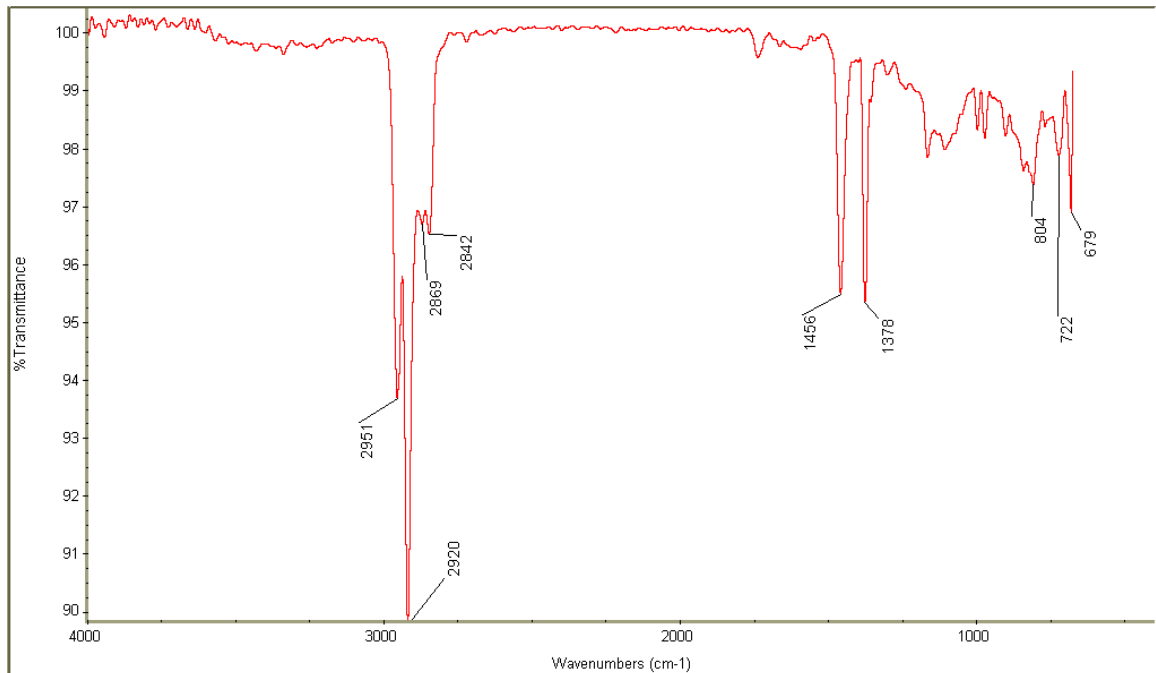


Fig 70: FTIR analysis of Sample 3

The DSC measures the thermal transitions of the sample with respect to time and temperature. Utilizing the DSC, melting points of the unknown material can be determined. This data is useful in identifying the unknown material and verifying the results of the FTIR. From the FTIR interpretation, initial composition of the polymer determined it was a polyolefin, probably a polyethylene-polypropylene. With this initial identification the thermal transition temperature ranges were determined. Polyethylene (PE) is semicrystalline material with a melting point ( $T_m$ ) between 110 and 140°C depending upon the type of polyethylene. Polypropylene (PP) is a semicrystalline material with a melting point ( $T_m$ ) near 155 – 165 °C. Blends and copolymers of these materials will manifest thermal behaviors dependent upon the ratio of the PE to PP. Sample 3 has thermal properties consistent with a polyethylene-polypropylene blend. The PE melting point of the blend is seen in the melting region of 115 - 125°C. The PP thermal property seen in the analysis is a melting region between 140 and 170°C with a peak near 160°C. The information determining this polymer to be a blend and not a copolymer is a separation of melting points of the PE and PP on consecutive heating runs. A DSC plot of Sample 3 can be seen in Fig 71.

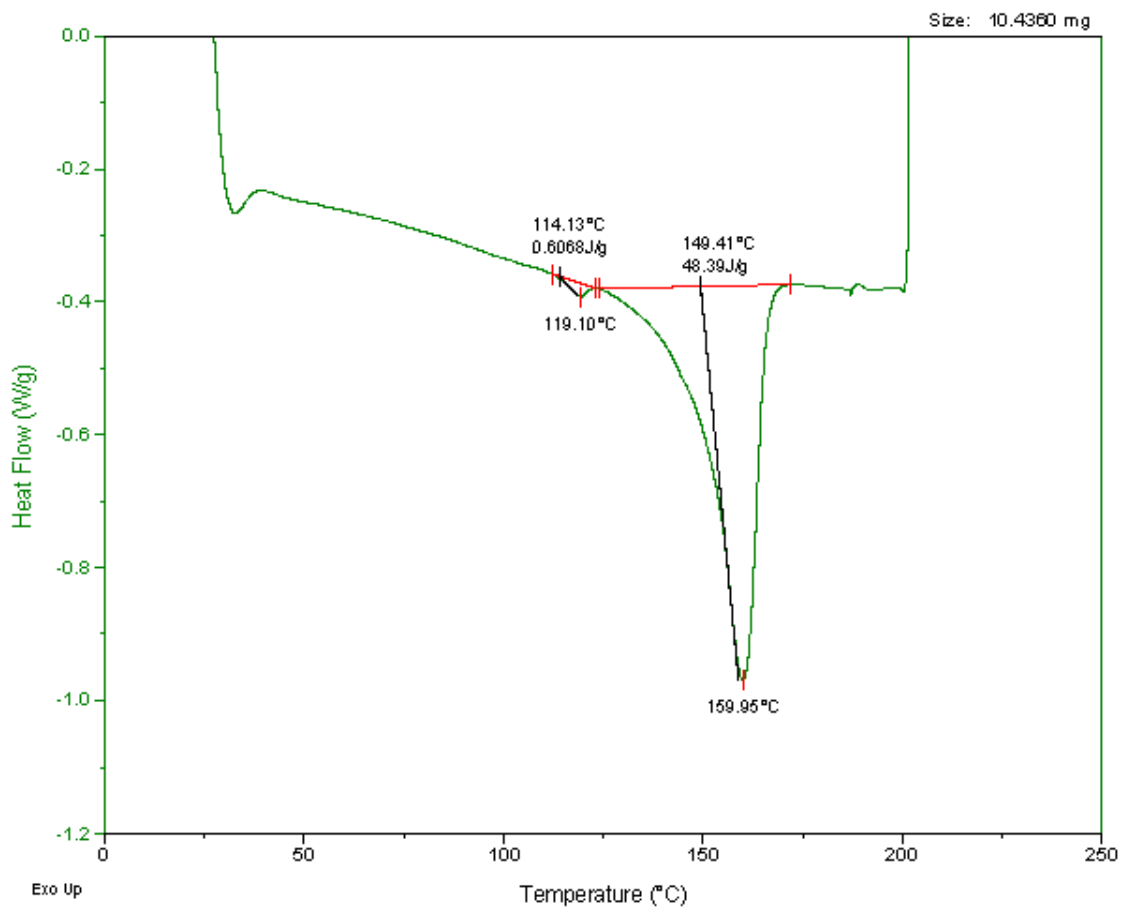


Fig 71: DSC plot of Sample 3

Thermal properties obtained from the DSC include:

Sample	PE Tm	PP Tm
Polyethylene	110 – 140 °C	---
Polypropylene	---	155 – 165 °C
Sample 3	115 – 125 °C	140 – 170 °C

These results confirm the FTIR initial determination of the composition of Sample 3 being a Polyethylene-Polypropylene blend.

Thermomechanical analysis (TMA) measures the change in dimension of a material with respect to time and or temperature. Obtaining the sample's thermal expansivity was the main goal of the TMA experiments. The upper temperature of the evaluation was determined to be a temperature just below the melting temperature of polyethylene. The molded part was studied to determine flow patterns and two directions were chosen. These directions can be used to determine sample anisotropy. The thermal expansivities of the these directions overlapped between 115 – 125  $\mu\text{m}/\text{m}^\circ\text{C}$ . This leads to minimal or no anisotropy. This lack of anisotropy also signifies the absence of fiber reinforcement in the sample which will be determined in the TGA evaluation. A TMA plot of Sample 3 is seen in Fig 72.

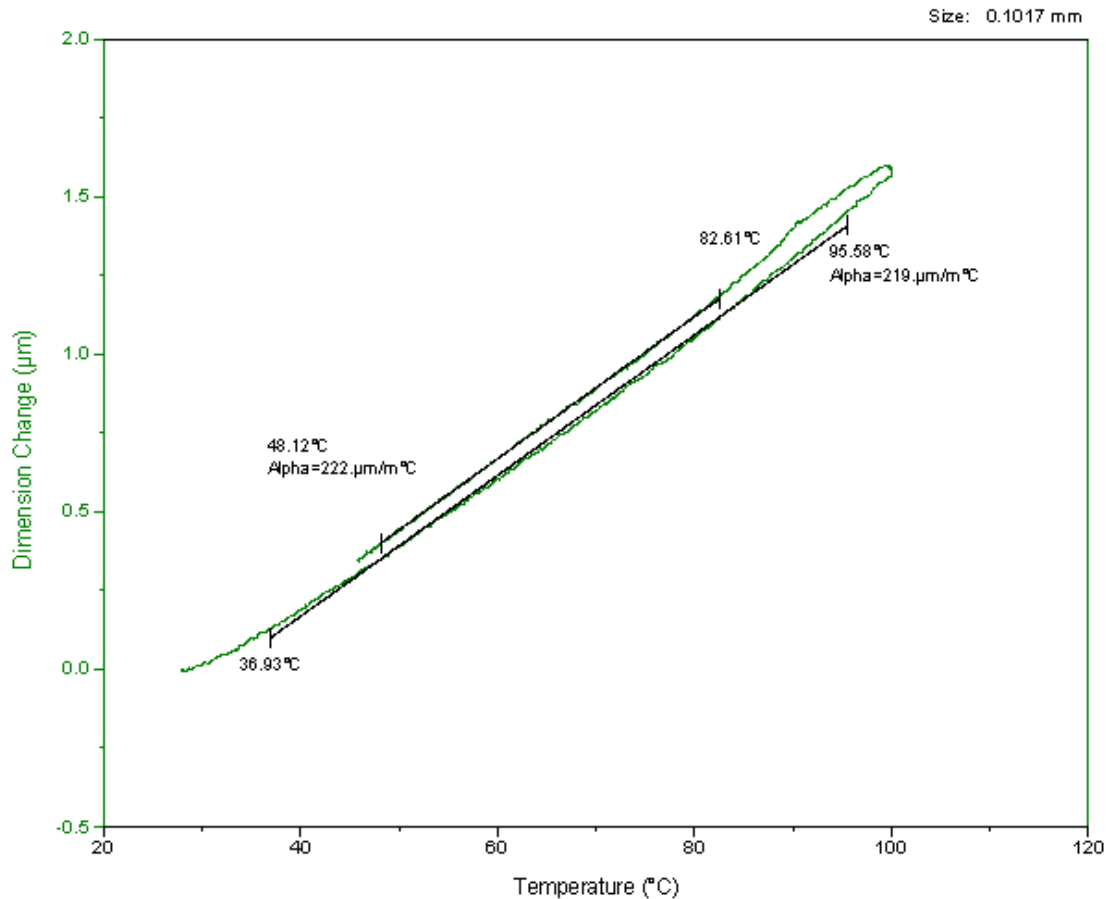


Fig 72: TMA of Sample 3

Dynamic Mechanical Analysis measures viscoelastic properties of a material as a function of time, temperature, and frequency. The previous evaluation on the DSC provided an upper evaluation temperature for Sample 3 on the DMA. Storage Modulus, Loss Modulus, and Tan  $\delta$  were evaluated on the DMA. These properties were characterized to determine Sample 3's viscoelastic property temperature dependence. Fig 73 is the plot of Sample 3's DMA analysis. This evaluation was performed to compare

improved materials viscoelastic properties against. It can be seen in the plot that there are no glass transitions in the temperature region evaluated.

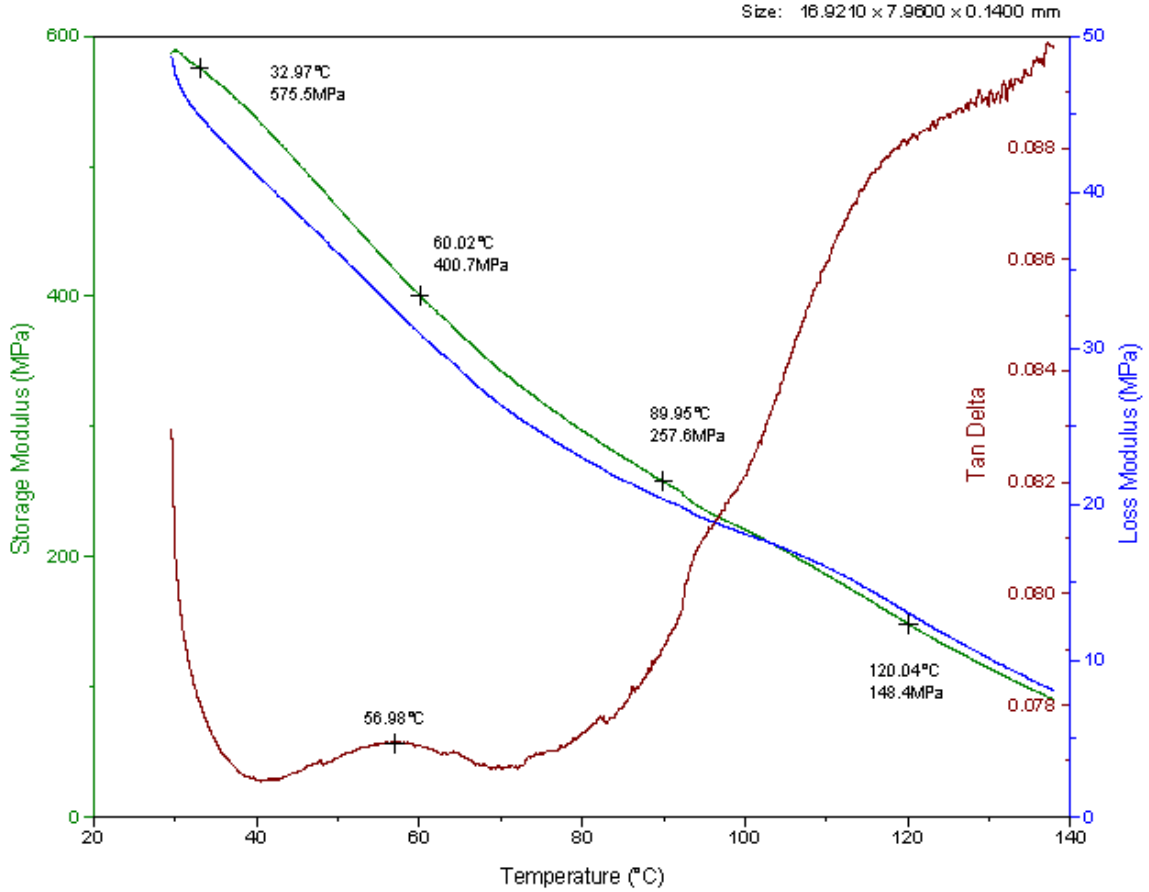


Fig 73: DMA of Sample 3

TGA measures weight change as a function of temperature and or time. In the TGA analysis, the minimum degradation temperature and the percent inorganic filler are of interest. The remaining percent ash allows for the determination of inorganic fillers, including glass fiber reinforcement, in the polymer. In Fig 74, Sample 3 has been

determined to have a minimum degradation temperature of 270 – 280 °C in air. This TGA plot also concludes that there is approximately 7.5 – 8.5 % inorganic filler. This inorganic residue was further analyzed determining there was no glass fiber reinforcement, which was consistent with the previous TMA evaluation. This low percent of inorganic filler is either a mineral used for colorant or flame retardancy.

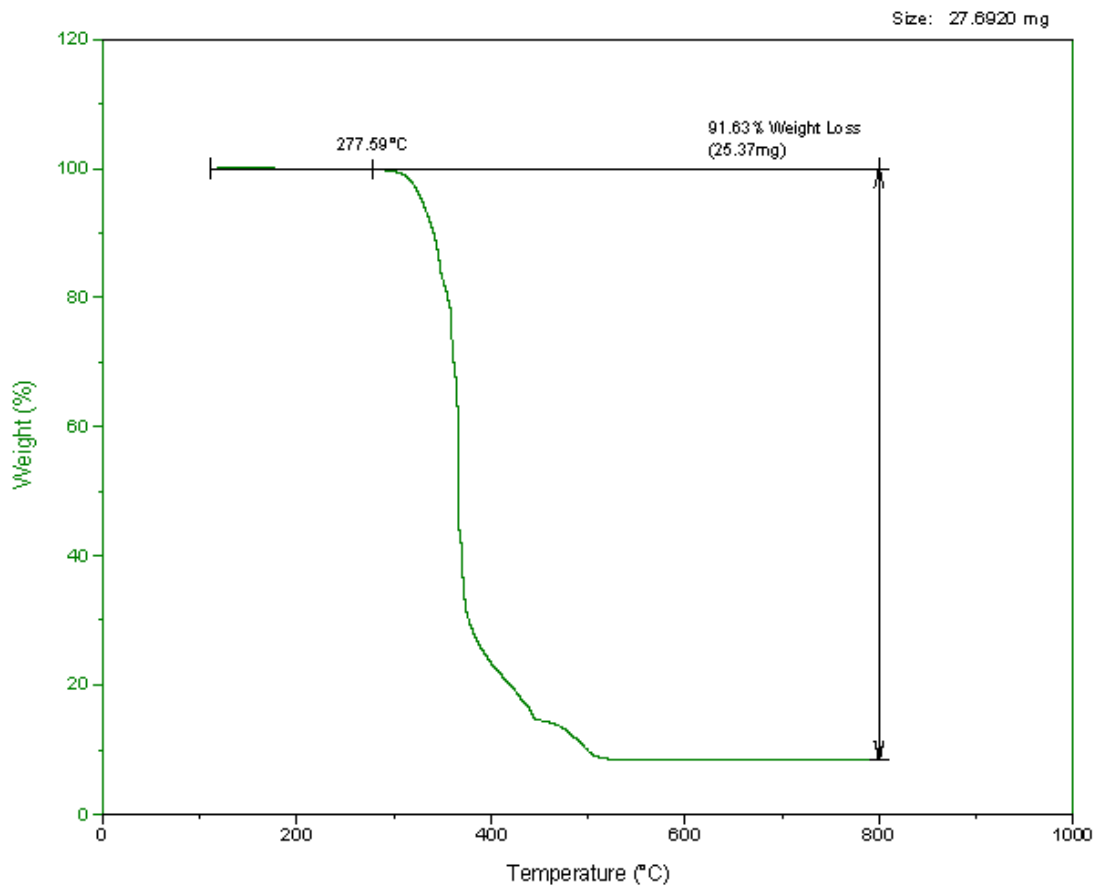


Fig 74: TGA of Sample 3

Rheology is the deformation and flow of materials. The viscosity function is necessary in order to determine the processability of a material over a given operational range of shear rates. This information is critical for molding equipment design and processing condition optimization. This data can be used to model the injection molding processing of critical components through computerized mold filling, packing, and cooling simulations. These simulations are very important for the proper sizing of mold part, runner, gate, and sprue dimensions.

Another useful tool of rheology is to predict the end product properties. This can be done in several ways by comparing zero shear viscosities of materials or by determining the shear rate dependence of the material. Rheological characterization techniques supply vital information regarding polymer material processability and possible MW changes (degradation) resulting from processing or conditioning. The storage modulus of a material is the portion of the sample which is completely recoverable. The loss modulus is the portion of energy that is lost due to friction and internal motion. It is not recoverable. The  $\tan \delta$  of a material is the ratio of the viscous to elastic component of the material. The measured visco-elastic moduli of the sample consists of storage and viscous contributions. Of these two moduli the useful one correlating to end-product performance (i.e., heat distortion) is the storage modulus as discussed earlier. By analyzing the storage modulus and  $\tan \delta$ , we can determine how the material reacts under the simulated real life conditions.

Fig 75 is a plot of the controlled strain torsion rheology data for Sample 3. Important data obtained from this plot include the shear thinning of the sample, the zero shear viscosity, and the cross over point of storage and loss moduli. The amount of shear

thinning of this material is important for mold filling and packing. This needs to be compared to future materials to ensure proper mold filling and packing. The zero shear viscosity of this material is near 200000 P. This can be used in the formula  $\eta = MW^{3.4}$  to obtain an approximate molecular weight. The cross over point of the storage and loss modulus marks the shear rate at which the elastic properties overcome the viscous properties. This is an important factor for real life applications.

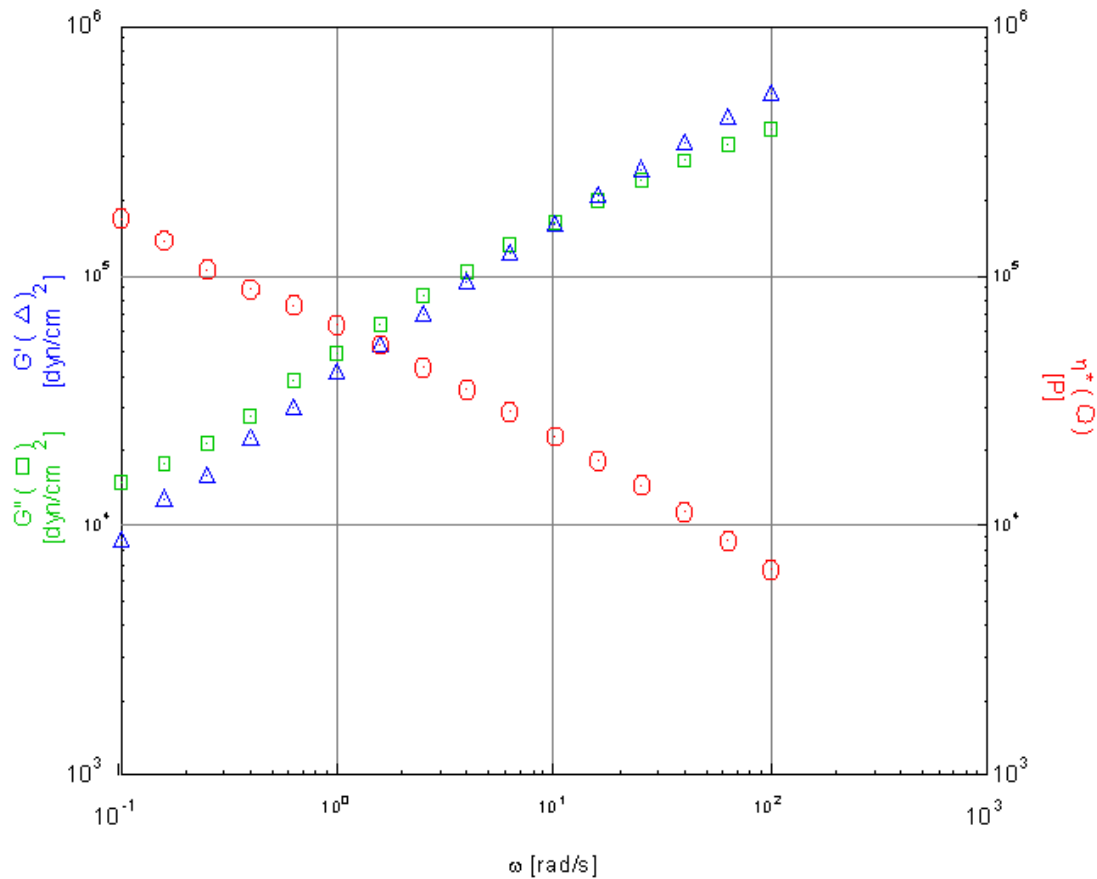


Fig 75: Rheology of Sample 3

## CHAPTER 5

### Discussion and Recommendations

#### 5.1 Sample 1

Sample 1 is used as an outdoor enclosure for telecommunication products. It's operation exposes it to UV radiation, extreme thermal cycling, rain, ice, and generally any other element possible in the continental United States. Sample 1 was evaluated to find an improvement material for replacement in similar enclosures. Many characterization techniques were joined to identify the composition of Sample 1. Through infrared analysis, thermal analysis, and rheological characterization it was determined that Sample 1 was an unfilled Polycarbonate-Poly(butylene therephthalate) blend.

Initially Fourier Transform Infrared analysis determined the base polymer chemistry to be a PC-PBT blend. This was performed through peak identification and correlation. Verification of the FTIR results was performed on the Differential Scanning Calorimeter. Through the use of the DSC, Sample 1's melting temperature and glass transition temperatures were determined. Sample 1 has a melting region of 210 – 230°C for the PBT portion of the blend. There are two glass transition regions associated with

Sample 1. The first glass transition region occurs between 85 – 90 °C and is also caused by the PBT portion of the blend. The second glass transition region occurs between 140 – 150 °C and is produced by the PC in the blend. This data was utilized in verifying the results of the FTIR and to set parameters for the remaining evaluations.

Dynamic Mechanical Analysis used the information obtained by the DSC as guidelines and produced the solid state viscoelastic properties of Sample 1. Due to this product's application, it was necessary to perform the DMA evaluation over a large temperature range. The evaluation was between –50 and 225°C. Important data obtained from this experiment included the storage modulus/temperature dependence and  $\alpha$  and  $\beta$  transitions. The modulus/temperature dependence is important because this product has an outdoor application where the temperature varies greatly. The  $\alpha$ -transitions determine the region at which there becomes a sharp decline in storage modulus. Sample 1 has 2  $\alpha$ -transitions. The first occurs between 90 and 100 °C and the second occurs between 125 and 135°C. These glass transitions establish the maximum useful temperature, with predictable modulus, to be between 60 and 75°C. The  $\beta$ -transition is equally important. The  $\beta$ -transition is caused by whole side chains and localized groups beginning to have enough space to move causing the material to begin to develop some toughness. This can be related through the  $\beta$ -transition peak on the Tan  $\delta$  plot. The size and location of the  $\beta$ -transition peak is important. The larger the  $\beta$ -transition the greater the materials ability to withstand an impact; however, if the impact occurs at a temperature lower than the  $\beta$ -transition there is not enough energy in the material to allow side chain movements and the material could fracture. It is important to ensure the  $\beta$ -transition is at a temperature lower than the application temperature. The  $\beta$ -transition for Sample 1 is between –20

and  $-10^{\circ}\text{C}$ . The size of the  $\beta$ -transition is small and could be used for comparison to future formulated materials.

Thermal Mechanical Analysis also relies on the previous characterizations and the product's application. Through TMA, the sample's thermal expansivity was determined and can be compared to other materials that come in contact with it. It is important that mating components have similar thermal expansivities so that through a temperature cycle these components don't expand and contract at different rates and become detached from each other. Sample 1 has a thermal expansivity of  $130 - 138 \mu\text{m}/\text{m}^{\circ}\text{C}$  in both flow and cross-flow directions; therefore, there is no anisotropy in this material. Also, this leans to the assumption that there are no fibers present in the sample.

Dielectric Analysis is an important characterization to determine the capacitance and conductance of a material. These properties are important if the product is used as an insulator or needs electrostatic discharge capabilities. The DEA analysis of Sample 1 shows the glass transition region, but the most useful utilization of this data is for comparison between similar materials to determine which most closely matches the needs of the product.

Thermogravimetric Analysis was used to verify the assumption created by the TMA regarding fiber reinforcement and to determine the minimum degradation temperature for use in subsequent rheological characterizations. The TGA evaluation determined there to be 2-3 % inorganic filler in Sample 1. This filler is probably colorant and/or flame retardant. The minimum degradation temperature for Sample 1 is  $305 - 310^{\circ}\text{C}$ , when combined with the melting temperature obtained by the DSC creates a processing window for use in rheological characterizations and material processing.

Through the combined extrusion and parallel plate rheology techniques, an evaluation can be performed predicting important polymer information. By fitting this data to the “Cross” model critical parameters including the Newtonian plateau viscosity ( $\eta_0$ ), a gauge of the breadth of the molecular weight distribution ( $k$ ), an indication of MWD ( $\tau^*$ ), and a power law or shear thinning index ( $n$ ) are generated.  $\eta_0$  is related to  $M_w$  and thus to the critical part end-use properties. As  $k$  increases, the MWD decreases. In addition  $\eta_0$ ,  $\tau^*$ , and  $n$  are direct indicators of extrusion or injection molding melt processability. These values are extremely important when trying to reproduce a material as a starting point for improved material development. The average molecular weight of Sample 1 can be determined by using the equation  $\eta_0 = MW^{3.4}$ . This is important for specifying the base polymer of the improved material. Also the molecular weight distribution of Sample 1 is not extremely broad. This is seen in the  $k$  value and is also utilized as a screening process for possible base polymers. Through the value of  $n$  it is seen that this material is midrange with respect to shear thinning which can also be seen in the cross model plot provided earlier and in the  $\tau^*$  value.

This product is used as an outdoor enclosure within the continental United States and sees a wide range of conditions; however, photodegradation is one of the most destructive elements that will come into contact with this product. This material can be improved with the addition of a UV stabilizer. There are many types of UV stabilizers that can be utilized for this application but the best one for this application would probably be carbon black. The addition of the correct amount of carbon black to the PC-PBT blend would produce many enhancements to the polymer characteristics on top of

the UV shielding feature including providing reinforcement for the polymer and producing anti-static properties.(11)

## 5.2 Sample 2

Sample 2 is a component used in telecommunication connectors. This part is a piece of a large component used for connection in the indoor environment. Due to its indoor use, it will not experience the range of conditions Sample 1 experiences. Sample 2 will generally remain at constant temperature ( $\pm 10^{\circ}\text{C}$ ) and humidity ( $\pm 30\%$ ) without any UV radiation, precipitation, or ice. Therefore, the properties of a material used for this component may be less stringent. Through a combination of six analytical techniques, including infrared analysis, thermal analysis, and rheology, Sample 2 was identified as an unfilled polycarbonate material.

Initial infrared analysis identified the base polymer of sample 2 to be polycarbonate. This determination was due to performing peak identification and correlation. These results were further verified by the DSC evaluation. In the DSC evaluation the glass transition of Sample 2 ( $144 - 149^{\circ}\text{C}$ ) was determined to be consistent with the glass transition of polycarbonate at  $145 - 155^{\circ}\text{C}$ . The TGA evaluation acquired the minimum degradation temperature of the sample and determines the percent inorganic filler. The minimum degradation temperature for Sample 2 is between  $420$  and  $430^{\circ}\text{C}$ . Sample 2 was determined to be an unfilled polymer by the 100% loss of mass upon heating to  $800^{\circ}\text{C}$  in air with the TGA.

DMA analysis was performed on Sample 2 from 0 – 165 °C at 10 Hz. Through the evaluation of the loss modulus, a glass transition was identified between 140 and 150°C. Through this range, there is a sharp decrease in storage modulus which determines the upper useful temperature of this sample to be below 140°C. The cross model evaluation of Sample 2 revealed a zero shear viscosity of 7300 poise. This can be used to determine the molecular weight of the sample and use this as the initial MW of the improved material. The  $\tau^*$  of Sample 2 is seen at approximately  $700\text{s}^{-1}$ . The shear thinning index (n) for Sample 2 is 0.19 meaning it doesn't shear thin very easily. The k value is 0.003 representing a broad molecular weight distribution. The master curve for Sample 2 was generated as a comparison for improved materials. The master curve takes the reference temperature from the peak of the loss modulus and shifts the remaining data to predict the data for extended times. The final evaluation of Sample 2 included complete Storage and Loss modulus curves from 0 – 300 °C at 1 Hz. In this plot the glass transition, taken from the peak of the loss modulus, is between 140 and 150°C as seen in the previous evaluations. This plot provides a complete temperature spectrum of viscoelastic data for comparison with future materials.

Sample 2 is used as an indoor connector in telecommunication products. This material could be improved by incorporating an anti-static feature into the material. The addition of the anti-static feature would help in many ways including reducing the static charge on the component that would attract dust and dirt to the point of connection and reduce the potential for shock to telecommunication workers. Typical thermoplastic materials have surface resistivities in the range of  $10^{14} - 10^{16}$  ohms while a dissipative material will have a surface resistivity in the range of  $10^{11} - 10^5$  ohms. (11)

### 5.3 Sample 3

Sample 3 is a fiber optic boot designed to fit over the fiber optic cable and dampen any shocks before it reaches and damages the fiber. This product is exclusively used indoors therefore will not have a large number of elements to contend with. This sample is a soft flexible material. Sample 3 was characterized to develop a base technology for this type of soft materials and as a base for new material development. Through a series of infrared, thermal, and rheological characterizations Sample 3 was identified as a Polyethylene-Polypropylene blend without any glass fiber reinforcement but 7.5-8.5 % inorganic filler.

FTIR analysis was initially performed on Sample 3 to help identify its unknown identity. This analysis found the presence of large amounts of CH<sub>2</sub> and CH<sub>3</sub> along with the presence of a long chain polymer peak. Further analysis revealed the absence of unsaturated peaks. This led to the initial FTIR identification of a Polyethylene and Polypropylene polymers. This initial assumption was verified through DSC. The DSC identified two melting peaks at 115 – 125 °C and 140 – 170 °C which were consistent with a Polyethylene-Polypropylene polymer. The DSC information determined this polymer to be a blend and not a copolymer due to the separation of the PE and PP melting peaks on consecutive heating runs.

The TMA evaluation was aimed at the thermal expansivity of the material and its anisotropy. Flow and cross flow thermal expansivities of Sample 3 overlapped between

115 and 125 $\mu\text{m}/\text{m}^\circ\text{C}$ . Similar perpendicular thermal expansivities means there is no anisotropy with respect to thermal expansion and most likely no fiber reinforcement.

The DMA analysis was performed to determine if there were any thermal transitions that are near the operational range of Sample 3 and to determine the viscoelastic properties of the operational temperature range. There were no transitions near room temperature that would cause the material to become hard and brittle and cause a failure during operation. The remaining viscoelastic data, including storage and loss modulus and  $\tan \delta$ , are used for comparisons of future materials.

TGA analysis revealed that the minimum degradation temperature of Sample 3 was between 270 – 280  $^\circ\text{C}$ . It also determined that there was approximately 7.5 – 8.5 inorganic filler. This filler was further analyzed to determine there was no glass fiber reinforcement, which was consistent with the TMA assumption. This low inorganic filler is either a mineral used for colorant or flame retardancy.

Rheological characterizations of Sample 3 determined many properties that are important for specifying a base material for material development. This analysis provided a plot of the amount of shear thinning of the material. This plot provides the useful shear/viscosity data required for the packing stage of injection molding to ensure proper part filling. Another extremely useful property of Sample 3 is the zero shear viscosity. From the analysis, it was estimated that the zero shear viscosity is near 200000 P. This will provide the sample's estimated molecular weight which is also utilized in material specification. An important artifact of Sample 3's rheological interpretation is the crossover point of storage and loss modulus. This is the point at which the elastic and viscous modulus are the same. Higher shear rates produce a larger viscous modulus than

elastic modulus and lower shear rates produces a larger elastic modulus than viscous modulus. Above this point, it is less likely to have fracture in a material.

Sample 3 is a fiber optic boot and is used exclusively indoors. There are not many elements that this material sees in its operational life. For a material of this type, there are standard fillers that must be in the material including flame retardants and smoke suppressors. Once these fillers are added in sufficient amounts to achieve the proper flame rating, the materials flexibility will be greatly reduced. Therefore when developing a material with equivalent or superior properties to this one, it is extremely important that the plasticizer must be optimized. There are several types of plasticizers that can be utilized in this application, and the one to use is dependent upon the required properties.

## CHAPTER 6

### Conclusion

It has become increasingly important to focus on the cutting edge of technology to remain competitive and survive in today's telecommunications industry. To do this, a company needs various resources dedicated to this cause. However, no matter how much a company puts into its research and development activities, there comes a time when a competitor produces a better, newer, and/or less expensive product. Another of these resources is the use of existing materials, as starting points, for which improved materials can be based. For this, a company must rely on the characterization of existing materials to bring that base technology into their company. Through this evaluation, the materials properties can be obtained and a material with improved properties can be developed easier, quicker, and cheaper.

There are many techniques that can be used in characterizing an existing material, but not every technique is required to obtain the desired goal. The techniques utilized depend upon the depth of identification that is required. For example, if the base polymer of a component is the only information needed, this can usually be determined with only a few techniques. If the exact make up of a material needs to be known, including its base polymer, filler content, filler particle size and distribution, molecular weight and

distribution, rheological characteristics, thermal properties, electrical properties, etc, it could take at least ten or twelve different techniques. Generally, for a quick overview of the sample's properties, most labs utilize the Fourier Transform Infrared Spectrophotometer (FTIR), Differential Scanning Calorimeter (DSC), Thermogravimetric Analyzer (TGA), Capillary Extrusion Rheometer, and Parallel Plate Rheometer in the characterization of various products. These techniques combined usually provide us with the base polymer composition, percent inorganic filler, operational temperature range of the material, molding temperature range, the material processing rheology, and other various properties.

Through a series of analytical techniques three different telecommunication products were characterized and their compositions were identified. From their compositions, improved materials can be developed. The first product identified was an outdoor enclosure of telecommunication products. Sample 1 required eight techniques to identify all the required characteristics. Through a series of FTIR, DSC, DMA, TMA, DEA, TGA, and torsion and extrusion rheology Sample 1 was identified as a Polycarbonate-Poly(butylene terephthalate) blend with no glass filler. Sample 2 is a component used in indoor telecommunication connectors. Through a series of six techniques, including FTIR, DSC, TGA, DMA, and torsion and extrusion rheology, Sample 2 was identified as an unfilled Polycarbonate homopolymer. Sample 3 is a fiber optic boot used at fiber optic connection points to avoid over flexing the fiber. Six different techniques were utilized, including FTIR, DSC, TMA, DMA, TGA, and torsion Rheology, to determine the composition of Sample 2 to be a Polyethylene-Polypropylene blend without any glass fiber reinforcement but 7.5-8.5 % inorganic filler.

There are many resources used in a company to maintain their edge on the competition, however many of these require large amounts of time and capital and don't always see favorable results. Through utilizing existing material that work fairly well in a circumstance and then improving their shortcomings, valuable time and money can be spent on other development needs. Why reinvent the wheel. If it already exists and it has proven to work then there is no reason to duplicate it, but there is reason to improve upon it. The ability of a company to develop superior materials with reduced development time and expense is an extremely important asset that most top companies practice.

## REFERENCES

- 1) Kevin P. Menard, Dynamic Mechanical Analysis, A Practical Introduction, CRC Press LLC, United States (1999)
- 2) John J. Aklonis, William J. MacKnight, Introduction to Polymer Viscoelasticity, 2<sup>nd</sup> Ed., John Wiley and Sons, New York (1983)
- 3) Christopher Macosko, Rheology, Principles, Measurements, and Applications, Wiley – VCH, New York, (1994)
- 4) T. Hatakeyama, F.X. Quinn, Thermal Analysis, Fundamentals and Applications to Polymer Science, John Wiley and Sons, New York (1994)
- 5) TA Instruments, DSC 2910 Differential Scanning Calorimeter Operator's Manual, TA Instruments Inc., Delaware
- 6) TA Instruments, TGA 2950 Thermogravimetric Analyzer Operator's Manual, TA Instruments, Inc., Delaware (1997)
- 7) Mars G. Fontana, Corrosion Engineering, 3<sup>rd</sup> Ed., McGraw Hill, United States (1986)
- 8) TA Instruments, DEA 2970 Dielectric Analyzer Operator's Manual, TA Instruments Inc., Delaware (1996)
- 9) Thermo Nicolet, Theory and Interpretation of Infrared Spectra, Nicolet Instrument Corporation, Wisconsin (1998)

- 10) Douglas A. Skoog, James J. Leary, Principles of Instrumental Analysis, 4<sup>th</sup> Ed., Saunders College Publishing, United States (1992)
- 11) John Murphy, Additives for Plastics Handbook, Elsevier Science LTD, United Kindom (1996)
- 12) D.A. Porter, K.E. Easterling, Phase Transformation in Metals and Alloys, 2<sup>nd</sup> Ed., Stanley Thornes (Publishers) Ltd., United Kindom (2000)
- 13) D.J. David, Ashok Misra, Relating Materials Properties to Structure, Technomic Publishing Company, Pennsylvania (1992)
- 14) David R. Gaskell, Introduction to the Thermodynamics of Materials, 3<sup>rd</sup> Ed., Taylor and Francis, Pennsylvania (1995)
- 15) Harry R. Allcock, Frederick W. Lampe, Contemporary Polymer Chemistry, 2<sup>nd</sup> Ed., Prentice Hall, New Jersey (1990)
- 16) J.R. Davis, ASM Materials Engineering Dictionary, ASM International, United States (1992)
- 17) James F. Carley, Whittington's Dictionary of Plastics, Technomic Publishing Company, Pennsylvania (1993)
- 18) N.B. Cotthup, L.H.Daly, S.E. Wiberley, Introduction to Infrared and Raman Spectroscopy, 3<sup>rd</sup> Ed., Academic Press, California (1990)
- 19) ULF W. Gedde, Polymer Physics, Kluwer Academic Publishers, The Netherlands (1999)
- 19) Witold Brostow, Performance of Plastics, Hanser Publisher, Munich (2001)
- 20) Witold Brostow, Science of Materials, Robert E. Krieger Publishing Company, Florida (1985)